IMSE

Institute for Materials Science and Engineering

CERAMICS

Technical Activities
1989

The twin structure in superconducting $YBa_2Cu_3O_{6+x}$ which results from cooling through the tetragonal-to-orthorhombic transition is shown in this top view of the Cu-O basal plane of the structure. The circles represent oxygen atoms which lie along b-axis midpoint sites. Adjacent twin domains have the a and b axes interchanged. Under an applied compressive stress as shown here, it is energetically favorable for the smaller a-dimension to be aligned along the direction of the stress. Consequently, oxygen atoms within the domains with the b-axis aligned along the stress will jump into adjacent sites, converting these domains into the more favorable configuration. The resulting untwinned crystals will be used to determine the role of twin boundaries in flux pinning, which contributes to the high critical current density in the material.

IMSE

Institute for Materials Science and Engineering

CERAMICS

S.M. Hsu, Chief
S.J. Dapkunas, Deputy Chief

NAS-NRC
Assessment Panel
February 1–2, 1990

December 1989

NISTIR 89-4148
U.S. Department of Commerce
National Institute of Standards
and Technology

Technical Activities 1989

TABLE OF CONTENTS

NOTICE

Though reference is made throughout the document to industrial firms and their products, such references in no way imply endorsement by the National Institute of Standards and Technology.

INTRODUCTION

INTRODUCTION

The Ceramics Division, established in 1985, provides measurement methods, standard reference data and materials, and scientific understanding to enhance the competitiveness of the U.S. advanced ceramics industry. This responsibility has been emphasized through the enactment of the Omnibus Trade and Competitiveness Act of 1988 which established the National Institute of Standards and Technology (NIST).

The primary impediments to the growth of the advanced ceramics industry are lack of reliability and high cost of ceramic components and devices. The Division programs address these issues through a broad range of research projects which focus on understanding the role of processing on performance and properties as well as mechanisms of behavior.

Fine powders (approximately 1 μm) from which advanced ceramics are made are crucial in determining the cost and final properties of a product. For this reason, the Divison has developed a strong capability in the synthesis, characterization and processing of powders. Reference materials of commercially relevant compositions have been prepared and characterization techniques assessed and developed. Through the auspices of the International Energy Agency (IEA), the Division has been the focal point for an international assessment of powder characterization techniques as well as leading the participation of U.S. industries. On a fundamental level, we have focused our efforts on the nature and effects of powder surface chemistry on agglomeration and ease of processing. To develop this understanding, we have established a solid state nuclear magnetic resonance (NMR) laboratory as well as a Slurry Characterization Laboratory. Processing studies have continued for both monolithic and ceramic matrix composites. Techniques for the measurement, of sintering stresses in composites have been extended to the development of techniques of stress control through fiber coating techniques, while Small Angle Neutron Scattering (SANS) techniques and high temperature X-ray diffraction have provided means to formulate and verify models of sintering behavior.

Improvements in the reliability of advanced ceramics, whether for structural or functional applications, require a mechanistic understanding of the modes of failure to which a ceramic is susceptible. To further our impact in this area, we have focused our efforts on the understanding of microstructural features which control brittle fracture and high temperature creep. Significant advances in the development of the theory of crack bridging have been accompanied by the development of techniques of measuring the surface forces of silica and alumina, both of which materials are constituents of advanced ceramics. In 1990, research will be initiated on dynamic fatigue of ceramics. Durability issues for structural ceramics, in addition to long term mechanical properties, have been addressed through the tribology program which is focused on developing an understanding of the role of microstructure, surface reactions and lubrication on the wear of advanced materials.

Efforts in the functional ceramic field have included, for electronic applications, the continuation of processing-property studies on piezoelectric materials as well as a major effort on high T_c superconducting ceramics. Research in the latter field has encompassed

phase diagram development for lanthanide series substitutions in the YBaCuO system as well as studies of the relationships of processing to microstructure and properties.

The microstructural features which limit the application of high temperature superconductors have been addressed as part of the NIST superconductivity initiative. Of primary concern in this field are the fundamental microstructural characteristics which limit the materials' current carrying capacity. A notable advance in understanding was provided through the synthesis of twin-free superconducting single crystals of the YBaCuO system (see cover).

Research in the optical materials area has included the development of techniques of deposition and analysis of diamond films which are expected to find application as protective coatings on a variety of detector windows. Synchrotron radiation analysis techniques have been developed to determine structural features of electronic and photonic materials and to relate these features to processing. To extend our capabilities in the optical materials field, construction and assembly of a MOCVD facility has been initiated to allow fabrication of thin film optical switching materials.

The Division has served as a link between academically oriented fundamental research and the applied needs of industrial technology. To fulfill this function, we interact intensively with both communities to both access and utilize state-of-the-art science and to apply this science to significant impediments to the implementation of advanced ceramics. Collaborative programs with academic institutions that have ceramic research programs, such as Rutgers, Pennsylvania State, Lehigh, University of California, Florida State, Cornell, Johns Hopkins, Drexel, Northwestern and the University of Illinois, have resulted in the active participation of 28 Guest Scientists in the Division's program. Industrial collaborations on projects of mutual interests have been undertaken with the Norton Company, 3M, Dupont, Chrysler, Cummins Engine Company, AT&T, Carborundum, Ford and Garrett, among others. Industrial support for our program has included both direct funding as well as contributions of goods and services as shown on the following diagram. Currently, 31 Research Associates from industry are participating in Division research projects. Contributions to the Ceramics community in 1989 were made through a variety of techniques. Division personnel have sponsored or organized 9 technical conferences in the past year to further technology in the field of advanced ceramics. This was accompanied by presentations to industry to ascertain needs and potential interactions. These latter activities resulted in identification of specific reference material and data needs. In 1989, three Standard Reference Materials were certified and six patent disclosures filed.

The desire to stimulate research in new areas not currently covered in the program has resulted in establishment of selected projects identified as "Exploratory Projects." These are intended to be conducted at relatively low levels with potential for expansion if significant results are found and if an impact on ceramics technology is foreseen. A category so identified is included in this report.

Looking towards FY 1990, we see continued effort to increase our
interactions with U.S. industries and expand the functional ceramics area.

S. M. Hsu
Chief, Ceramics Division
September 1989

1989 BUDGET - CERAMICS DIVISION

Other Agency
40 %

SRM/SRD/ONDE
2 %

STRS-Base+Initiative
37 %

Indus. Direct Funds
6 %

Indus. Goods & Serv.
15 %
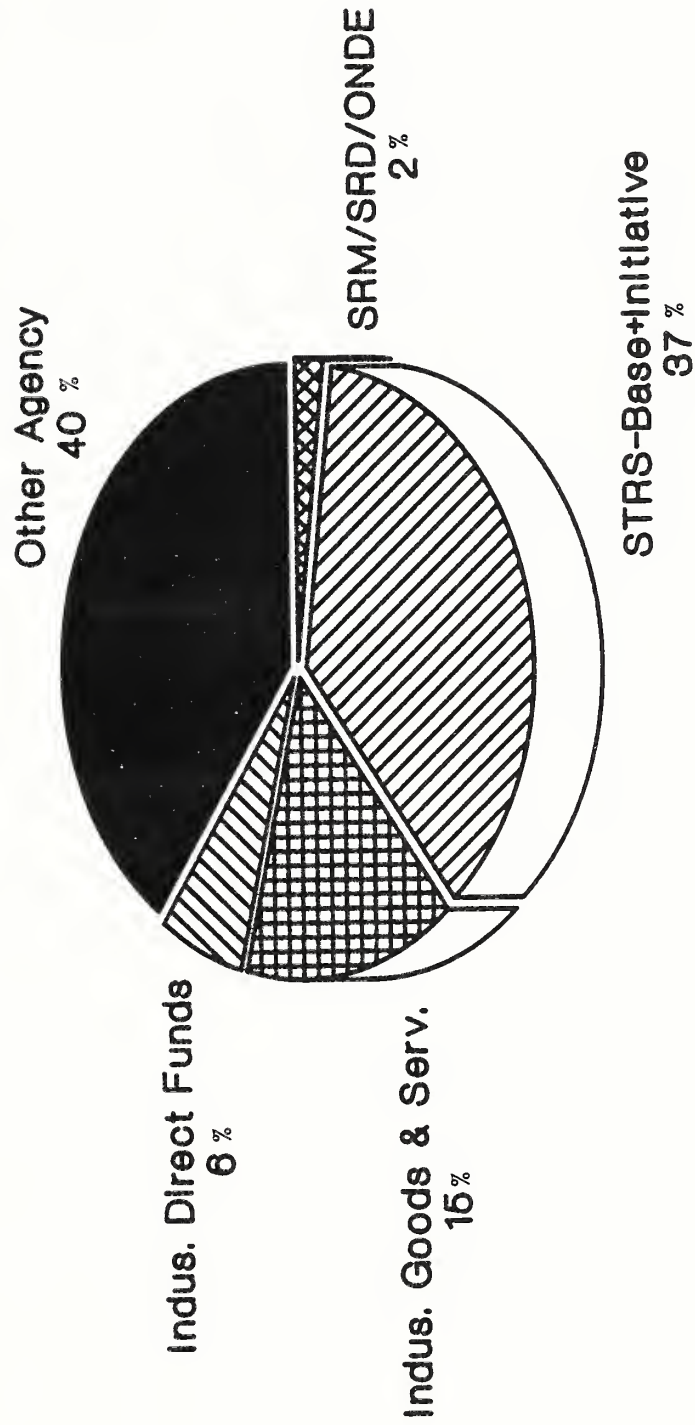
TECHNICAL ACTIVITIES

STRUCTURAL CERAMICS

STRUCTURAL CERAMICS

Overview

Structural ceramics, with high temperature strength, wear resistance and chemical stability, have been identified as materials with a wide variety of potential applications. These include heat exchangers for temperatures above 900°C or in corrosive environments; heat engine components such as turbochargers, valves, valve seats, bearings, wear pads, gas generator turbines, seals and cylinder liners; hot gas filters; and a variety of biologic implants.

The potential market value of ceramics in these applications has been estimated to be as high as four billion dollars per year and to have an impact of several hundred thousand jobs attendant on their introduction. Conversely, loss of a domestic dominance of the advanced ceramics market can result in the loss of jobs to foreign manufacturers and a significant increase in the balance of payments deficit. The recognition of these factors has resulted in the establishment of national programs to further the development of advanced ceramics technology in the United States. Major programs in both Defense and Civilian agencies of the government as well as industry have allocated approximately eighty million dollars of publicly funded research to this field. However, consensus studies have shown that the United States is viewed as not having the lead in implementation of these materials.

Significant barriers to the implementation of advanced structural ceramics can be summarized as unacceptable cost and inadequate durability and reliability. Our program is focused on addressing these barriers through an integrated set of projects which extend from powder characterization and processing to determinations of material performance in selected applications within the context of the processing-structure-property-performance relationships.

Program Structure

The focus of powders research at the Ceramics Division is on synthesis, characterization and processing. The primary objective of these activities is to further the reliability and reproducibility of advanced ceramic components manufacture by development of improved starting powders, characterization procedures, standards, and the science and technology base for ceramics processing. This is conducted in an integrated effort from the early steps of synthesis of well characterized, deagglomerated powders to the understanding of processing effects on the microstructural aspects of ceramics. The connection between powder characteristics and processing and performance originates with the recognition that powders are complex and their characteristics are often spatially distributed within particles, between particles and at the surface of particles. There is a critical need for standard reference materials with certified physical and chemical properties.

The Division continues to play a key role in an international, interlaboratory comparison of powder characterization methods conducted under the auspices of the International Energy Agency (IEA). The results have provided an important basis for the establishment of measurement procedures and standards that are vitally needed for the international commerce of advanced ceramic powders and materials.

The performance of structural ceramics in terms of reliability and durability is addressed through our programs in mechanical and tribological properties.

Our program on mechanical properties has as its objective the development of techniques and mechanistic theories to understand the fracture and long term, high temperature behavior of monolithic and composite ceramics necessary for their commercial application. Specific projects are focused on the processing-property relations between microstructural features and resulting properties including toughening behavior in structural ceramics and development of models for the fracture behavior of continuous fiber-reinforced, ceramic matrix composites. This latter work involves test development as well as preparation, characterization, and testing of composite systems.

The primary objective of the Tribology Program is the development of data and guidelines as well as a scientific understanding of the tribological behavior of advanced ceramic materials required for their reliable technological application through the development of test and analysis methodologies as well as the mechanistic theories of wear. The primary focus in our research is on the characterization of the tribological interface including analysis of chemical reactions and formation of tribochemical films, physical and mechanical behavior of surface films, and the microstructural aspects of deformation and fracture process leading to wear and failure.

Project Listing

Projects comprising the structural ceramics program are as follows:

IEA Powder Characterization Round-Robin*

Powder Surface and Colloid Chemistry*

SANS Analysis of Sintering Phenomena*

Surface Analysis and Oxidation of Silicon Carbide Whiskers and Nitride Powders

Ceramic Fiber Coating

Coating of Fibers in Fiber-Reinforced Ceramic Composites by Colloidal Processing Routes*

Sintering of Fiber/Whisker-Reinforced Ceramic Composites*

12

Processing, Microstructure, Mechanical Properties and Machining Performance
of Silicon Carbide Whisker-Reinforced Composites

Composite Testing*

New Technique (Slide Compression Test) for Measuring Interface Friction and
Interface Debond Toughness for Aligned Ceramic Composites

Fracture Mechanics Approach for Characterizing Toughening Mechanisms in
Ceramic Composites

Surface Forces of Ceramic Materials*

Microstructure Bridging, Toughness and Strength in Ceramics*

Tensile Creep of Whisker-Reinforced Silicon Nitride*

Creep and Creep Rupture of Silicon Carbide

Glass Science and Technology

Fracture Mechanics Models for Wear Transitions in Ceramics*

Wear Mechanisms of Ceramic Materials*

Tribological Coatings and Films

Mechanisms of Abarsive Wear in Lubricated Contacts

Self-Lubricating Ceramic-Matrix Composites

Self-Lubricating Metal-Matrix Composites

Tribological Characteristics of Synthesized Diamond Films

Advanced Liquid Lubricants*

Nano-Indentation and Scratch Testing

Standards and Cooperative Measurement Activities*

Numeric Database for Tribology*

Structural Ceramics Database*

*These projects are selected for expanded descriptions to illustrate the
program.

Significant Accomplishments

Significant technical accomplishments in the structural ceramics program
include the following:

o   Completed an international round-robin on powder characterization,
    involving physical and chemical properties of five powders. Two major
    reports on this round-robin work were prepared.

o   Established a laboratory facility for characterization and processing
    of dense slurries. The major characterization techniques include
    electrokinetic sonic amplitude (ESA) and rheology measurements.

o   Developed a colloidal coating method for ceramic fibers to enable
    interface control during sintering of ceramic composites. Alumina
    coatings of varying thickness and grain size were applied.

o   Analyzed pore structure and change in porosity during densification of
    alumina using small angle neutron scattering and models of pore
    shrinkage were verified.

o   Thermochemical treatment of polymer-derived silicon carbide fibers was
    investigated and potential mechanisms of degradation were identified.

o   High temperature X-ray diffraction was used for in-situ measurements
    of stress development during sintering of ceramic composites.

o   Standard Reference Material 674a was certified as a set of internal
    standards for quantitative analysis in X-ray diffraction. This
    standard is expected to improve accuracy of quantitative XRD data.

o   Preliminary measurements of the forces existing between silica-silica
    and mica-silica surfaces in varying environments have been determined
    using the Israelachvili surface forces apparatus. Determinations of
    the viscosity of water in thin films have shown that it is identical
    to that of bulk water to thicknesses of about 10 nm or greater.

o   Creep and creep rupture behaviors of siliconized silicon carbide
    (Si/SiC) and of silicon nitride (Si_3N_4) with and without whisker
    reinforcement have been characterized in tension using a laser imaging
    system. Characterization of the damage using analytical electron
    microscopy has shown significant differences between two grades of
    Si/SiC, and that damage accumulates at glassy regions along the
    whisker-Si_3N_4 interfaces.

o   A facility for investigating the creep and creep rupture behavior of
    ceramic materials in tension up to 1700°C in air has been constructed.
    Data will be collected by laser imaging.

o   The general validity of a model to predict the R-curve behavior of
    alumina ceramics has been confirmed by fitting the theory to
    indentation-strength data for a "standard" alumina with a well-
    characterized microstructure. Substantial flaw tolerance for alumina
    materials with large R-curves has been demonstrated.

o   Processing techniques developed for studying residual stresses and
    distortions in ceramic-matrix composites have been applied to both
    whisker- and fiber-reinforced ceramics. Controlled oxide coatings
    applied to the fibers by sol-gel techniques have been shown to
    influence the initiation of sintering stresses.

o   A fracture mechanics model was formulated to account for the observed
    transition from low to high wear of advanced ceramics. Experimental
    results were obtained on α-alumina under different test conditions and
    temperatures ranging from ambient to 800°C. The test results and the
    model indicate that the wear transition is controlled by a fracture
    process at the trailing edge of the contact circle. The most
    important parameters are load, coefficient of friction, elastic
    modulus, toughness, and hardness.

o   A feasibility study has shown that ceramic-matrix composites
    containing solid lubricants as a second phase can produce low
    coefficients of friction. The primary mechanism for the reduction in
    friction is formation of transfer films on the contact surface
    consisting of materials from both surfaces, as well as tribochemical
    reaction products.

o   A study has been concluded on self-lubricating composites to define
    the material and tribological requirements for lubricating cages in
    rolling contact bearings for space applications. Based on these
    requirements, selected materials have been evaluated and models of
    their lubricating behavior have been developed.

o   A cooperative research agreement was initiated with Akzo Chemical Co.
    to develop high temperature liquid lubricants for future engines. The
    research, in progress, will draw upon the technology base developed by
    NIST on the DOE-ECUT Tribology Project and utilize test methods
    developed at NIST to assess new formulations.

o   A personal computer-based system containing numeric data for tribology
    has been developed at NIST and is now ready for release. This is the
    first such information system for tribology in the U.S., and consists
    of 368 records of different materials or test conditions, in a format
    that contains 50 different information fields. The system is intended
    for both experienced tribologists and also for engineers in materials
    or other specialties who may need to make design choices pertaining to
    tribological hardware.

o   A prototype structural ceramics database for use by equipment
    designers has been developed and distributed to industrial
    sites for field testing.

The Powder Characterization and Processing research activities include synthesis, characterization and processing of ceramic materials for advanced structural applications. This research is directed toward the improvement of the reliablity and reproducibility of components through the development of scientific understanding of behavior of powders and development of unique characterization and processing techniques.

For bulk and surface characterization of powders, suspensions and ceramics, the group has established the following facilities: X-ray diffraction, analytical scanning electron microscopy, Fourier transform infrared spectroscopy, solid state nuclear magnetic resonance, and electrokinetic sonic amplitude. These facilities are complemented by other techniques at the NIST or at universities through cooperative arrangements.

Crystalline structure and microstructure of particle ensembles are characterized with high temperature X-ray diffraction (XRD), and small angle neutron and X-ray scattering (SANS and SAXS). The application of these techniques to model powder systems for characterization of agglomerate microstructures has been initiated. In addition, the high temperature XRD has been used to evaluate environmental effects in the sintering and microstructure evolution of superconductor powders.

IEA Powder Characterization Round-Robin

S. G. Malghan, L. S. H. Lum, R. G. Munro, A. L. Dragoo and S. M. Hsu

The overall objective of the International Energy Agency (IEA) characterization effort is the enhancement of the quality, reproducibility and reliability of powder characterization measurements and, consequently, of ceramic powders. Through a program of interlaboratory comparison of measurements the participants sought to:

- Survey methods currently in use for characterization of ceramic starting powders.

- Establish a base of data and experience which would identify unique sets of properties and methods useful for powder evaluation and comparison.

- Determine the extent of agreement between laboratories, to identify areas for further measurement research and to recommend useful standards which would aid international commerce.

The analysis of powder characteristics includes particle size distribution, particle morphology, elemental composition, crystalline/noncrystalline phases, surface area, density and other physical properties. Based on extensive discussion among the participants, the powders selected for this program were:

17

GTE (Ube) silicon nitride, SNE-10
Kemanord/IV-D silicon
H.C. Stark (< 5 μm) silicon carbide
Toyosoda yttria stabilized zirconia
H.C. Stark (LC-10) silicon nitride

The data were compiled and evaluated and one report on data has been published. The final report including data, procedures, technical analysis, conclusions and recommendations will be published by the end of 1989.

Analysis of the data has shown good agreement for the determination of N and O in Si_3N_4, and O in SiC by fusion and combustion and for Al and Fe in Si_3N_4, SiC and Si by inductively coupled plasma. Additionally, specific surface areas of all five powders by single and multipoint BET showed good agreement among all laboratories.

Based on detailed analysis of the data, a draft report was prepared containing recommendations and conclusions. Current participants have reviewed this draft and expressed that the following general areas shall be included in future studies.

a. Comparison of size distribution data from selected techniques using tightened sample preparation procedures.

b. Improvement of precision in major impurities determination by inductively coupled plasma (ICP), direct current plasma (DCP), and atomic absorption spectroscopy (AAS).

c. Determination of surface and interface chemical data of powders using spectroscopic and electrokinetic techniques.

Powder Surface and Colloid Chemistry

D. C. Bartenfelder, P. Pei, P. S. Wang, S. G. Malghan and S. M. Hsu

One part of the research program is centered on explorations of the measurements of electrokinetic properties of surface active agents (SAA) using a Matec acoustophoretic titrator in the electrokinetic sonic amplitude (ESA) mode. This technique would allow for determination of particle polarity through the isoelectric point (IEP) and electrochemical potential from the zeta potential.

A second part of research was initiated to remove surface contaminants by solvent leaching and measure the effect of these treatments on the colloidal properties of these slurries and surface chemistry of particles. The modification of powder surface chemistry is intimately related to its colloidal properties and ultimately to its dispersion-flocculation behavior. Alumina powder was used with water (pH~3 and 9), isopropanol, and hexane as the washing media. The rationale for media selection was to establish a gradation in oxidation potential and solvent polarity, thus monitoring surface hydroxylation a nd leaching efficiency effects. In

addition, the contribution of carbon to the surface from the organics was to be evaluated.

The results from the acoustophoretic titrations of the surface active agents did not exhibit amphoteric (reversible) properties with alternating acid-base titrations. In contrast, they exhibited a chemical specificity to initial pH titrations and titration repetition. The anionic and cationic SAA's migrated to opposite polarities with consecutive acid-base titrations. This phenomena is demonstrated by the multiple ESA values (0.004, 0.012, 0.046) at pH 7 and continuously more positive polarity of the anionic-acrylate (Darvan C) after repeated acid-base-acid titrations, Figure 1. These multiple ESA values at a specific pH indicate a change in the molecular configuration and chemical properties of the SAA. In addition, multiple IEP's were identified with the specific titration route, Figure 2. There appears to be the possibility of two IEP's for the specific surface active agent that is dependent on the initial pH of titration. The polyacrylate (Darvan C) exhibited an IEP~6.6 when the SAA was titrated in an acid-base sequence. However, when a titration sequence of base-acid was used, an IEP~10.1 was identified. In addition, there was no instance when both IEP's were present in any of the titration sequences. The appearance of multiple IEP's requires greater consideration when selecting a surface active agent for a specific processing scheme.

The results from the water washing treatments of alumina powder revealed that the slurry pH decreased with time from an initial 10.3 to 9.4 after three weeks and three wash cycles, thus indicating consumption of hydroxyl ions from solution. Consequently, the isoelectric point (IEP) of the powder shifted to higher pH values with aging, (Figure 3). In addition, ultrasonication of the slurry accelerated the process of hydroxyl ion removal from solution. Results are shown below

Treatment of Suspension	IEP
Unaged, Unultrasonicated	8.3
Unaged, Ultrasonicated	8.5
Aged (2 weeks), Ultrasonicated	9.2

In addition to the increase in IEP, there was a commensurate increase in electrical conductivity (EC) of the suspensions, indicating surface dissolution of alumina. The EC increase in aged natural-pH samples was on the magnitude of two to three-fold; whereas, the pH 3 slurries increased by a magnitude of over 10-fold. Particle/agglomerate size (median size, d_{50}) decreased with ultrasonication treatments and pH modification as shown below:

Treatment of Suspension	Size, d_{50} (microns)
Unaged, Unultrasonicated	1600
Aged, pH 3, Unultrasonicatd	770
Aged, pH 3, Ultrasonicated	630
Aged, pH 9, Ultrasonicated	870

Both pH and ultrasonication played an important role in reducing particle/agglomerate size, with pH exhibiting the dominant influence. Washing of the alumina powder with isopropanol and subsequent measurement of IEP in aqueous environment, yielded an IEP of 8.3. This value was in line with that of the fresh powder, indicating that the isopropanol washing had little effect on the interface chemistry of the alumina powder.

Fourier transform infrared (FTIR) and Raman spectroscopic techniques were used in a complementary manner for characterization of chemical constituents in ceramic powders. Minor amounts of carbon and hydroxide were identified on the surface of the alumina powder with FTIR. The washed materials exhibited slightly greater hydroxides content, but marked levels of nitrogen, most likely as nitrate, in the low pH-washed materials. This observation is consistent with the use of nitric acid used for pH adjustment. Typically, the diffuse reflectance sampling method is employed for infrared powder analysis, in which the bulk powder is diluted in an inert KBr matrix. In contrast, the Raman analysis uses a backscattering geometry with a microscope optics system for direct analysis.

Surface sensitive x-ray photoelectron (XPS) spectroscopy was used to analyze surface impurities (including hydroxides) on the alumina powder processed under various conditions. The initial powder exhibited a 2:3 aluminum:oxygen stoichiometry with 22% surface carbon contamination. After water leaching treatments there was an increase in the surface hydroxyl content. With continued leaching, XPS was able to identify and discriminate hydroxyl and oxygen on the surface, showing an increase in the hydroxide content at the expense of oxide.
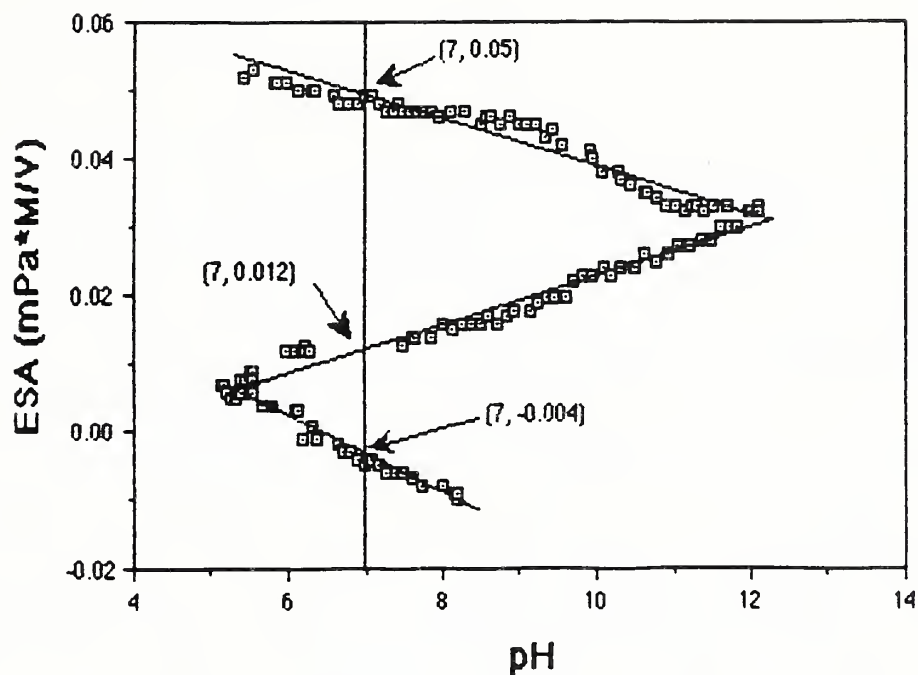
Figure 1.   Multiple electrokinetic sonic amplitude (ESA) values at pH 7 for the consecutive acid-base titration of an anionic surfactant (Darvan C).
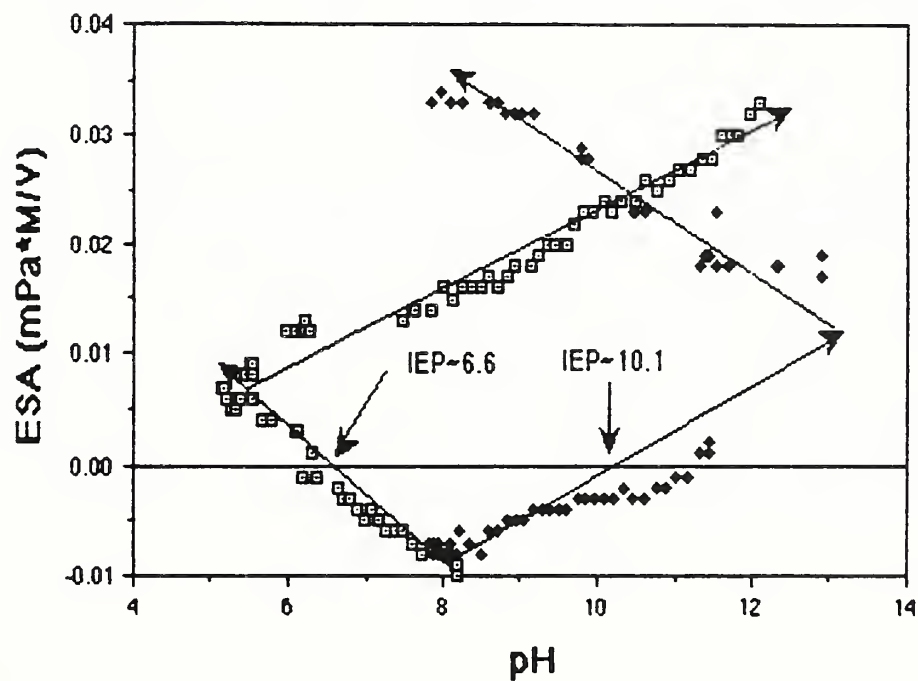
Figure 2.   Determination of isoelectric point (IEP) for an anionic surfactant (Darvan C) as affected by alternating acid-base initial titrations.

THE ELECTROKINETIC SONIC AMPLITUDE (ESA) OF ALUMINA SLURRIES AS A FUNCTION OF AGING AND pH FOR DETERMINATION OF DISPERSION BEHAVIOR.
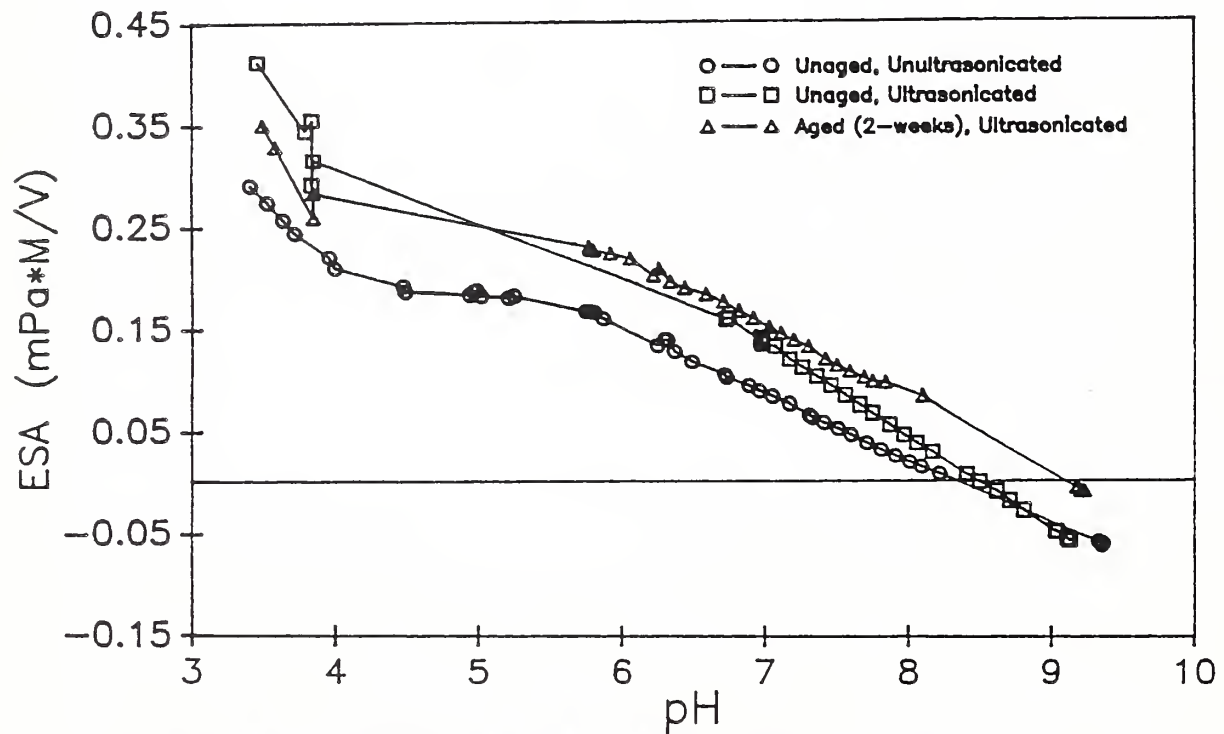
ESA is the pressure amplitude per unit electric field generated by the colloidal system, and is directly related to zeta potential, a potential at the slipping plane. At ESA~0, the colloidal system exhibits instability or flocculation.

Figure 3. The electrokinetic sonic amplitude (ESA) of alumina slurries as a function of aging and pH for determination of dispersion behavior.

SANS Analysis of Sintering Phenomena

G. G. Long, J. P. Cline, J. Ritter, and S. Krueger[1] and R. A. Page[2]

[1] Polymers Division
[2] Southwest Research Institute, San Antonio, TX

Until now, it has been very difficult to perform quantitative microstructure studies of ceramics in the early and intermediate stages of sintering because the relevant size range (0.08-10 μm) is beyond the resolution of standard techniques, and the density is between 55% and 90% of theoretical. The multiple scattering formalism developed by Berk and Hardman-Rhyne at NIST successfully addresses these issues. We have applied their formalism to the problem of microstructure evolution during the sintering of pure alumina and this application has led to the first detection of the transition from one sintering mechanism to another by small angle neutron scattering.

The samples were made by conventional sintering of Baikowski alumina powder (CR6, 6m^2/g) that had been slip cast to an average green density of 53% theoretical density (TD). Samples were removed from the furnace at different times during the sintering process to yield examples of material between 56.5 and 98.9% TD.

Using the multiple scattering analysis formalism, the radii of curvature of pores were determined as functions of neutron wavelength for each of eight samples. Figure 4 shows the measured (symbols) radii of curvature and the theoretical (solid lines) fit of radii. The densities measured volumetrically and those determined by fit of the neutron scattering data are shown in the inset to the figure.

Figure 5 shows the effective average pore radius for the alumina samples as a function of percent theoretical density determined from the multiple scattering formalism ($R_{eff}(0)$) and from a single particle (viz., Porod) method ($R_{eff}(\infty)$). The multiple scattering determinations, which are strongly weighted to the larger volume particles, indicate that the average effective pore radius for the distribution within the alumina decreases in the intermediate sintering stage and increases sharply in the final stage. The Porod determinations, which are made from the total surface scattering area, indicate an average effective pore radius that is slowly increasing during the intermediate stage of sintering and rapidly increasing during the final stage. Both methods show a break between the intermediate stage processes, in which the pores are believed to be open, and the final stage processes, in which the pores become sealed off. The multiple scattering and the Porod analyses are combined to model the total pore size distribution during each step of thermal processing.
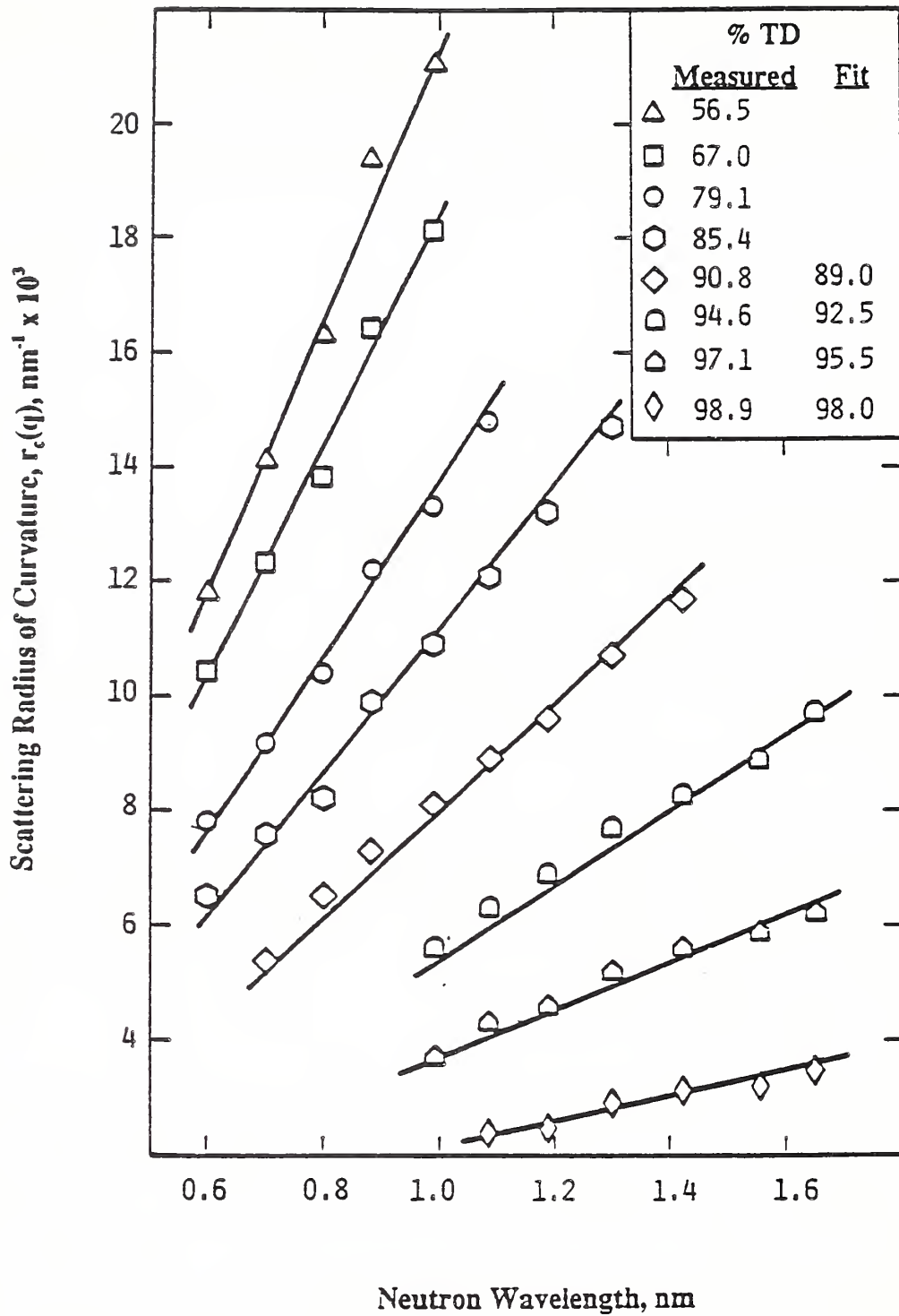
Figure 4. Radii of curvature measured (symbols) and theorectical radii
(solid lines). The insert indicates densities measured
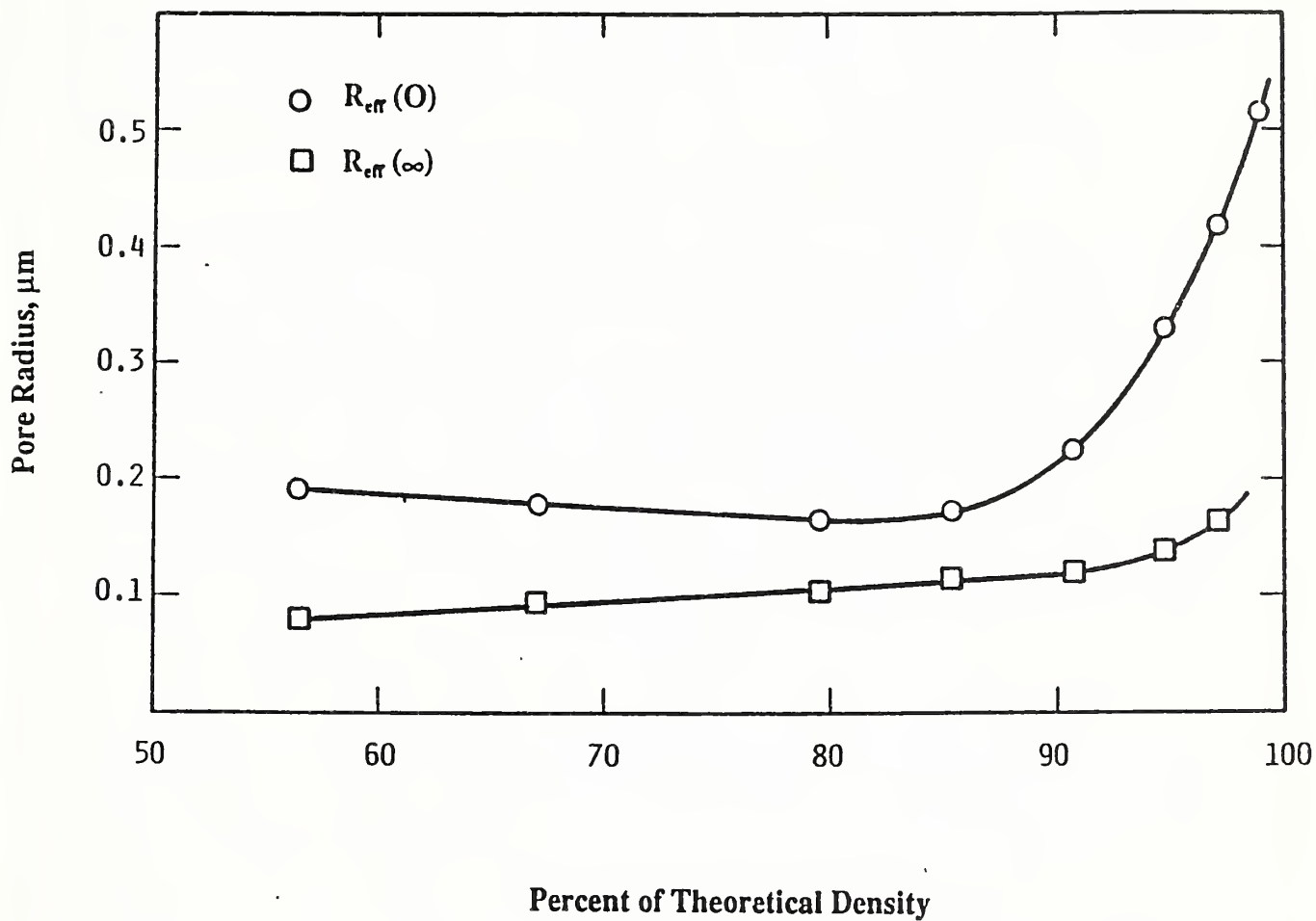volumetrically and measured by means of SANS.

Figure 5. Effective average pore radius as a function of %T.D. as determined by multiple scattering, $R_{eff}(0)$, and by single particle Porod measurements.

Surface Analysis and Oxidation of Silicon Carbide Whiskers and Nitride Powders

P. S. Wang

Measurements of surface structures and surface oxidation activation energies of silicon carbide whiskers and silicon nitride powders (with and without yttrium oxide) have been carried out. Surface sensitive x-ray photoelectron spectroscopy (XPS) was used to determine changes in the surface oxide film which occurred as a result of heating in air at temperatures from 600° to 1000°C. Equations were derived for the calculation of surface oxide film thickness from the SiC (or Si_3N_4) to SiO_2 2p intensity ratios. Oxidation was found to follow a linear rate law in this temperature range for the first 100 Å of oxide growth.

The SiC whiskers and Si_3N_4 powder were obtained from commercial sources. The samples were placed in alumina crucibles and heated in air for 0.5, 1.0, 2.0 or 4.0 hours at the desired temperatures. A carbon 1s scan of the as-received SiC whiskers shows the peaks at binding energies of 282.9 eV, 284.8 eV and 286.5 eV can be identified to be from SiC, free carbon or hydrocarbon and C-O, respectively. The Si 2p peaks from SiO_2 and SiC are at 100.3 eV and 102.9 eV, respectively, as were observed from the 2p scan. An increase in SiO_2 intensity from the oxide layer on the surface of the SiC whiskers was observed with increasing oxidation time.

From the ratio of the Si 2p intensities of SiC and SiO_2, the thickness of SiO_2 overlayers can be determined as a function of heating time and temperature. From previous work it is known that, if R is the ratio of the SiC 2p intensity to the SiO_2 2p intensity, then we have

$$R = R^* [e^{-t/\lambda}/(1-e^{-t/\lambda})] \qquad (1)$$

where t is the SiO_2 layer thickness, λ is the inelastic mean free path of the Si 2p photoelectron, and R^* is the 2p ratio of the pure SiC to the completely oxidized SiC. Equation (1) can be solved in terms of the SiO_2 layer thickness to give

$$t = - \lambda \ln[R/(R+R^*)]. \qquad (2)$$

The oxide layer thickness on the SiC whiskers was determined from Equation (2) for each heating time and temperature. The value of λ was determined from the data to be 29 Å. The error, δt, in a particular thickness measurement, can be determined by differentiating Equation (2) to give:

$$\delta t = - \lambda [R^*/(R+R^*)] (\delta R/R) \pm \lambda [1/(R+R^*)] \delta R^*, \qquad (3)$$

where the value of ($\delta R/R$) is determined from the Poisson noise in each spectrum. For each of the three temperatures, the least-squares linear fits to the data gave correlation coefficients >0.98 which is indicative of the agreement. The SiO_2 layer thickness, t, in angstroms (Å), is then given by the equations

$$600°C : t = (2.82 \pm 0.40)h + (14.9 \pm 0.9) \qquad (4)$$
$$700°C : t = (5.85 \pm 0.11)h + (25.1 \pm 0.3) \qquad (5)$$

$$800°C : t = (17.67 \pm 0.51)h + (33.5 \pm 1.2) \quad (6)$$

where h is the heating time in hours. The linear rate constants are then given by the slopes of these three lines and an Arrhenius type plot will give the activation energy. The activation energy was determined to be 17.2 ± 2.8 kcal/mole for SiC whiskers.

The studies for Si_3N_4 powders with and without Y_2O_3 as sintering aid indicate that the presence of Y_2O_3 seems to speed up the surface oxidation. The details of the reaction mechanism are yet to be investigated.

Ceramic Fiber Coating

D. C. Cranmer

Control of the fiber/matrix interfacial region is crucial to being able to tailor the properties of ceramic matrix composites. The successful coating will permit mechanical clamping of the fiber by the matrix while preventing or inhibiting strong chemical reactions between the matrix and reinforcement. One demonstrated way to achieve this control is to use coatings of either carbon or boron nitride; however, the optimum coating composition and thickness are not known. The present project will investigate carbon, nickel, and other coatings of various thicknesses on several fibers. Fiber/matrix properties will be determined using either an indentation test or a single fiber pull-out test. Carbon coatings of about 5 microns thickness have been deposited on alumina and mullite fiber tows. Using both coated and uncoated fibers, changes in the interfacial properties will be compared and correlated with the interface chemistry. Additional coatings of Ni on SiC monofilament are being prepared by Chris Johnson of the IMSE Metallurgy Division.

An apparatus for putting oxide, nitride, or carbide coatings has been constructed. A schematic of this apparatus is shown in Figure 6. As shown, an organometallic solution is applied to the fiber. This solution is then hydrolyzed to form an oxide, followed by heating to about 500°C to complete the conversion of the organometallic to oxide and to drive off remaining organic components. The process forms an oxide coating of about 150-200 nm. It can be repeated to make thicker coatings, if desired. The process to make a nitride coating is substantially the same, except the hydrolysis step is replaced by an ammonialysis step. An electrochemical cell is now being added in order to permit us to apply metallic coatings to the fibers.
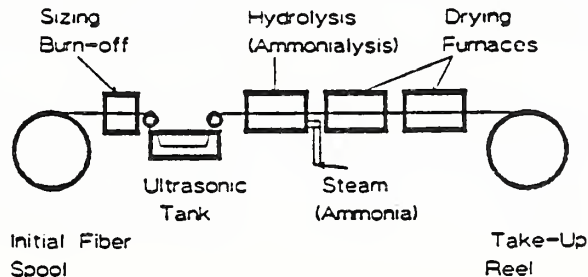

Figure 6: Schematic of organometallic precursor apparatus for fiber coating.

Coating of Fibers in Fiber-Reinforced Ceramic Composites by Colloidal Processing Route

S. G. Malghan, D. B. Minor and C. P. Ostertag

In the colloidal processing route, a stable suspension of the particles to be coated is formed, and coating of these particles on the fiber is enhanced by surface modification of the fiber. Surface chemistry of a given particle in contact with a liquid is described by its zeta potential, adsorption density (inorganic or organic species), type of adsorption (physical versus chemical), chemical composition of the bulk phase, etc. The formation of colloidal suspensions is governed by the application of appropriate physical and surface chemical forces to attain a maximum amount of repulsion between the particles. A stable suspension of particles is characterized by measurements of rheological properties, settling rate, agglomerate size, etc.

In the case of coating SiC_f (silicon carbide fibers) with alumina particles the following unit operations are involved:

* Surface cleaning of fibers
* Imparting a desired surface charge on the fibers
* Preparation of alumina powder suspension in a liquid
* Stabilization of the suspension
* Adsorption of alumina particles on the fibers
* Drying of coated fibers
* Repetition of coating steps to obtain increased thickness

Several experiments have been carried out with Sumitomo (AKP-15 and 50) alumina powders. The primary variables examined were:

* Size of alumina particles-- mean size of 0.2 and 0.7 micron.
* Thickness of alumina coating on SiC_f

Other variables have been examined to observe their effects on coating thickness. The coated fibers were examined by scanning electron microscopy for determining the thickness, morphology of particle packing, and uniformity of particle size in the coating. These results are illustrated in Figures 7 and 8.

Two sets of fibers coated with 0.2 and 0.7 micron alumina were sintered to determine the effect of particle size and thickness of the coating on temperature at which densification initiates and sintering stresses are minimized. These results demonstrated beneficial effects of the coating thickness and particle size variation. Sintering results are presented in the following highlight "Sintering of Fiber Whisker-Reinforced Ceramic Composites Through Fiber Coating."

The colloidal approach to coating of fibers has been demonstrated only for the case of SiC_f. However, the same concept with minor modifications can be used for coating other reinforcing agents, such as whiskers, platelets and even particulates.

Additional studies are in progress to examine some of the unit operations (dispersion, surfactant adsorption, etc) in greater detail to understand limitations of the process.
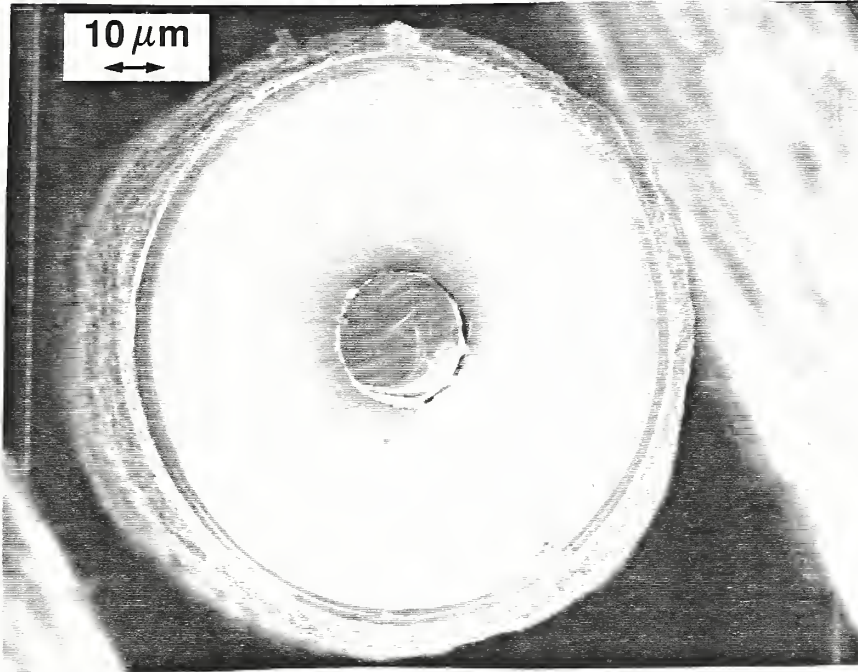
Figure 7. Electron micrograph of 6 micron thick coating of 0.7 micron alumina particles after 25 dippings.
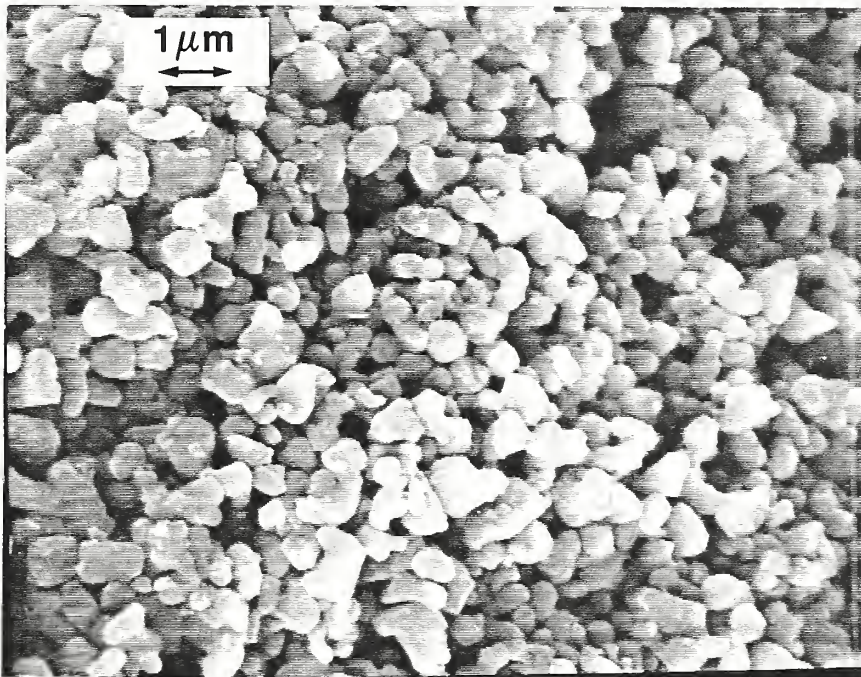

Figure 8. Micrograph showing morphology and uniformity of particle coating of 0.7 micron alumina particles.

Sintering of Fiber/Whisker-Reinforced Ceramic Composites

C. P. Ostertag and S. G. Malghan

Sintering of ceramics reinforced by whiskers or fibers is impeded by
stresses generated by the differential shrinkage between the weak, porous
ceramic matrix and the dense reinforcing agents. During the sintering of
fiber- and whisker-reinforced composites, the ceramic matrix densifies ap-
proximately thirty to forty percent by volume, while the fibers, or
whiskers, which are already fully dense do not densify at all. Fibers
and/or whiskers cause stresses to develop during sintering because of the
constraints that they impose on the contracting matrix. During the
densification process, the fiber is put under hydrostatic compression.
Stresses in the matrix normal tc the fiber axis are tensile in the circum-
ferential direction and compressive in the radial direction. Parallel to
the fiber axis, stresses in the matrix are tensile because of shrinkage
constraints. Stresses that develop due to the presence of fibers or dense
inclusions are known as heterogeneity stresses, to differentiate them from
the applied stress and from the sintering stress. Heterogeneity stresses
occur primarily in the vicinity of the reinforcing agents and cause
microcrack formation in the matrix. Heterogeneity stresses also inhibit
densification of the composite.

To avoid sintering damage, it is important either to reduce the generation
of heterogeneity stresses or to modify the response of the matrix to these
stresses such that no microcracks form. To employ effective methods for
reducing or avoiding these stresses, it is necessary to know when they
initiate and in which stage of the sintering process they are responsible
for the crack formations. A model composite system has been developed,
which can be used to assess the magnitude of stresses in unidirectionally
oriented fiber-reinforced composites. The stress is measured by means of a
sandwich compact, which consists of a layer, or plane, of SiC fibers
sandwiched between two layers of ceramic powder of different thicknesses.
Upon sintering, this configuration produces an asymmetric stress field
across the thickness of the specimen, which results in the bending of the
compact, which can be characterized by the curvature of the fibers. To
reveal the time and temperature at which the stress initiates, the sinter-
ing experiment was observed in-situ. A video camera was mounted in front
of an open tube furnace to monitor the bending of the sample bars. The
sintering experiments, including both the heating and cooling cycles, were
recorded on videotape. Bending of the fibers and, hence, the development
of the stress in the matrix began during the heating cycle, before the
actual sintering temperature was reached. The resulting stress development
depended strongly on the fiber content and fiber spacing. The higher the
fiber content, the larger the bending and the lower the stress initiation
temperature.

In-situ observations of the sintering process revealed that heterogeneity
stresses initiate during the heating cycle. It was hypothesized that
heterogeneity stresses which develop during the early stage of sintering
(at low matrix density, hence, low matrix strength at the point of stress
initiation) are responsible for the sintering damage observed in sintered
fiber-reinforced composites. Therefore, to produce damage-free composites,
stresses have to be suppressed in the early stage of the sintering process.

Furthermore, cavities or cracks that form during the early stages in the densification process do not close, but grow during subsequent densification, since the shrinkage differential (hence the stress buildup) between the fiber and the matrix increases with the increasing temperature and annealing time. The hypothesis was proven right based upon experiments where the composite densification was influenced only during the initial stage of sintering (i.e. heating cycle) by changing the heating rate and by applying uniaxial compressive stresses to the composite sample to avoid shrinkage along the fiber axis.

Lowering the heating rate from 50°C/min to 16°C/min reduced the stress development and hence the bending of the composite. The shrinkage of the matrix along the length of the fibers was inhibited during the heating cycle by applying a uniaxial compressive load perpendicular to the fiber axis. Applying the load during the heating cycle inhibits shrinkage of the matrix along the length of the fibers and hence eliminates stress development in the early stages of sintering. Uniaxial compressive stresses in the range 0.5 to 2.3 MPa were applied to green ceramic composites during heat-up to identify that stage of the sintering process that is responsible for detrimental microstructure development such as crack formation. A compressive stress of 1.5 MPa delays stress development until the density of the matrix is high enough to withstand heterogeneity stresses. A compressive stress of 1.5 MPa during the temperature range of 1100°C to 1350°C and 1.3 MPa and 1.6 MPa during the temperature range of 1100°C to 1450°C completely suppressed the sintering damage formation. The formation of crack was avoided once the matrix density reached 65% of theoretical, even though stresses built up later as a consequence of sintering.

Stresses which develop during the early stage of sintering are the most detrimental in achieving a damage-free composite due to the low matrix density and hence the low matrix strength at the point of stress initiation. Hence, the stress development needs to be delayed until the matrix density is high enough to withstand the stresses associated with the reinforcing fibers. A colloidal processing route for coating fibers with alumina was developed and the effects of fiber coatings and coating thicknesses on the stress initiation during the heating cycle was studied. The curvature of the composite during the heating cycle for uncoated and coated fibers with small (d=0.2 μm) and large (d=0.8-1.0 μm) particle-size alumina powders is illustrated in Figure 9. For the uncoated fibers in the fiber plane, the bending of the composite starts at 1300°C and increases with increasing temperature. Coating the fibers with fine particle-size alumina powder was assumed to enhance the creep and hence the stress relaxation. However, the coatings of fine particle-size alumina enhance the bending and hence the stress development in the composites during the heating cycle. During sintering of the model composite containing the fibers with a coating thickness of 4 μm, the bending and hence the stress initiates at 1265°C and increases steadily, exceeding the curvature of the composite of the uncoated fibers during the entire heating cycle. The strongest bending was observed for the coating thickness of 16 μm of the

fine particle-size powder. Furthermore, the bending initiates at the
earliest stage during the heating cycle, at 1200°C. Therefore, the
densification rate dominates over the creep rate in early stage sintering
of alumina and hence the stress was enhanced by the coatings of the fine
particles. The coarse particle coating achieved the desired results of
delaying the stress initiation to higher temperature and hence high matrix
strength. For the coarse-size alumina coating to a thickness of 10 μm, the
bending of the composite was considerably reduced and most importantly the
bending was retarded, which resulted in delayed stress initiation to
1325°C. The coarse particle-size coatings appear to reduce the stresses by
acting as a buffer layer between the matrix and the fiber. These experi-
ments reflect the importance of the fiber/matrix interface with respect to
stress enhancement (small particle-size powder) and stress retardation
(coarse particle-size powder) during the sintering of fiber-reinforced
composites. Even small interfacial layers of few microns considerably
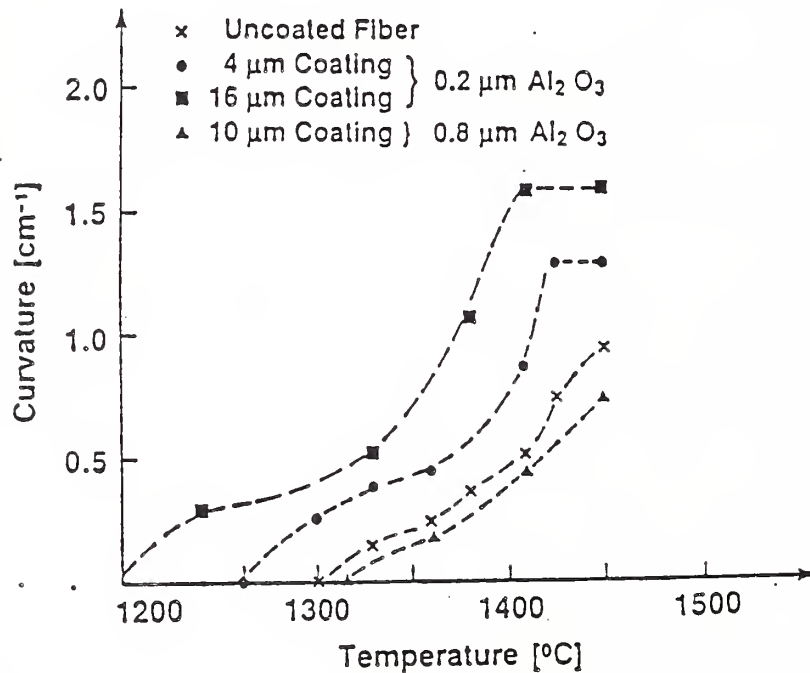influence the stress state during sintering.

Figure 9. Curvature vs. temperature plot showing changes in
         stress initiation temperature and level of residual
         stress as a function of coating particle size and thickness.

Processing, Microstructure, Mechanical Properties and Machining Performance of Silicon Carbide Whisker-Reinforced Alumina Composites.

J. Barta[1], E. R. Fuller, Jr., R. F. Krause, Jr., J. F. Kelly, P. S. Wang, D. C. Cranmer, E. Lagergren[2], R. N. Kacker[2], P. F. Jahn[3] and G. Scheyer[3]

[1] Research Associate, ISCAR Ceramics, Inc.
[2] Statistical Engineering Division, Center for Computing
                                   and Applied Mathematics
[3] Industrial Collaborator, ISCAR Ceramics, Inc.

Two statistically designed (one-half fractional factorial) experiments were conducted to establish the applicability of statistically designed experiments for materials research and to study the relationships between the performance of whisker-reinforced, ceramic matrix composites and their processing conditions, chemistry, microstructure, and properties. Two composite compositions of a SiC whisker-reinforced alumina composite were prepared by using a different diameter for nominally the same whisker. Blending procedure and whisker volume fraction were not varied. Hot-pressing parameters were varied over the ranges: temperatures from 1600°C to 1800°C; pressures from 28 to 41 MPa; and times from 30 to 60 min. Processing parameters were correlated by regression analysis with microstructure (density, alumina grain size, and homogeneity), mechanical properties (flexural strength, hardness, and fracture toughness), and machining performance (flank and nose wear).

Several conclusion can be drawn from the studies thus far. From the primary analysis: 1) temperature and pressure have a large effect on density, hardness and machining performance (expt. 2) with 1700°C and 41.4 MPa, respectively, producing the best billets; 2) possible interactions between temperature and pressure indicate that a combination of 1600°C and 27.6 MPa gave poor quality billets; 3) processing conditions in expt. 1 are very robust, giving uniform data over the entire range of conditions; 4) processing time had little effect on the responses studied; and 5) no differences in response were detectable between center and edge test pieces.

From the secondary analysis: 1) mean hardness and mean strength are strong predictors of machining performance; and 2) mean density is a strong predictor of both mean hardness and mean strength.

Our program on mechanical properties has as its broad objectives: (1) the generation of new theories and data to elucidate fracture and deformation mechanisms in brittle materials; (2) the development of fracture methodology for studying the fundamental forces that exist between two near surfaces; (3) the investigation of ceramic microstructures and their relationship to mechanical behavior; and (4) the understanding of the deformation and fracture properties that govern the mechanical response of ceramics at high temperatures. Specific projects are focussed on the processing-property relations between microstructural features and resulting properties including toughening behavior in structural ceramics and development of models for the fracture behavior of continuous fiber-reinforced ceramic matrix composites. This latter work involves test development as well as preparation, characterization, and testing of composite systems.

The primary objective of this program is to experimentally determine the relationships between the fracture behavior of fiber-reinforced ceramic composites, the properties of the individual components, and the interface between the fiber and the matrix. A second objective is to establish mechanical test procedures appropriate for these composite systems. The increased understanding of the fracture process will be used to develop strong, damage-tolerant materials.

Composite Testing

D. C. Cranmer, M. Barsoum[1], M. J. Koczak[1], J. Chou[1], U. V. Deshmukh[1] and T. W. Coyle[2]

[1] Drexel University, Philadelphia, PA
[2] Ecole Nationale Superieure de Mechanique, Nantes, France

A number of model and commercial composite systems have been examined by a number of different test procedures. These systems include borosilicate, soda-lime-silica, and calcia-titania-silica glass matrices reinforced with SiC monofilament (SiC_m), a lithium aluminosilicate glass-ceramic matrix reinforced with SiC multifilament tows (SiC_t), a chemically vapor infiltrated (CVI) silicon carbide reinforced with SiC_t, and several alumina-chromia-chrome metal matrices reinforced with Al_2O_3 fibers. The effort is divided into three parts: 1) measurement of the fiber/matrix interfacial properties, 2) determination of thermal expansion mismatch effects on the fiber/matrix interfacial properties, and 3) development and comparison of various test methods for determining fiber/matrix interfacial properties. The interfacial properties of interest include interfacial frictional stresses and fiber/matrix debond strength which determine the balance between matrix microcracking, at which point environmental effects can become important, and graceful failure of the composite.

Several techniques are available for determining the fiber/matrix interfacial properties including indentation techniques, pull-out tests, and others. A schematic diagram of an instrumented indenter developed in the Division for making these measurements is shown in Figure 10. It is a

commercially available microhardness tester which has been modified to directly measure the displacement of the diamond and force applied to the fiber. The displacement of the diamond can readily be converted to fiber displacement to obtain the complete load-displacement curve. The movement of the diamond is obtained from a pair of capacitance probes which sense the change in the gap between the probe and the target. The probes are initially calibrated using a laser interferometer. The load on the fiber or specimen is obtained from a strain-gauge load cell mounted underneath the specimen. A schematic of the expected force[2]-displacement behavior for a push-thru type of test is shown in Figure 11. The three regimes which can be seen in the figure are: 1) initial loading of the fiber prior to complete debonding of the fiber from the matrix, 2) a plateau region where slip-thru of the fiber in the matrix after complete debonding has occurred, and 3) contact of the diamond with the matrix. A typical result for a SiC_m-borosilicate matrix composite is shown in Figure 12. In this figure, two plateau regions are evident. The first occurs when the carbon core of the monofilament slips in the SiC fiber and the second when the SiC slips in the matrix.

Table 1 lists the values of the interfacial strength and/or frictional stresses determined for each of the systems mentioned above. As can be seen in the table, a wide variety of interfacial properties can be obtained, depending on the composite system desired. Measurements of fiber/matrix interfacial properties of the mixed ceramic/metal matrix composites can be correlated with the processing conditions and matrix compositions used in fabricating the material.

Table 1: Interfacial Properties

Composite System	Debond Strength (MPa)	Frictional Stress (MPa)
$Na_2O-B_2O_3-SiO_2/SiC_m$	9-10	3
$Na_2O-CaO-SiO_2/SiC_m$	?	14
$CaO-TiO_2-SiO_2/SiC_m$	3	3
$Li_2O-Al_2O_3-SiO_2/SiC_t$	30-50	2-30
CVI SiC/SiC_t		
As Received	0.5-4	0.5-4
Oxid.(500°C,100 hr)	5-6	?
Oxid.(500°C,1000 hr)	4-5	?
Oxid.(1000°C,100 hr)	5-6	?
Oxid.(1000°C,1000 hr)	8-9	?
$Al_2O_3-Cr_2O_3-Cr/Al_2O_3$		
50/50 Al_2O_3/Cr_2O_3	30-40	?
75/25 Al_2O_3/Cr_2O_3	>200	?
90/10 Al_2O_3/Cr_2O_3	>750	?

During FY 89, we have completed an initial comparison of three methods of measuring fiber/matrix interface properties: indentation push-in, indentation push-out, and single fiber pull-out. Of the three, the pull-out test provides the most direct information but suffers from being usable only with large diameter monofilaments. The push-in test provides only information about the interfacial frictional stresses while the push-out test can be used to determine both frictional stresses and debond strengths in some instances. Both indentation tests can be used for either large or small diameter fibers. Also completed this year is a determination of the effects of thermal expansion mismatch between the fiber and matrix. Above a certain value of the mechanical clamping stress as dictated by the mismatch, the matrix microcracks, resulting in an inadequate material. With too small a mismatch, the frictional pull-out is small, resulting in little damage tolerance.
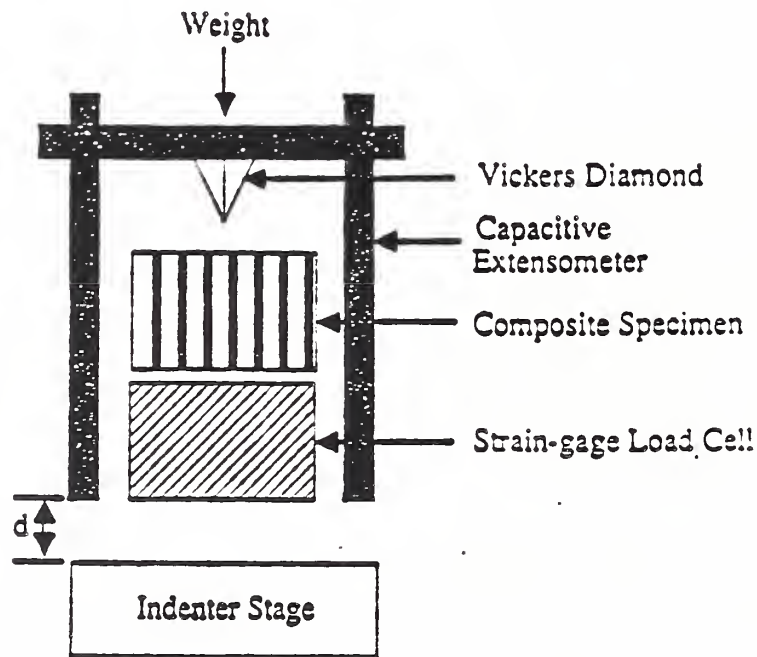
Figure 10:   Instrumented indenter capability developed during FY88. Results obtained during FY89 indicate the self-consistence of the indentation tests (push-in and push-out) with the single fiber pull-out test.

The equations shown in the figure:

$$1 = \frac{2\pi R^2 E_f \delta}{F}$$

$$\tau = \frac{m}{4\pi^2 R^3 E_f}$$

$$\tau = \frac{F}{2\pi R t}$$

$1 < t$
$(1 >> r)$

Diamond contacts matrix

Fiber slips through matrix

Fiber pushes into matrix

Fiber Displacement (δ)
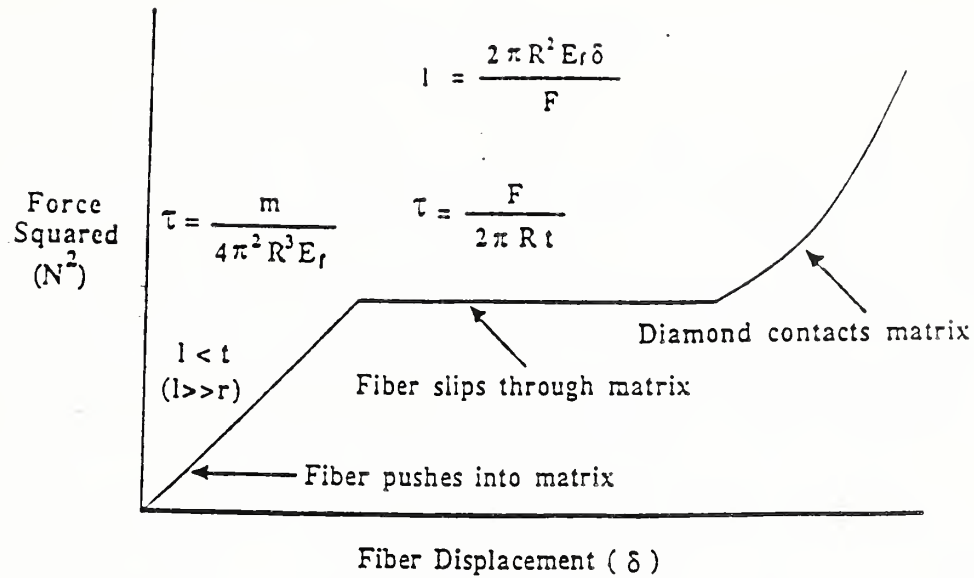
Figure 11:   Schematic of (force)^2 - displacement curve for fiber push-out test.

Second plateau yields debond strength of 9.9 MPa for SiC slipping in matrix

First plateau yields debond strength of 36 MPa for C core slipping in SiC

SCS-6 SiC./Borosilicate Matrix Indentation Push-out Test Load = 150 g

Figure 12:   Indentation push-out on SiC monofilament/borosilicate glass Load = 150g. Both core and fiber move.

New Technique (Slice Compression Test) for Measuring Interface Friction and Interface Debond Toughness for Aligned Ceramic Composites

D. G. Brandon[1], E. R. Fuller, Jr., N. Shefri[2], and M. Terasaki[2]

[1]Guest Scientist, Technion - Israel Institute of Technology
[2]Academic Collaborator, Technion - Israel Institute of Technology

A quantitative test was developed for measuring debond interface toughness and interface friction of aligned fiber-reinforced, ceramic matrix composites. The test involves the compression of a polished slice of a locally aligned composite which is cut normal to the reinforcement. The bottom surface of the slice is compressed at a constant strain, while the top surface is compressed at constant stress. Debonding of the fibers occurs at the top surface due to the compressive strain mismatch between the fibers and the matrix, resulting in the protrusion of the fibers from the matrix. On removing the load the fibers partially relax back into the matrix, with the degree of relaxation depending on the frictional stresses at the fiber-matrix interface. The test has the major advantage that measurements are made on actual processed composites and not on individual fibers. Furthermore, since the test is comparatively simple to perform, there are few limitations to either the dimensions of the reinforcement or to the loading system. Indeed, it should be feasible to extend the method to quasi-aligned, whisker-reinforced composites, as well as to tests performed at elevated temperatures or in controlled environments.

The slice compression test (SCT) specimen is a lapped and polished slice of a ceramic composite cut normal to the local direction of reinforcement. The s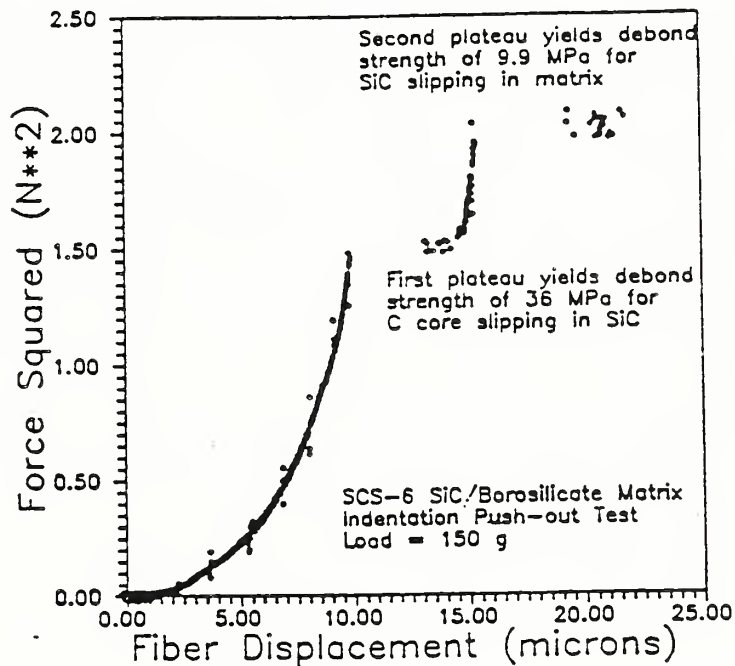lice is uniaxially compressed between two platens, one a hard, high-modulus ceramic and one a soft, ductile metal. For our initial studies on a Nicalon fiber-reinforced glass ceramic, the hard platen material was hot-pressed silicon nitride, and the soft platen was aluminum. Once general yielding of the aluminum was established, this soft platen imposed a condition of uniform stress (pressure) on one side of the composite slice, and hence ensures a condition of maximum elastic mismatch between the matrix and the reinforcement at this surface. An annealed, commercial purity aluminum (1100 grade) was used for this platen.

On loading the test slice, fiber debonding and relative sliding initiate from the surface under uniform pressure and propagate down the fiber/matrix interface. For most ceramic composites the fibers are stiffer than the matrix, and, thus, the fibers progressively indent the soft platen with increasing load. In some cases (e.g., Nicalon fiber preforms chemically infiltrated with a SiC matrix), the matrix has a higher stiffness, and the fibers then slide back into the matrix during compressive loading. In either case, the soft, plastically deformable platen retains an impression, after the load has been released, of the maximum fiber displacement with respect to the matrix while under load (elastic relaxation of the platen is negligible compared to the plastic deformation occurring in this indented region. During the unloading cycle the fibers can relax partially back into the matrix. The extent of relaxation reflects the magnitude of the frictional forces which restrict fiber sliding. At the end of the test the soft metal thus retains a "negative image" of the extent of fiber displace-

ment under maximum load, while the composite slice contains information on the residual fiber/matrix displacement after unloading.

Initial experiments were conducted on a Nicalon-reinforced lithium aluminosilicate (LAS) glass-ceramic matrix composite provided by Dr. J. J. Brennan of United Technologies Research Center. These materials included both uniaxially reinforced samples and biaxial 0°/90° laminates of Nicalon/LAS III in both the as-pressed and the ceramed conditions. The samples were sliced perpendicular to the direction of reinforcement and diamond polished. Under loading at a constant displacement rate of nominally 50 μm/min, general yielding of the aluminum platen occurred at about 50 MPa; matrix microcracking parallel to the compression direction became general above about 180 MPa (and led to partial disintegration of the specimen). The pressure interval between 50 and 180 MPa thus constituted the working range for the present experiments.

The depth of the fiber indentations into the soft aluminum platen and the extent of residual fiber protrusion from the matrix after relaxing the load were measured by two techniques: (1) changes in optical focus and (2) parallax shifts in a scanning electron microscope (SEM). The optical technique was sensitive to surface displacements of the order of 0.2 μm, and quite reproducible. The SEM technique gave values that were reproducible to better than 0.1 μm when viewed at a tilt angle of at least 45°; accuracy depends on the assumed circular cross-section of the fibers and the magnification calibration of the SEM. Note that measurements of maximum indentation depth and of residual fiber protrusion must be made for the same fiber to analyze interface properties for a series of individual fibers. This was accomplished with microstructural markers to identify corresponding sections.

A SCT specimen prepared from a 0/0° laminate of Nicalon-reinforced LAS III (unceramed) was loaded to a stress of 100 MPa, and the extent of fiber indentation and residual protrusion was measured from SEM images taken at a tilt angle of 65°. A typical fiber indentation depth in the aluminum platen was a 2.7 μm, while the residual protrusion of the same fiber was 1.6 μm. The calculated debond length for this fiber, 6.7 mm, was greater than the thickness of the slice (3mm), implying that the fibers were fully debonded. The calculated value of the interface frictional shear resistance was 37 kPa.

Fracture Mechanics Approach for Characterizing Toughening Mechanisms in Ceramic Composites: Influence of Ductile Interfacial Layers

E. P. Butler[1], E. R. Fuller, Jr., T. R. Palamides[2], and H. M. Chan[3]

[1] Guest Scientist, Lehigh University
[2] Guest Scientist, Drexel University
[3] Academic Collaborator, Lehigh University

A fracture mechanics specimen known as the double-cleavage drilled-compression (DCDC) specimen was used to study crack-fiber interactions and toughening mechanisms in a model composite system of a borosilicate glass matrix reinforced with SiC monofilaments. Fiber toughening for a single monofilament was measured from changes in the applied stress intensity

factor with crack length. Interface friction and interface toughness, properties which influence toughening, were measured independently with single fiber pull-out tests. The influence a thin ductile interfacial layer on toughening was examined by electrodepositing a nickel coating on the SiC fiber. Results from single-fiber pull-out tests indicated that both the sliding friction and the interface toughness were greater for the glass/nickel interface than for the nickel/SiC interface. In agreement, the toughening increment for the nickel-coated fibers was generally less than that of as-received fibers. The fracture toughness increment for the nickel-coated fibers initially decreased with increasing coating thickness, but gradually increased again up to that of the as-received fibers at a coating thickness of 22 μm.

Surface Forces of Ceramic Materials

R. G. Horn, D. T. Smith, K. W. Schantz and W. Haller[1]

[1]Research Associate, Electronic Materials Group

In the latter part of 1988, a dedicated Surface Forces Laboratory was established in the Division. The facility is based on a technique developed by Israelachvili in which the forces acting between two ultra-smooth solid surfaces, usually mica, are determined as a function of their separation in various vapor or liquid media. Over the past decade, this technique has proven very successful in elucidating the forces arising from van der Waals interactions, electrical charges on the mica surfaces, adsorption effects, capillary condensation and surface tension, and molecular packing effects in a liquid. Such forces play an important role in the behavior of various systems including brittle fracture and colloidal processing, but the limitation to mica surfaces has been a severe restriction on their wider applicability.

Recently we have removed this limitation, by developing a method of preparing silica surfaces which are sufficiently smooth and clean to enable us to make sensible measurements of the surface forces between them. The trick is to melt and close the end of a silica tube, then rapidly blow it out so that it sets into a large, thin-walled bubble. The surfaces of the bubble are very smooth, with rms roughnesses measured by surface profilometry and atomic force microscopy in the range 0.3 - 0.5 nm. Two fragments taken from such a bubble can be mounted in the surface force apparatus, which can then be filled with any vapor or liquid environment of interest.

Our results show that in a dry inert gas the silica surfaces adhere, as expected, from van der Waals forces. In the presence of water vapor, there is a comparable adhesion, resulting in this case from capillary condensation effects. However, when the surfaces are immersed in liquid water (or electrolyte solution) there is no adhesion. There is a long-range repulsion due to the formation of an electrical double-layer, and its range decreases as electrolyte concentration increases (Figure 13). This follows theoretical expectations, but the classical theory also predicts that the van der Waals attraction should become dominant at short range, causing the surfaces to adhere, which we do not observe. Rather, there is a strong repulsion measured when the surfaces approach within 2 - 3 nm, which is attributed to the hydration of the silica surface. The strength of this

additional repulsion does not appear to depend on electrolyte concentration.

The observation of a hydration force such as this implies some ordering of the water molecules in the immediate vicinity of the surfaces, and in the past it has commonly been believed that this ordering would also affect the viscosity of the thin water film. This is a quantity which we are also able to measure by studying the rate of thinning of the liquid film as the solid surfaces are pushed together. Our results (Figure 14) show no deviations of the viscosity from that of bulk water, as seen from the agrement between our data (open circles) and classical hydrodynamic theory (solid line). This indicates that although the water molecules are on average ordered in some way to cause the hydration repulsion, they nevertheless remain mobile on the time scale of our measurements. This is important to know, since the viscosity of thin liquid films is a key parameter in colloidal stability, tribology, crack kinetics and other areas.

Our development of a method of studying silica surfaces in this way opens the doqr to many future investigations. The large body of work on mica has shown that surface force measurements give a great deal of useful information about the surface chemistry of the material, for example surface charging mechanisms, the adsorption behavior of surfactants and polymers, and the ordering of particular liquids adjacent to the surface. Now this can be done comprehensively for silica, and also for other glass compositions. Furthermore, glass surfaces are readily modified chemically (mica is not), so that we can explore, for example, the effects of silane coupling agents or chromatographic derivatization.

Another possibility which is now open is to investigate surface forces and adhesion between dissimilar materials. One of our prime interests will be to relate such measurements to intergranular fracture in ceramics, and matrix-filler debonding in composite materials.
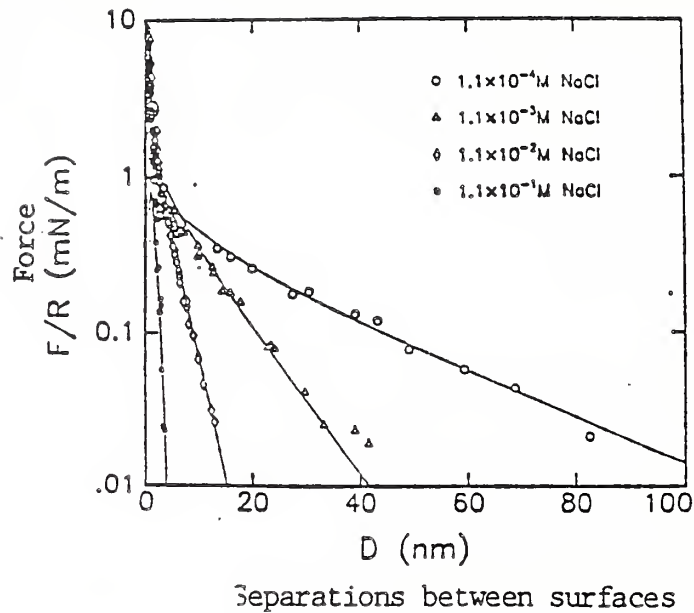
Figure 13:   Forces between silica surfaces as a function of
separation in several difficult electrolyte
solutions. Note strong repulsive force occurring at
2-3 nm as surfaces are brought into contact.
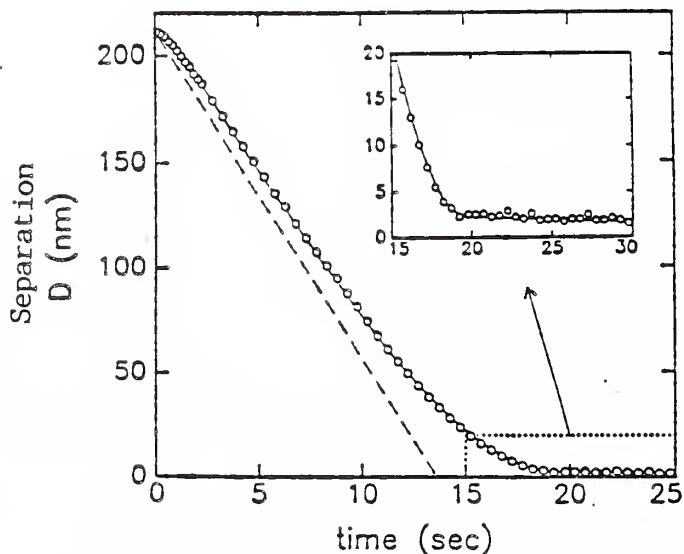
Figure 14:   Distance between two silica surfaces separated
by a thin film of water as the surfaces are driven
together over time. If there were no viscous drag, the
separation distance would follow the dashed line. With a
viscous liquid present, the response predicted by classical
hydrodynamic theory (solid line) fits the experimental data
(open circles) extremely well.

42

Microstructure Bridging, Toughness And Strength In Ceramics

B. R. Lawn, S. J. Bennison[1], S. Lathabai[1], J. Rodel[1] and J. Runyan[2]

[1] Guest Scientist, Lehigh University
[2] Coop Student, Virginia Polytechnic and State University

This research program is directed toward a fundamental understanding of the governing role of microstructure in the strength and toughness properties of structural ceramics like aluminas. We now appreciate that the toughness characteristics of structural ceramics like aluminas can be a strong function of crack size, i.e. they exhibit "R-curve" behavior. Perhaps the most important practical manifestation of R-curve behavior is an associated "flaw tolerance", i.e. an insensitivity of the strength to the initial crack size. Such flaw tolerance is of special interest in the context of reliability, because it offers the structural engineer the prospect of a well-defined design stress; flaw distributions and statistics are then no longer such critical factors in materials evaluation. Part of our project over the past year has been spent in analyzing these tolerance properties, with the express aim of providing guidelines to materials processors as to the levels of defect and porosity content that structural materials may be able to withstand in service. Contrary to the prevailing wisdom in the ceramics community, we suggest that in many cases a processing philosophy based on the elimination of all flaw populations may be counter-productive; judicial incorporation of defect structures may actually improve strength properties, by enhancing the crack-interface bridging restraints.

Our achievements in this area are summarized as follows. The micromechanical mechanism of R-curve behavior has been physically identified in aluminas and other monophase ceramics as bridging, by interlocking grains at the interface behind the crack tip. This behavior has been mathematically modelled in terms of frictional tractions at the boundary between the interlocking grain and embedding matrix. Thermal expansion mismatch internal stresses have been evaluated as the key element in generating significant energy-dissipative friction. The general validity of the model has been confirmed by fitting the theory to indentation-strength data for a "standard" alumina with a well-characterized microstructure. From this fit, we have been able to evaluate all essential microstructural parameters (grain-matrix friction, bridge rupture strain, etc.) needed to extract the complete R-curve. With this "calibration" on "reference" material, the strength and toughness behavior of aluminas of different microstructures, e.g., grain size have been predicted. Confirmation of these predictions has been obtained by comparing with actual data on aluminas processed in our own laboratories with a wide range of grain sizes. Substantial flaw tolerance for alumina materials with large R-curves has been demonstrated. In one instance, we have shown that the strength of an alumina of grain size 20 μm is almost totally insensitive to large defects, e.g. pores, in excess of 100 μm. We have begun our own processing program, beginning with aluminas with different grainshape, e.g., elongated grains to maximize interlocking and bridging, to test predictions for optimal strength, thence toughness. We have begun also to fabricate alumina-based composites, e.g., with an aluminum titanate second phase, to increase internal residual stress levels and thereby increase the R-curve characteristic. The first results indicate substantial gains in the flaw tolerance.

Our future goals are:

(i) To focus on in-house processing to provide a unique processing-properties approach to designing stronger and tougher ceramics. To this end, we will continue to develop a formal NIST-Lehigh University link, through AFOSR sponsored funding, to strengthen our materials development capability.

(ii) To extend the bridging principles systematically to model composites (e.g. two-phase, whisker-reinforced, etc.), in light of the growing evidence that the bridging mechanism may be a primary source of toughening in most non-transforming ceramics. Also, to continue to investigate the micromechanics of bridging using new NIST scanning electron microscope fixture for in situ observations of propagating cracks.

(iii) To investigate fatigue and wear properties of the same ceramics that show optimal flaw tolerance; recent work in our laboratories suggests that possible trade-offs between flaw tolerance and these other properties may sometimes be necessary.

Tensile Creep of Whisker-Reinforced Silicon Nitride

S. M. Wiederhorn[1] and B. J. Hockey

[1] IMSE, Institute Scientist

In this program, the tensile creep behavior of two whisker-reinforced composites is being studied: SiC whisker-reinforced hot-pressed Si_3N_4, and SiC whisker-reinforced Al_2O_3. In flexure, these two materials behave quite differently in creep; SiC whiskers improve the creep resistance of the Al_2O_3, but have little effect on the Si_3N_4. The collection of creep data in tension should help elucidate the reasons for the difference in behavior of these two materials. Currently most of our data has been collected on the whisker-reinforced Si_3N_4. This work is being conducted with active collaboration of GTE, which is making materials for us to test, and will iterate the structure and composition of the composite to attain the best mechanical behavior.

To date, tensile tests have been conducted on both whisker-reinforced and whisker-free hot-pressed silicon nitride, in both the annealed and unannealed state. Tensile creep results have also been compared with results obtained on material subjected to compressive creep deformation. Characteristic of the deformation of this material is transient creep behavior, especially on specimens that sustained creep loads for times approaching 1000 hr. This behavior is observed on both whisker-reinforced and whisker-free material. An extreme example of this behavior is shown in Figure 15 for a whisker-free material that was subjected to a tensile load for ≈1000 hr. As can be seen, there is no steady state region on this curve. For shorter test periods, ≈100 hr., "apparent" steady state creep is achieved before failure; however, microstructural examination of the specimens by transmission electron microscopy suggests that this "steady state creep" is merely a balance between work-hardening and the cavitation that eventually leads to component failure.

Whisker reinforcement in this material appears to have little effect on the creep resistance of the material. Thus, in Figure 16, whisker-reinforced materials creep more readily than materials lacking reinforcement. Results for specimens tested in the unannealed state indicate that the creep rates for both sets of material are almost identical at high creep rates. For low creep rate tests, tests that last ≈1000 hr., annealing occurs in both types of materials. In this case, the creep resistance of the whisker-free material is approximately ten times that of the whisker-reinforced material. Similar results were obtained on materials that have been annealed for extended periods before testing; the whisker-free material exhibits a higher resistance to creep.

Investigations of these materials by transmission electron microscopy suggest that many of the observations discussed above are a consequence of phase transformations that occur during the long term exposures. In the as-received state, the whisker-reinforced material contains considerable amounts of glass at the SiC whisker-Si_3N_4 interface. This glass is introduced into the composite as a consequence of an amorphous layer on the whiskers before processing the composite. Smaller amounts of glass are present at Si_3N_4-Si_3N_4 interfaces. In the unannealed specimens, this glass promotes deformation by enhancing grain boundary sliding and solution re-precipitation at contact sites between grains. Large amounts of glass at the silicon carbide whisker surfaces appear to nullify the beneficial effect of the whiskers on the creep rate, so that creep in the as-received composite is no better than that of the whisker-free material. GTE is currently changing the composition of the composite to reduce or modify the glass at the whisker interfaces, which hopefully will improve the creep resistance of this material.

Annealing improves the creep resistance of both the whisker-free and the whisker-reinforced materials, due to devitrification of the glass within the materials. Crystalline materials tend to be more resistant to creep than amorphous materials of the same composition, hence, devitrification is used as a standard method of improving the creep resistance of nitride ceramics. Enhancement of creep resistance is more apparent for the whisker-free material, where a factor of 10 reduction in the creep rate is observed for short failure times. Improvement in the creep resistance of the whisker-reinforced material occurs primarily at low creep rates, where cavitation does not control the creep behavior. At high creep rates, cavity formation and crack growth dominate the behavior of both the annealed and unannealed, whisker-reinforced specimens, so that devitrification due to annealing had no effect on the creep rate.

A comparison of the creep behavior of whisker-reinforced materials in tension and compression indicates a much greater resistance to creep in compression. To achieve the same creep rate, the applied stress must be twice as high in compression as in tension, Figure 17. Furthermore, the stress exponent of the creep rate is less in compression, ≈2.5, than in tension, ≈4. This difference in behavior indicates a difference in creep mechanism in the two modes of loading. Based on microstructural analyses of tensile specimens, cavitation cracks form during the creep of this material in tension. Cracks are more prevalent at the higher creep rate. Since crack formation enhances the rate of deformation, the fact that more cracks are formed at the higher creep rates suggests that the higher stress

exponent in tension is a consequence of the cavitation process. In compression, the slope and position of the creep curve is almost identical to data obtained on this material by other researchers. Microstructural analyses of the deformed material by the same researchers showed no evidence of significant cavitation or crack formation, suggesting that the deformation process did not depend on cavity formation. Based on their observations, grain boundary sliding was identified as the primary mechanism of deformation for this material. However, additional experimentation is needed to establish modes of accommodation during compressive creep.

Differences in creep behavior in tension and compression are not only of interest scientifically, but have important practical implications. Normally materials at high temperature are loaded neither in states of pure tension nor pure compression, in which case both states of stress contribute to the rate of deformation. When rates of creep in tension and compression differ substantially, then time dependent shifts in the stress distribution occur, shifts that can lead to a factor of two error in the estimated maximum stress within a component. To assure the reliability of engine components, these creep-induced modifications in the stress distribution must be ascertained.

During the coming year, high temperature work on whisker-toughened ceramic materials will be continued. The silicon nitride grade of material will be modified (at GTE) to reduce the amount of glass in the composite so as to increase its resistance to creep. In addition, creep measurements will be initiated on SiC whisker-reinforced aluminum oxide. Transmission electron microscopy will be used to clarify differences in mechanical behavior for these two materials.
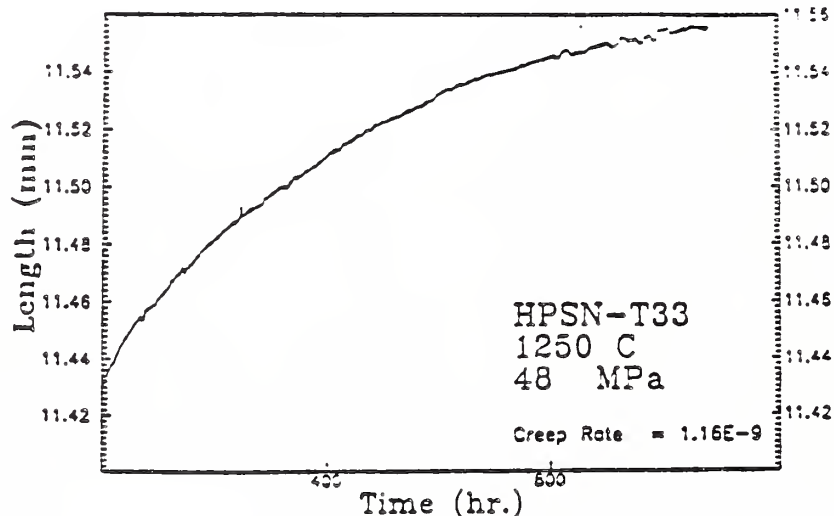
Figure 15:   Whisker free specimen tested in the as-received state. Extended deformation gives no indication of a steady state region of deformation.

46

HPSN-Tension
1250 C
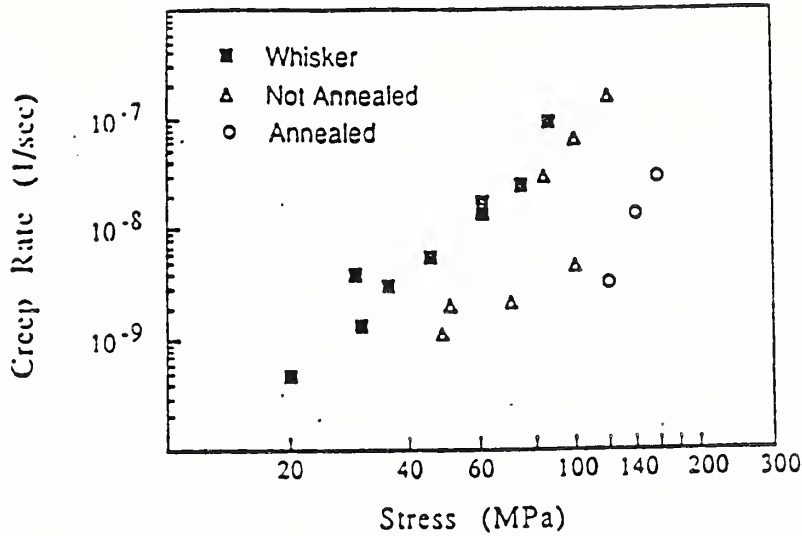
Figure 16:   Effect of whisker reinforcement on the creep rate
              of hot-pressed silicon nitride. Annealing improves
              the creep resistance of the whisker-free material
              by a factor of ≈ 10. The open symbols, circles and
              triangles, are data collected on whisker-free
              material.

HPSN-1200 C
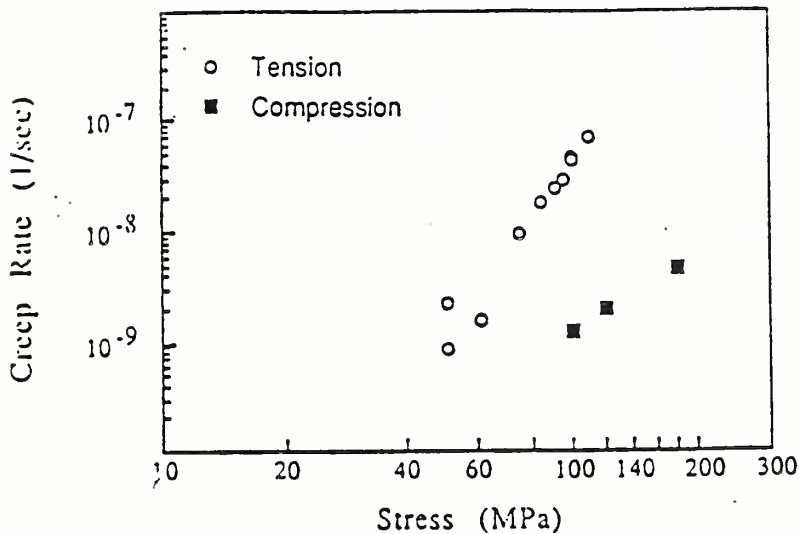
Figure 17:   Effect of the sign of the applied stress on the
              creep rate. For a given creep rate, approximately
              twice as much stress is needed in compression as
              in tension. This same sort of behavior has been
              observed on other materials.

Creep and Creep Rupture of Silicon Carbide

S. M. Wiederhorn[1], B. J. Hockey, T.-J. Chuang, D. E. Roberts and D. C. Cranmer

[1] IMSE, Institute Scientist

The development of new ceramics holds promise for use of high efficiency, enhanced performance of structural systems in high temperature, stress-bearing environments. However, before ceramics can be used in industrial applications, issues concerning reliability and service life remain to be resolved. Accordingly, we have been studying the creep and creep rupture behavior of model ceramics at elevated temperatures. During the past year, the creep and creep rupture behavior of a grade of siliconized silicon carbide having a large grain microstructure was investigated and compared with a similar grade of material having a uniform fine grain microstructure. Grain size enhancement resulted in cavity formation at the boundaries between the large grains of silicon carbide and the silicon. These cavities grew along the silicon-silicon carbide interface, forming large cracks that limited the amount of deformation allowable in the material and were the eventual cause of component failure. Although the cavity nucleation process in the fine grain material was similar, the small size of the grains limited the size of the cracks that could form as a result of the creep process. As a consequence, the fine grain material was found to be more ductile, tolerating a greater degree of creep before failure. Work on the effect of microstructure on creep has shown that the fine grain material appears to creep via a diffusional mechanism, while the large grain size material appears to creep via a different, as yet unidentified mechanism.

Creep rupture behavior of non-oxide ceramics in tension and flexure has also being used to predict the lifetime of compressively loaded "C"-rings. Using a maximum strain criterion for failure and the previously determined experimental data, the lifetime of the "C"-rings was predicted. Experimental determinations of the creep rupture life and depth of the damage zone of the "C"-ring agreed well with the predictions, thus demonstrating the general applicability of the technique to ceramic materials.

Glass Science and Technology

D. C. Cranmer, D. H. Blackburn, and D. A. Kauffman

The most significant area of glass technology involves the use of these materials as sensors and devices. The specific technologies we have been exploring include fluoresence and changes in this property as a function of exposure to various forms of radiation. A large variety of glass compositions will fluoresce when exposed to various forms of radiation. One particular application of interest is the detection of ultraviolet radiation which strikes the Earth. Such a sensor would permit real-time measurement of UV radiation as a function of other variables such as atmospheric ozone concentration, thus confirming current atmospheric theories. A series of twelve Pb-Al phosphates which fluoresce when exposed to UV radiation were melted and provided to Dr. Ambler Thompson of the Radiation Physics Division of the Center for Radiation Research. These

materials will be exposed and their fluorescence measured over time to determine their fluorescence half-life and chemical stability. Another application relies on fluoresence shifts to detect and discriminate between gamma radiation and neutrons. This project is being conducted in conjunction with Dr. William McLaughlin of the Center for Radiation Research's Ionizing Radiation Division. A set of nominally identical Eu glasses will be prepared, one containing normal Li, the other containing Li^{VI}. To date, four glasses have been prepared. Two of these glasses contain normal Li, the other two, Li^{VI}.

Another significant area of glass technology is that of optical devices and components. A number of applications for ultraviolet lasers exist, provided components which transmit and process the appropriate UV wavelength can be made. One particular example requires the development of an optical isolator for use at 308 nm. A green praesodymium glass containing 5 mole % Pr appears to transmit UV light in the appropriate wavelength region. The most suitable composition appears to be a phosphate-based matrix containing Pr. Two such compositions have been prepared, one using P_2O_5, the other using $Na(PO_3)_3$, and supplied to the U. S. Naval Research Laboratory for incorporation into their ring dye laser. The quality of the glasses differs depending on the starting materials with the $Na(PO_3)_3$ yielding a higher quality glass. Based on this work, a patent disclosure has been filed for this material. In other laser systems, europium-based glasses have been identified as potential optical components. Changes in the optical properties as a function of Eu concentration and host glass composition have been observed in our previous work in this area. The host glass in this prior work was a silicate-based material. Four glasses have been melted containing 5 mole % Eu_2O_3 and 15 mole % of either MgO, SrO, BaO, or CaO. These will be used to determine the effects of glass modifier ions on the optical properties of the glass.

In yet another application, there are presently no completely acceptable materials available for use as a neutron stop in a beamline. Those that are available are either powders which are difficult to handle or solids such as LiF which are subject to environmental attack. A durable glassy material containing Li^{VI} would provide improved properties over currently available materials. This project is being conducted in conjunction with Dr. Craig Stone of the Center for Radiation Research, Radiation Source and Instrumentation Division. The approach being taken is to develop appropriate, chemically durable glass compositions containing Li^{VI}, which will be exposed to a neutron source to determine their ability to stop neutrons. Initial compositions have been fabricated and supplied to Dr. Stone. The glasses are being taken to a neutron source at MIT for study of their properties.

The ability to control the chemistry and crystallization behavior of many glasses has led to the creation of the class of materials known as glass-ceramics. One interesting area where these materials are finding new applications is in dental technology. The problem of providing improved dental materials which have improved structural properties while maintaining tooth appearance is one which has beset the dental materials community for a number of years. Previous research in this area has identified a family of glass-ceramics which might be applied to other structural materials and provide the appropriated visual characteristics. Three

appropriate glasses which can be heat treated to form glass-ceramics have
been melted and provided to the American Dental Association's Health
Foundation. (This effort is conducted at NIST.)   Promising compositions
will be modified as needed to maintain appearance.

A number of analytical instruments require the use of standard glass disks,
spheres, and particulates.   Using conventional glass melting techniques and
a unique apparatus for making spheres, we provide a number of glasses in a
variety of shapes for use in instrument calibration.   The glasses are
provided to the Gas and Particulate Science Division of the NIST Center for
Analytical Chemistry (CAC).   During this year, we have provided six glasses
in various forms to the CAC for development of new microanalytical
standards.   This particular effort has resulted in the issuance of 13 glass
standards in the past 11 years.   These kinds of standards can be used to
characterize a variety of air pollutants.   In one particular case, five
sets of glass microspheres having known and differing concentrations of Fe,
Al, Ca, Ti, Mg, K, and Si have been provided to Professor Mark Scotto of
the University of Arizona.

The primary objective of the Tribology Group is the development of the science and technology base to provide scientific understanding, critical data, and design guidelines for new and improved tribomaterials. This information is needed for mechanical systems requiring high performance, durability, and cost effective designs. The output from the tribology program will allow wider usage of engineered ceramics, coatings, self-lubricating composites and advanced liquid lubricants, as well as realistic models for prediction of performance and reliable data and information for design and selection of new materials for advanced applications. The tribology program is divided into five thrust areas: 1) ceramic tribomaterials, 2) tribological films, 3) self-lubricating composites, 4) advanced liquid lubricants, and 5) computerized databases. The primary focus in our research is on the characterization of the tribological interface including analysis of chemical reactions and formation of tribochemical films, physical and mechanical behavior of surface films, and the microstructural aspects of deformation and fracture process leading to wear and failure.

Fracture Mechanics Model for Wear Transitions in Ceramics

S. Jahanmir, X. Dong and S. M. Hsu

Our investigation deals with deformation and fracture which precedes the process of wear particle generation. The first step in the process of wear particle generation in the absence of pre-existing microcracks is the nucleation or initiation of microcracks. Microcracks can be nucleated by several mechanisms, such as dislocation pile-ups, twin intersections and strain incompatibility. In an elastically deforming region localized microplastic deformation may lead to microcrack nucleation by one of the listed nucleation processes.

In order to analyze the conditions for initiation of plastic flow and subsequent microfracture in the absence of pre-existing flaws, the von Mises flow rule was used with the state of stress under a sliding contact. The results of this analysis for the case of 6.35 mm diameter alumina ball sliding on a smooth alumina surface at different temperatures indicated a strong influence of temperature and the coefficient of friction on the initiation of yield in alumina. As either the temperature or the coefficient of friction is increased, a lower value of applied load is needed to initiate plastic flow and subsequent failure by microcrack nucleation at grain boundaries.

Pre-existing flaws, such as microcracks at the grain boundary triple-points in ceramics, may preempt the requirements for microcrack nucleation process. Propagation or extension of pre-existing flaws by the tensile component of stress was analyzed using linear elastic fracture mechanics. This analysis applies to a homogeneous, isotropic and linear elastic semi-infinite plane subjected to a combination of normal and tangential surface forces. Experimentally determined values of critical stress intensity factors were used in the calculations to predict fracture initiation at different temperatures. The results of the analysis clearly showed that

the critical failure load for the extension of pre-existing flaws depends strongly on the coefficient of friction. The temperature dependence is very slight, due to the mild influence of temperature on fracture toughness of alumina.

Wear tests were conducted in a reciprocating ball-on-flat high temperature tribometer to evaluate the theoretical failure predictions. The specimens for the wear tests consisted of 6.35 mm diameter balls made from 99.5% purity α-alumina and 19 mm diameter disks with a thickness of 3 mm made from 99.8% α-alumina. The alumina balls were used in the as-received condition with a highly polished surface of 0.01 μm RMS. The disks were polished with a 1 μm diamond paste to a final surface roughness of 0.1 μm.

The wear results indicated that a transition occurs in wear from a value of wear coefficient $K \approx 10^{-6}$ to a much larger value of $K > 10^{-4}$ as the load is increased above a critical threshold value. The data also suggest that the coefficient of friction increases from 0.5 to 0.8 or higher, as the wear transition occurs.

The wear data and the operating conditions for this series of experiments are summarized in Figure 18. The open data points designate test conditions where $K << 10^{-4}$, whereas the solid data points correspond to $K > 10^{-4}$. In order to clearly identify the repeat tests, some of the data points were slightly shifted on the figure. The theoretical curves for the initiation of failure by plastic flow and by crack extension in the tensile zone corresponding to a friction coefficient of 0.55 are also plotted in Figure 18. Comparison of the theoretical curves with the boundary between the filled data points and the open points indicates that microfracture in the tensile zone, not plastic flow, is the dominating process for the observed transition for low to high wear. It is clear that at loads lower than the predicted loads for microfracture, the wear coefficients are very low. However, at loads larger than the predicted values, large wear coefficients are always observed. The repeat tests near the transition point sometimes produces high wear and other times low wear. This can be expected due to the instabilities near the transition point.

The wear tracks for all the tests exhibiting low wear showed no evidence of fracture. However, the wear tracks corresponding to the condition of high wear, after two hours of testing, showed extensive damage in the form of microcracks and debris accumulation. Some evidence for grain boundary fracture were also observed.

The theoretical prediction of severe wear by microfracture in the tensile zone agrees with the experimental results for test conditions above room temperature. The tests at room temperature, in Figure 18, did not result in a large wear coefficient predicted by the model. Since the friction coefficient for these tests correspond to 0.4, the theoretical microfracture load must be recalculated with this value of friction coefficient. This calculation resulted in a failure load of 39.2 N. Above this load, numerous microcracks were observed on the worn surface; but, these cracks appeared to be stable. Even after 24 hours of testing the wear coefficient was approximately 10^{-6}.

52

Examination of specimens tested at room temperature showed an interesting feature which was absent from the other specimens tested at higher temperatures. Typical examples are shown in Figure 19. These cylindrical debris, which were observed only on the wear track, are approximately 0.2 μm in diameter, and range from 1 to 5 μm in length. It is hypothesized that the reaction of water vapor with the alumina surface may produce thin hydroxide films, which are then rolled by the sliding and reciprocating action at the contact producing the observed cylindrical debris.

To confirm the presence of aluminum hydroxide on the wear track, μ-FTIR was used. The results of this analysis conducted on three different positions are shown in Figure 20. All three spectra show a strong peak at 1035 cm^{-1} which corresponds to α-alumina. It should be recognized that this spectral feature is not directly due to a vibrational mode energy absorbtion, but rather represents an IR reflectivity phenomena of α-alumina related to its frequency dependent dielectric constant. Comparison of the three spectra obtained outside the wear track (A) on the wear track (B), and on the wear debris accumulated at one end of the wear track (C), indicates the presence of -OH region around 3600 cm^{-1}. This information confirms the presence of hydroxide on the surface of the alumina specimen, especially in the debris accumulated at the end of the wear tracks. These hydroxides have a layered structure with relatively weak bonding between the layers, and are much softer than the alumina substrate. Formation of such tribochemical films on the alumina surface may explain the low coefficient of friction of alumina at room temperature. The same film, which has different elastic properties than the substrate, can modify the magnitude of the contact stresses and result in a deviation between the theoretical predictions and the experimental results.

The proposed model and supporting experimental evidence clearly confirm that a simple linear elastic fracture mechanics analysis can be used to predict the onset of catastrophic wear in alumina, and perhaps in other ceramics. The proposed model and the experimental results offer several important conclusions that are worthy of discussion. It is confirmed that crack propagation in the tensile zone controls the transition from "mild" to "severe" wear. In this respect, reduction of contact stress or reduction of the coefficient of friction can prevent the wear transition. Furthermore, surface films generated by tribochemical reactions or intentionally deposited on the surface may prevent the wear transition if their mechanical properties are different than the substrate. Several investigations have in fact shown that surface films alter the state of stress both in the film and in the substrate. This conclusion is quite important since different investigators have shown the possibility of the formation of tribochemical films on ceramic surfaces. Therefore, by controlling the sliding environment, one may be able to control the wear transition through tribochemical film formation.
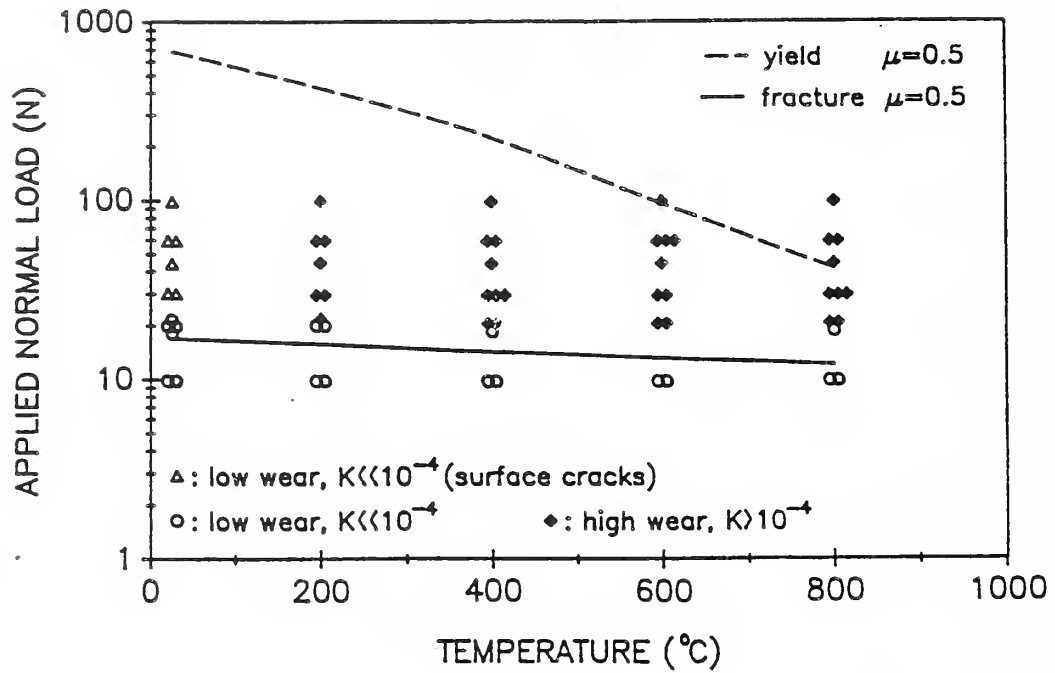
Figure 18:   Comparison between test results and theoretical
               prediction for failure by plastic yielding and
               microfracture.
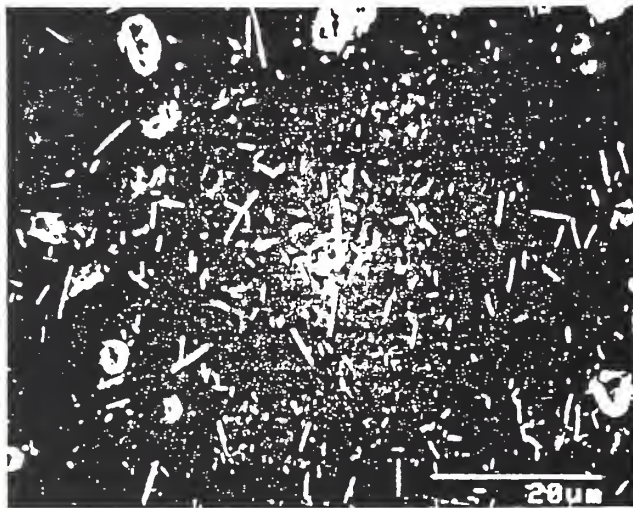
(a)   (b)

Figure 19:   SEM micrographs showing typical wear debris on the
               wear track for tests conducted at room temperture. (b)
               is a higher magnification of (a).
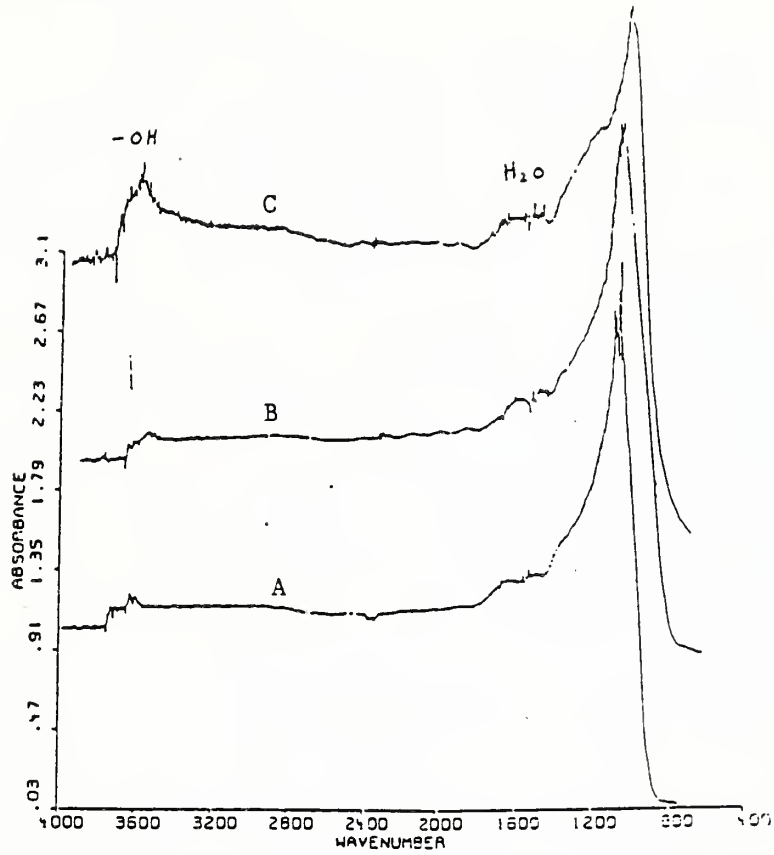
Figure 20: FTIR spectra on the alumina surface, A - unworn region,
B - on the wear tract and C - piled-up debris at the
end of the wear track.

Wear Mechanisms of Ceramic Materials

S. M. Hsu, R. G. Munro, S. W. Lee[1] and Y. W. Wang[2]

[1] Guest Scientist, University of Illinois at Chicago
[2] Guest Scientist, University of Tsinghua

The present effort in the study of wear mechanisms in ceramics examines the basis for the development of a laboratory test methodology that could be used in the screening of materials prior to engine testing. Central to this objective is a means of characterizing the wear properties of a material in such a manner that the limitations of the material are readily determined. Towards that end, the concept of quantitative wear maps for ceramic materials is being developed.

A single wear map is a graphical display of the wear of a material under systematically prescribed conditions, shown as a function of simultaneous control variables such as sliding speed and contact load. Figure 21a shows an example of the wear of alumina. This map has three identifiable regions: low wear; transition to high wear; and high wear. The wear maps methodology is a concept that uses a comprehensive set of such wear maps for the analysis of wear.

The wear maps methodology, therefore, examines a material under a full spectrum of tribological conditions. The emphasis of this approach is firstly on determining what material characteristics limit or control the boundaries between critical and noncritical operating regions. This materials aspect of the wear map approach provides essential information both for materials screening and for materials design. Secondly, the method examines how the system and environmental variables may be used to enhance the useful operating regions. Figure 21b shows how the wear map of Figure 21a is transformed when a paraffin oil is added to the wear test. Notice especially how the influence of the speed variable has been reduced causing the low wear region to be greatly expanded.

In general, the wear of a material depends on the details of the system in which that material is used. The extent of wear of a particular component may depend on the operating conditions (speed, load and temperature), machine characteristics (contact geometry, alignment, motion, and vibration), environment (lubricants, gaseous atmosphere, oxidation, and surface reactions), and materials properties (composition, mechanical and thermal properties defects, surface roughness, and surface contaminants). Consequently, a comprehensive set of wear maps must investigate the relations among speed, load, temperature, time, and environment.

When such a set of wear maps has been constructed, it is then possible to deduce the dominant mechanisms that influence the limits of the distinct wear regions and transition zones. For a mechanistic analysis, the quantitative wear data are supplemented by SEM and TEM microstructural observations. The result of such an analysis is a wear mechanism map. Figure 22 shows a mechanism map for alumina tested using water as a lubricant. In the mildest wear regime, wear appears to result from plastic deformation. As the degree of wear severity increases, the wear process

evolves from plastic deformation to grain pullout, then to pullout and intragranular fracture, and finally to large scale intergranular fracture.

Such analyses of materials conducted systematically within the context of the wear maps methodology will enhance the ability of designers to select the materials most appropriate to their operating conditions or to focus their attention on the specific mechanisms that need to be controlled to increase the lifetimes of their components.

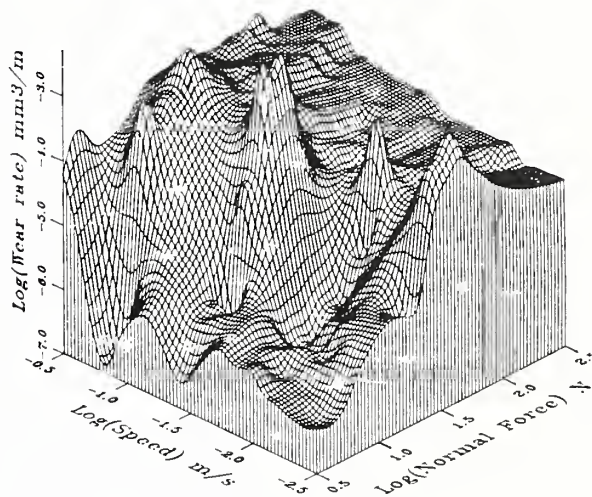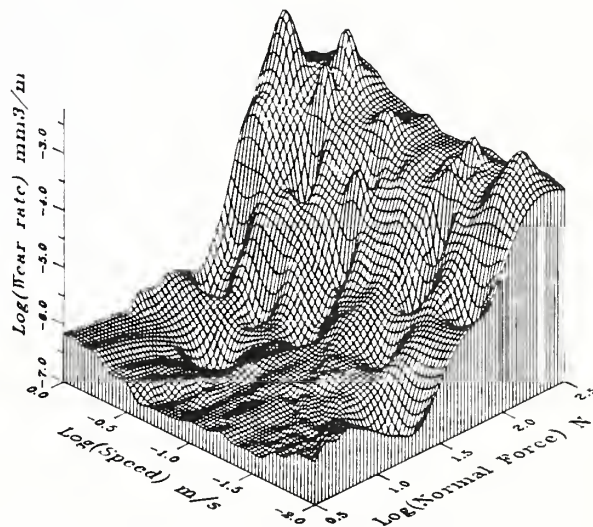Figure 21a. Wear map of alumina under dry conditions

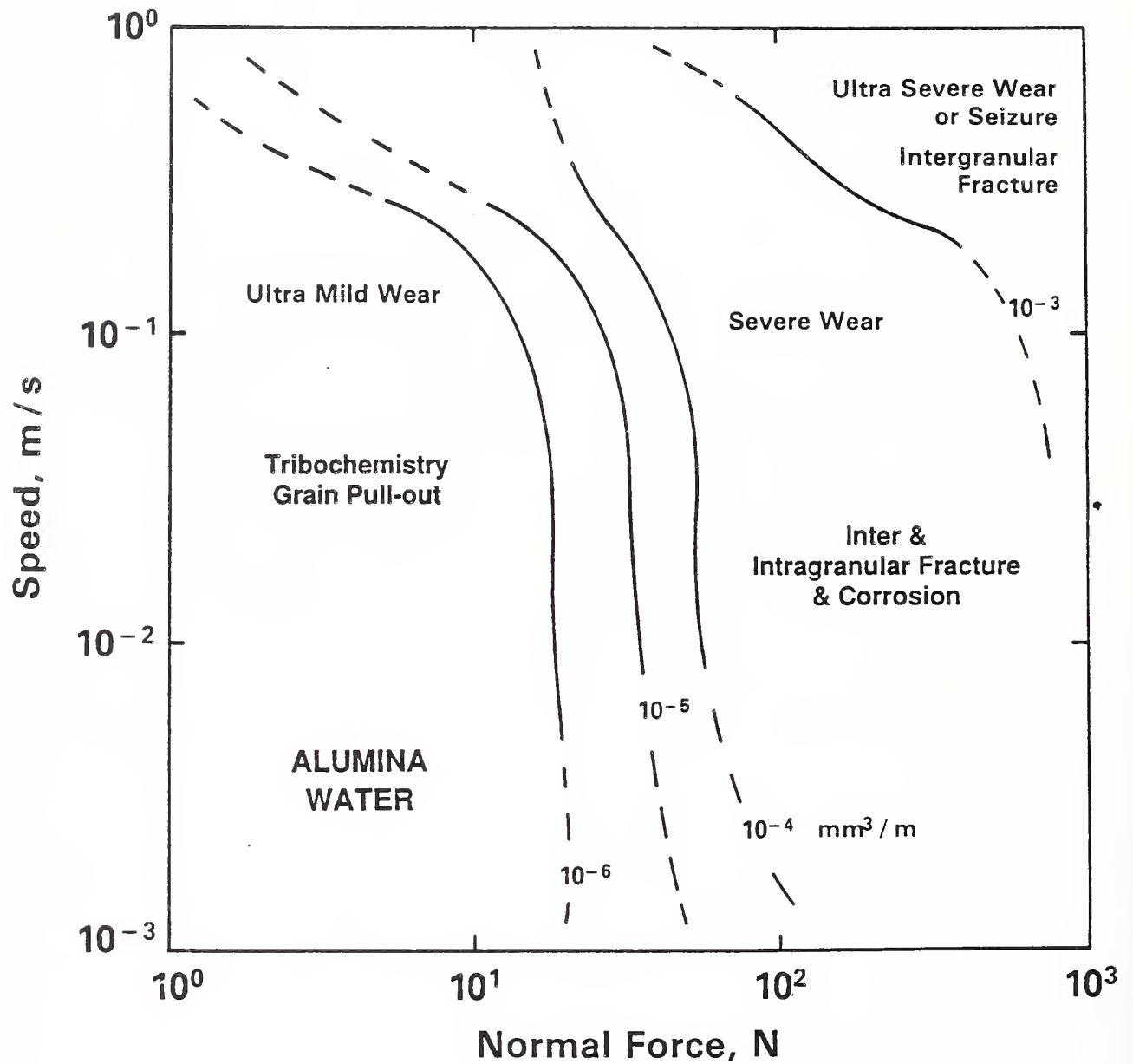Figure 21b. Wear map of alumina under paraffin oil

Figure 22. Mechanism map of alumina lubricated with water

Tribological Coatings and Films

A. W. Ruff, M. B. Peterson, L. K. Ives, E. P. Whitenton, T. J. Strakna and
W. W. Duvall

The research in this project focuses on tribological characteristics of
composition-modulated alloy surface coatings, and on transition effects in
friction and wear of different tribological films. The experimental
approach involves both surface analysis and subsurface microstructural
characterization; this provides data to aid in modeling the observed wear
and friction phenomena. The results should provide the needed
understanding for future development of wear-resistant materials, coatings,
and surface treatments for practical applications. Such developments can
have a significant impact, since in many applications it is not possible to
use lubricants and thus the materials themselves must have suitable wear
and friction properties.

Research on tribological characteristics of composition-modulated alloy
(CMA) coatings has continued. The coatings, made at NIST, were prepared as
alternate layers of nickel and copper, deposited on steel, at layer
spacings down to 1.5 nm. The total coating thickness was typically 25 μm.
Sliding wear studies were completed under both unlubricated and lubricated
conditions against 52100 bearing steel counterfaces using a crossed-
cylinder geometry. It was found that the CMA Ni-Cu coatings had
significantly more wear resistance than the pure copper and nickel
coatings. Figure 23 shows wear rate results for two CMA coatings in
comparison with pure Ni and pure Cu deposited in the same manner. The
coatings were slid against 52100 steel surfaces in air at the indicated
loads for distances up to 10 m. It is seen that wear of the Ni and the Cu
coatings at all loads exceeds that for the CMA materials. Further, for
loads less than 17.6 N, the CMA coatings have a wear rate less than 1/5
that of the pure Ni. The smallest layer thickness alloy (10 nm) shows the
greatest wear resistance of the four materials. An analytical model of
dislocation behavior in a layer microstructure during the plastic
deformation associated with wear has been developed to explain these
results. The model allows for three effects associated with these unique
microstructures: 1) layer spacing effects (smaller spacings give greater
wear resistance); 2) dislocation line energy difference effects, associated
with composition; and 3) layer interface thickness and structure difference
effects. The model is currently being tested by measurements on the
smallest layer (1.5 nm) spacing alloys.

During the past year this project also has studied thin oxide film solid
lubrication mechanisms near a severe wear transition boundary. It is well
known that the friction and wear characteristics of solid bodies in sliding
contact are determined by the properties of a thin layer on the surfaces.
During sliding, instantaneous contact is usually at only a few asperities
of relatively small total area compared to the apparent area of contact.
Since the majority of the load is supported by these asperities, the
stresses and temperatures, except at extremely low sliding speeds and
loads, are very high. Thus, the surface material is subject to plastic
deformation, fracture, mechanically and thermally induced phase
transformations, chemical reaction with the surrounding media, and
mechanical mixing of the material in the contact. Although the presence of

this tribolayer or film is widely recognized, its properties have been studied in only a few cases.

In the initial phase of this project an extensive search of the literature (1900 - 1989) was conducted to determine the role of oxides in controlling the friction and wear properties of metallic alloys. Two approaches were selected: (1) adding elements to alloys (e.g., Mo, B, W, Re, V) which would result in the formation of lubricating oxides and (2) adding elements which would assist in forming dense, compact and adherent oxide films. In the experimental phase of the program high temperature alloys have been slid against silicon nitride at elevated temperatures to generate films for evaluation in terms of composition, structure, morphology, and mechanical properties. Figure 24 shows the topography of the film developed on a silicon nitride surface after sliding against M50 steel at 600°C in air. The topography was determined by means of stylus profilometry. The film is primarily oxide with some metal. Characteristically, the film is not continuous and consists of patches and regions of varying height. Film topography appears to correlate with the observed coefficient of friction and wear rate. The film topography itself depends strongly on the alloy composition.
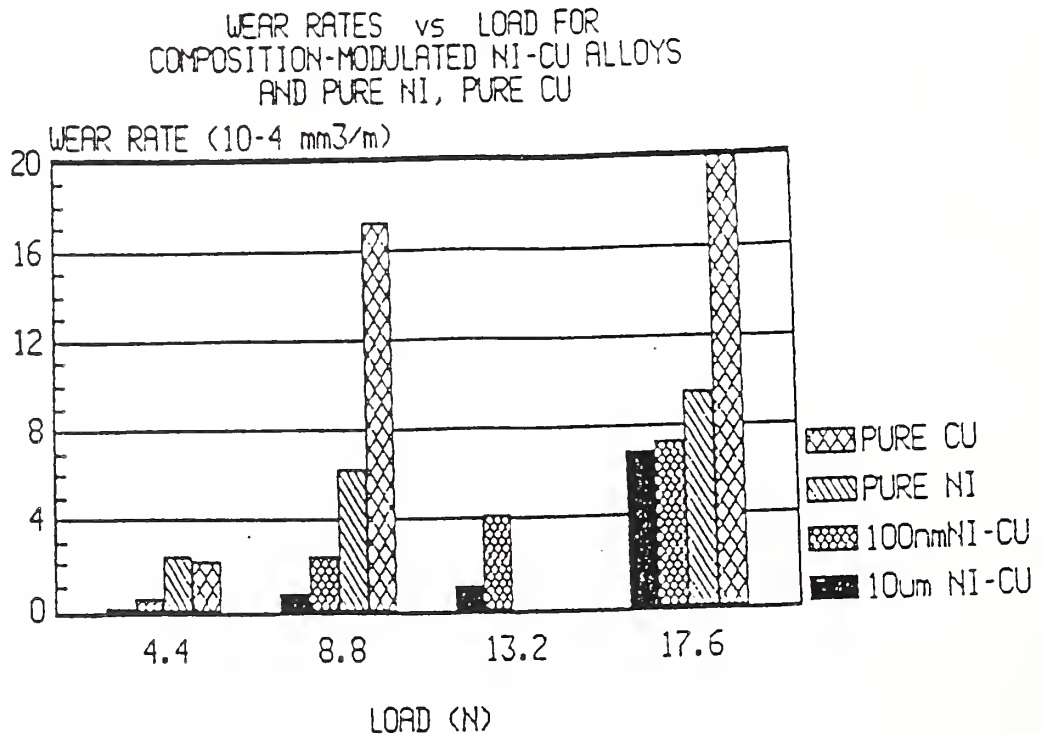

Figure 23:   Wear results for two composition-modulated alloys in comparison with pure materials, showing load dependences.
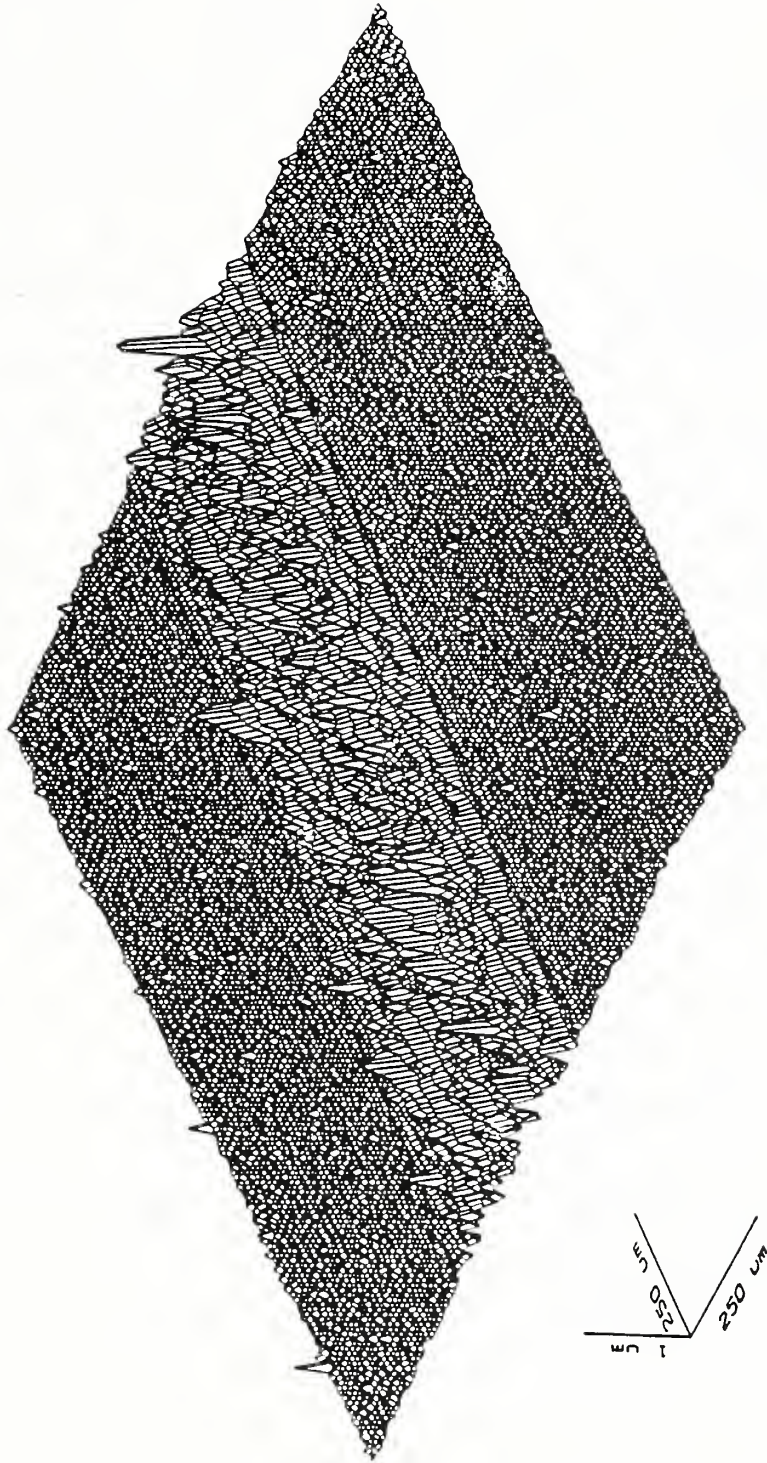
Figure 24: Topography of film, measured by stylus profilometry, generated by sliding a silicon nitride against M50 steel at 600° in air.

Mechanisms of Abrasive Wear in Lubricated Contacts

L. K. Ives and E. P. Whitenton

Wear by extraneous abrasive particles is an important and often the predominant mode of wear in sliding lubricated contacts. The purpose of this project is to study the mechanisms which are responsible for this form of wear. A number of different mechanisms can be postulated. These involve direct abrasion of the surfaces and removal of surface films by hard particles as well as the interaction between abrasive, adhesive and lubricated wear processes.

The Department of Energy is supporting the development of diesel engines capable of operating directly on pulverized coal, primarily as a 50% water slurry. Efficient combustion has been demonstrated with this fuel; however, operating engines have experienced an extremely high rate of wear. One critical area of wear is at the piston/ring cylinder wall contact. The high wear rate is directly associated with the presence coal-fuel and combustion particles which enter the contact during sliding. Mineral matter in the coal rather than the coal itself is generally thought to be the main agent responsible for wear.

In the first stage of this project, samples of coal-fuel and diesel exhaust particulates have been characterized with respect to shape, size, and composition.

Laboratory wear tests have been conducted to investigate the wear characteristics of the coal-fuel and exhaust particulates, as well as to study the operative wear mechanisms under controlled conditions. The wear test device used employed a pin-on-disk configuration. The pins were of 52100 steel (62 HRC) and the disks of 0-2 tool steel (62 HRC). A highly refined paraffinic mineral oil was used as the lubricant. Wear test results are shown in Figure 25. It is seen that the unburned coal-fuel particles resulted in only a small increase in wear rate compared to tests without particles. Exhaust particulates, however, resulted in a five fold increase in wear rate.

Wear by exhaust particulates was also compared to wear by quartz, aluminum oxide, and magnesium oxide particles. As an example, Figure 26 shows results obtained with 5 wt% of these particles in mineral oil. Results for three different sizes of quartz particles are shown. Wear rate is seen to increase rapidly with increasing particle size. A strong dependence on particle hardness is also demonstrated. Aluminum oxide (2000 kg/mm^2) is substantially harder than the steel specimens (850 kg/mm^2) and causes a very high rate of wear. Quartz (1000 kg/mm^2) is somewhat harder, while magnesium oxide has about the same hardness. The lower wear rates with quartz and magnesium oxide are consistent with their lower hardness. The exhaust particulates are expected to have about the same hardness as quartz; however, they produced the smallest wear rate among the particles studied. This may be explained by the fact that a significant portion of the exhaust particles consisted of relatively soft coal, which is shown in Figure 25 to cause only a small increase in wear rate. Other factors, such as the spherical shape of many of the exhaust particles may contribute to their lower abrasivity.

Examination of worn surfaces and other studies in this project to investigate the effect of particle concentration, applied load, and specimen surface roughness indicate that the wear mechanism can range from a condition in which direct abrasion is predominant to one in which abrasion plays only an indirect role.
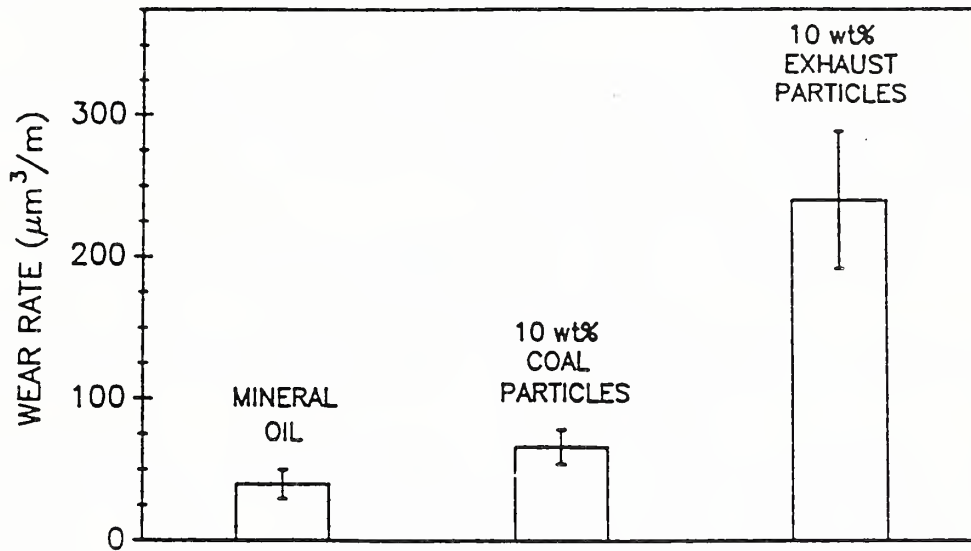

Figure 25:   Effect of particle additions to mineral oil on wear of 52100 steel in pin-on-disk wear tests.
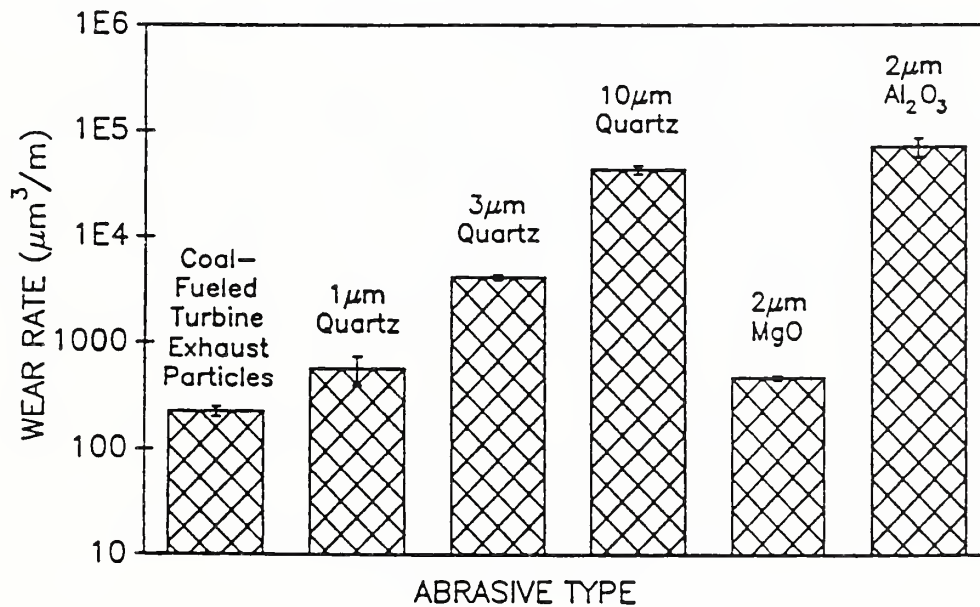

Figure 26. Pin-on-disk wear test results comparing effect of different types of particles at a concentration of 5 wt % in mineral oil.

Self-Lubricating Ceramic-Matrix Composites

S. Jahanmir, M. B. Peterson and A. Gangopadhyay[1]

[1]Research Associate, University of Maryland

Friction and wear behavior of several advanced structural ceramic materials have been studied in detail for the past few years. It has been observed that the friction coefficient of ceramics is generally high (0.5 -0.8) under unlubricated sliding conditions and thus limits their use as tribological components. However with liquid lubrication, the friction coefficient of ceramics can be reduced typically to 0.1 which is acceptable for many applications. Therefore, durable solid lubrication appears to be the key to meet these operational needs.

The aim of this research was to explore whether the high friction coefficient of ceramic materials can be reduced by incorporation of solid lubricants in a ceramic matrix. The ceramic materials chosen for this investigation were alumina and silicon nitride using graphite intercalated with $NiCl_2$ as the solid lubricant.

The wear tests were conducted using a pin-on-ring test configuration. The pin holder was modified to accommodate two pins. In the ceramic-steel tests, two ceramic pins of either alumina or silicon nitride were used. In the solid lubricated test, one of the ceramic pins was replaced with intercalated graphite. In order to obtain a reference value for the friction coefficient, one set of tests were conducted with two intercalated graphite pins in contact with the steel ring.

The friction coefficient of alumina sliding against steel was found to be 0.48; but, when one of the pins was replaced by an intercalated graphite pin, the friction coefficient was reduced to 0.20. The friction coefficient of silicon nitride sliding on steel was 0.45, and by the replacement of one silicon nitride pin by one intercalated graphite pin, the friction coefficient was reduced to 0.17. The friction coefficient of intercalated graphite sliding against steel was 0.14, which is somewhat lower than that of the solid lubricated ceramic-steel contact.

The specimen surfaces were analyzed to elucidate the mechanisms responsible for reduction in friction. The combination of Raman and FTIR spectroscopies confirmed that the films on the steel surface were discontinuous and consisted of both Fe_2O_3 and silicates. The transfer film formed at the interface between silicon nitride, intercalated graphite, and steel consists of a mixture of very fine particles of graphite (roughly 40 40 Å) silicates and Fe_2O_3. The formation of this transfer film on the mating surfaces is responsible for the observed low friction coefficient. The analysis of worn surfaces of steel ring and alumina pins confirmed that sliding of alumina and intercalated graphite against steel also results in the formation of a discontinuous transfer film of graphite and nonoxide on both the steel ring and the alumina pin.

The experimental results and analysis of the transfer films have confirmed that solid lubrication provides a viable way to improve the tribological performance of ceramics. It is necessary, however, to find ways to

incorporate the solid lubricant phase in the ceramic matrix and develop self-lubricating ceramic-matrix composites.

Self-Lubricating Metal-Matrix Composites

A. W. Ruff, M. B. Peterson and E. P. Whitenton

Composite materials consisting of copper metal-matrices with a solid lubricant phase of intercalated ($NiCl_2$) graphite (IG) have been prepared and studied in sliding wear against type 440C stainless steel at normal temperatures in air. Sliding wear tests were carried out using a pin-on-ring tribological test system. The interfacial film formed during sliding wear was found on both the composite pin and on the steel ring. The interfacial film is comprised of system wear products, namely, IG, copper, and steel (probably Fe, Cr, Ni oxides).

In summary, intercalated ($NiCl_2$) graphite in copper provides a lubricating, wear-reducing film when worn against 440C steel. Friction coefficients can be as low as 0.15 in air. Volume wear rate decreased by a factor of 5x with a full IG film present in the contact, and by a factor of 4x with a composite specimen containing 12 vol. % IG in copper. Increasing IG content above 15 vol. % leads to increasing wear due to loss of composite strength. Composite worn surface morphology shows three significant mechanisms: (1) lubricating interfacial film formation at the exit region of the soft phase; (2) recession from the average surface at the soft phase locations; and (3) collection of wear debris in the recess at the entrance region, thus removing some of the wear debris but blocking part of the soft phase area.

Tribological Characteristics of Synthesized Diamond Films

S. Jahanmir, L. K. Ives, D. E. Deckman, E. N. Farabaugh and A. Feldman

The present study has focussed on determining the tribological characteristics of the system silicon carbide sliding against diamond coated silicon carbide in air. The coefficient of friction was measured during the experiments, and the wear rates of both diamond and silicon carbide were determined. Laser Raman spectroscopy, scanning electron microscopy, and energy dispersive x-ray analysis were used to analyze the wear processes.

Diamond films were deposited on silicon carbide disks by means of the hot filament chemical vapor deposition (CVD) method. The different coating thicknesses of 2-6 μm and 4.3 μm were used to evaluate the possible effect of film thickness on wear. In the absence of a diamond film, the friction coefficient rises initially as the load is increased; at the higher loads, it stabilizes at a value of 0.70 ± 0.10. The diamond film resulted in reduction in friction coefficient by almost one order of magnitude to a value of 0.08 ± 0.02.

A comparison was made between the wear rates of the disk in the SiC/SiC and SiC/diamond film tests. Wear reduction by four orders of magnitude is observed for the tests on diamond film.

Wear debris generated during sliding was analyzed. For both SiC vs. SiC and for SiC vs. diamond film, analysis indicated a high concentration of Si and O with a small amount of C, Al and W. (Al and W are sintering aides in the SiC ball.) This suggests that wear of SiC involves tribochemical reaction with the air environment to produce SiO_x.

The low coefficient of friction obtained with the diamond film may be attributed to the presence of a relatively soft silicon oxide layer in the contact.

Advanced Liquid Lubricants

J. M. Perez, C. S. Ku, B. E. Hegemann, P. Pei and S. M. Hsu

The development of advanced lubricants for future applications is critical to the advancement of technology involving the lubrication of advanced materials. Manufacturing processes and machining, magnetic recording devices, advanced aerospace engines, more efficient low heat rejection engines, transportation and power generation are a few examples of technologies with critical lubricant needs. High temperature lubrication efforts consist of the following: lubrication of ceramics using improved synthetic fluids, lubricant interaction with ceramics, high temperature additive chemistry and the mechanism of oxidation and deposit formation at high temperatures. The reaction mechanisms at high temperatures involves an understanding of the relationship between molecular structure and thermal oxidative stability. Understanding how changes occur at the interface under severe tribochemical conditions is the first step in controlling the process.

During the previous year, information on a number of synthetic fluids and their interactions with various materials were developed. New research on the chemistry of high temperature additives was initiated. The basic information on base stocks, lubricants and additives and the research on the relationship of chemical structures to thermal and oxidative stability of the materials has led to the selection of a novel combination of base fluids and additives for some of the new technology applications. One lubricant developed by the Tribology Group at NIST was evaluated against state-of-the-art lubricants using several laboratory test methods developed by NIST. Comparison of thermal stability and oxidation stability are found on Figure 27. A significant improvement was obtained.

A key to how effectively an additive will perform in a lubricant is the compatibility of the additive with other components in the fluid. To understand the effect of various constituents in petroleum base stocks on the performance of additives, two petroleum stocks were studied. A 300 neutral fraction and a 600 neutral fraction from two different sources were chromatographically fractionated into several fractions. The fraction containing polar constituents was further subdivided into seven subfractions, including three acidic, three basic and one neutral subfractions. The subfractions were chemically analyzed and their interaction with some commercial additives characterized. The additives are commercial antioxidants and include a phenol, an amine and a multipurpose dithiophosphate. The phenolic additive is in itself slightly acidic and would not be expected to interact significantly with the

subfractions, except possibly the basic constituents. The phenol was the least active of the three additives and the least effective of the three. The amine was antagonistic with the acidic fractions and only the zinc dithiophosphate showed synergistic effects with all fractions.

The catalytic effect of steel was evaluated. The phenyl-α-napthylamine (PAN) was most dramatic in that it reduced the oxidation induction period from about 40 to 20 minutes. This is probably due to a strong interaction of the amine with the steel surface. When the polar constituents are added, the effectiveness of the amine is further reduced by reaction of the constituents in the fractions with the remaining amine groups. Chemically, the amines are basic compounds and can donate electrons to substances deficient in electrons. Therefore, PAN would readily interact with compounds in the acidic fractions reducing PAN's function as an antioxidant. With the basic fractions, the polar constituents become more antagonistic to the PAN at concentration levels of 3 wt % or higher. This may be due to solubilizing of some of the metal.

Zinc dialkyl dithiophosphate (ZDDP) is synergistic to all polar subfractions, bases and neutral compounds except the weak acids in fraction PCN-3. The presence of steel reduced the pressurized differential scanning calorimeter (PDSC) induction time to ZDDP from 22 to 10 minutes. The effect of the subfractions, as shown in Figure 28, is truly synergistic in that the induction time with most of the subfractions at higher concentrations actually exceeds the 22 minutes. This indicates the additive not only offset the effect of the metal surface but also increased the antioxidant effectiveness of the ZDDP.

Research to establish an understanding of the tribochemistry occurring at the surface using laser-Raman and Fourier transform infrared (FTIR) analyses continued as part of the effort to establish an understanding of additive and substrate interaction. Fluorescence of the lubricant as it is being oxidized continues to limit the use of laser-Raman in this area, but the method was shown to have application in the study of non-lubricated surfaces. Use of diffuse reflectance infrared (DRIFT) and micro-FTIR techniques were valuable in identifying and detailing the chemistry of substrate-lubricant interaction products. The DRIFT technique was used to obtain reference spectra of model compounds such as might be found on the surface as a reaction product, and work is now in progress to look at thin films of compounds adsorbed on metals.

THERMAL STABILITY

OXIDATION AT 220°C
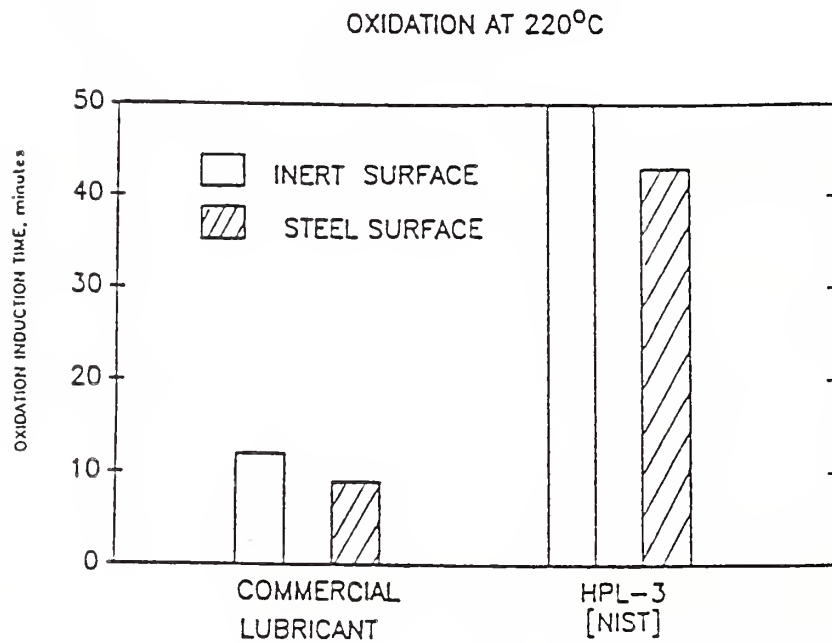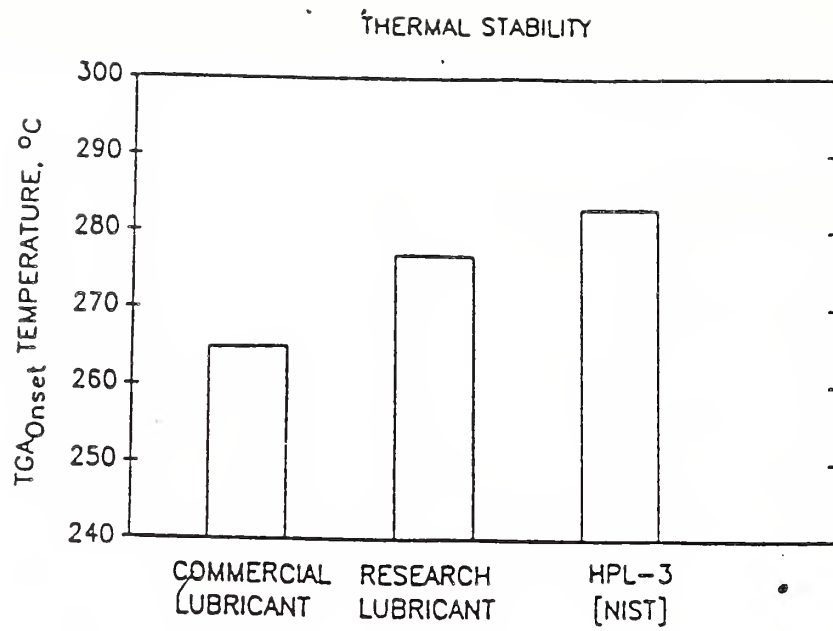

Figure 27:   Future lubricants research using thermogravimetric analysis
              (TGA) and differential scanning calorimet (DSC). TGA onset
              in upper figure is the TGA temperature at which
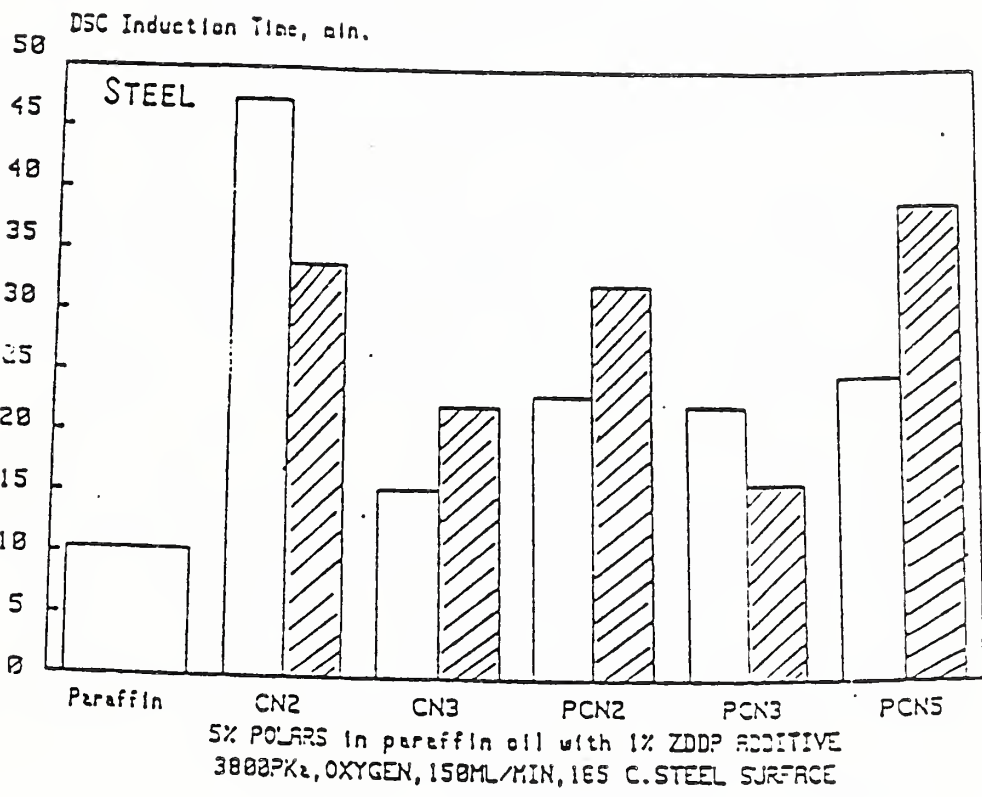   significant material loss begins.

Figure 28: Additive susceptibility with polar base stock fractions.

Nano-Indentation and Scratch Testing

A. W. Ruff and E. P. Whitenton

A nano-indentation and scratch testing apparatus is being planned and constructed. This tester will in principle permit measurements of material properties such as microhardness, elastic modulus, yield strength, ductility, toughness, friction coefficient, plowing resistance, and others, including rate effects of these properties. Microscopic examination of the indentations and scratches will provide further information. This method can be used with homogeneous bulk materials, but should be most advantageous in studying inhomogeneous materials, thin films, coatings, and materials having had surface treatments. It may offer previously unavailable information on coating micromechanical properties, coating wear and friction properties, and coating/substrate adhesion.

The new instrument will operate over the same range of load and speed as described above. In addition, it will be able to translate the specimens under load to produce scratches. The load waveform can be held constant during the translation, or it can be varied in a preset pattern. The scratching resistance force will be measured by a transducer. All control and data analysis will be carried out by a dedicated lab computer, using software developed within the project. One of the first applications of the system will be to characterize tribological films on sliding contact surfaces.

Standards and Cooperative Measurement Activities

A. W. Ruff and S. Jahanmir

An interlaboratory measurement comparison has been carried out among 16 U.S. tribology laboratories as part of a larger effort involving six countries within the VAMAS (Versailles Advanced Materials and Standards) Wear Test Method Activity. The Tribology Group at NIST acted as the U.S. coordinating laboratory. This interlaboratory measurement round was actually the second such effort; the summary of the results of the first effort has been published previously. The second round was designed to examine additional material pairs and also to investigate some different test conditions: a lower test load and the use of a lubricant in the sliding contact region. The results of these two interlaboratory studies are being used in the process of developing a U.S. standard for pin-on-disk wear tests through the ASTM Committee G-2 on Wear and Erosion.

The first round of interlaboratory tests involved one "advanced material", aluminum oxide, and one traditional material, AISI type 52100 bearing steel. The materials were provided to each laboratory in the form of disks and balls. Both friction and wear were measured. Reproducibility of friction and wear values was judged to be good in terms of usual tribological data.

The second round, recently completed, involved a new material and a range of desired humidity levels during the test. The new test material was hot pressed silicon nitride (85% Si_3N_4, 8% Y_2O_3, 5% Al_2O_3; HV 1500 - 1800). A humidity range of 50 ± 10% (relative) was specified for the test

environment. The other test parameters were unchanged. A total of 16 U.S. laboratories agreed to participate in this round (the total world group was comprised of 38 laboratories). Five U.S. laboratories followed this standard test plan. The remainder of the U.S. group was to carry out two other types of tests involving low load (2 N) conditions and lubricated conditions (using a highly purified paraffin oil lubricant).

The principal standard condition findings were: variability in ball wear volume ranging from 11% for ceramic/ceramic to a large value of 50% for steel/steel and variability of average friction coefficient of about 15% for all combinations. Further, average ball wear volume was smallest for the mixed ceramic/ceramic couple and for steel/silicon nitride. The principal low load findings were: considerable variation in friction coefficient for all materials, ranging from about 33% to 50%. This was larger than found for the standard condition load of 10 N. The principal findings under lubricated conditions were: average friction values closely similar for all five material combinations, ranging from 0.09 to 0.12; variation in friction values among the laboratories, ranging from 10% to 50%; and ball wear volume lowest for the material combinations including a ceramic member, ranging from 4×10^{-5} to 8×10^{-4} mm^3.

In summary, the results of VAMAS Round 2 for the U.S. laboratories showed that the test and measurement methods used were well established and basically sound. It was agreed that standardization efforts through the ASTM should be pursued. Some problems were identified in connection with differences among the test systems used in Round 2; improved machine characterization is needed. Data variability would probably be reduced if the test systems were more identical.

Activities in ASTM Committee G-2 on Wear and Erosion continued in several areas. A draft standard for Wear Testing with a pin-on-disk apparatus was written at NIST. Data and information obtained in the process of carrying out the VAMAS activity was included. The draft standard has proceeded through the subcommittee level in the process of revision. It is currently undergoing a main committee ballot. When the document is completed, it will be the first U.S. standard covering this popular wear test system design. A commercial instrument is already being marketed based on details within the proposed new standard.

A Workshop was organized with NIST staff leadership on Computer Utilization in Tribology, and held at the December 1988 meeting of ASTM G-2. Ten presentations were made involving areas such as computer control of wear test systems, databases of tribology information, and expert systems for material selection. A summary of the Workshop has been published by G-2. In view of the growing importance of this area in tribology, a permanent subcommittee on Computerization in Wear and Erosion was formed at the last G-2 meeting to continue to address appropriate subjects. The subcommittee is chaired by an NIST staff member.

Numeric Database for Tribology

S. Jahanmir and A.W. Ruff

A computerized tribology information system, named "ACTIS", is presently under development at NIST. Support for this effort is also being provided by the Department of Energy, Department of Defense, National Science Foundation, American Society of Mechanical engineers, and Society of Tribologists and Lubrication Engineers.

The full ACTIS system is planned to consist of six components: Numeric, Design, Newsletter, Bibliographic, Research-in-Progress, and Product and Services Directory. The primary users were identified to be tribology researchers, applications engineers, and design engineers. ACTIS will be developed in stages. A personal computer (PC)-based system is being developed currently in Phase I. Self-contained PC disks containing evaluated numeric data, both materials data and tribology data, will be available in fall 1989; an expanded version that also includes four design codes will be available shortly afterward.

Based on information developed at the workshop, a set of 50 data fields was identified for use in a numeric database on friction and wear of materials and on material properties. Evaluated data have been assembled and loaded into that format using commercial database management software. The present ACTIS numeric database ("Tribomaterials I") contains about 370 records. The data are organized for direct application by the user in material selection, wear model calculations, tribological component design, and with other software codes such as stress and temperature calculations. Areas covered by the data are shown in Figure 29.

An important consideration has been the method by which the user would search the database. A database searching scheme has been developed that involves the user working with two selection screens. The two screens list a total of 34 fields that were judged to be of principal interest. Two forms of tabular output result from each searching process. The first is a screen labeled Summary Report that lists each record returned from the search, and each field that was marked on the two selection screens. This summary presents the user with a preliminary idea of materials and data available in the database that satisfy the stated interest. It is then possible to select any of those records using the PC spacebar and bring up on the screen a Complete Report of all 50 fields for that record. The user can toggle between the Summary Report and the Complete Report for any record in the process of deciding which record(s) satisfy his interest. The complete report for that record(s) can then be printed as hard copy. Graphical output, either screen or hard copy, is possible from the present ACTIS database by using commercial memory-resident software.

In summary, a computerized tribology information system is under development. A numeric database has been completed and will be marketed this fall. Future expansions including additional numeric data and sets of design codes will be prepared later.

```
                    ┌─────────────────┐
                    │     Numeric     │
                    │   Data Base     │
                    └─────────────────┘
```

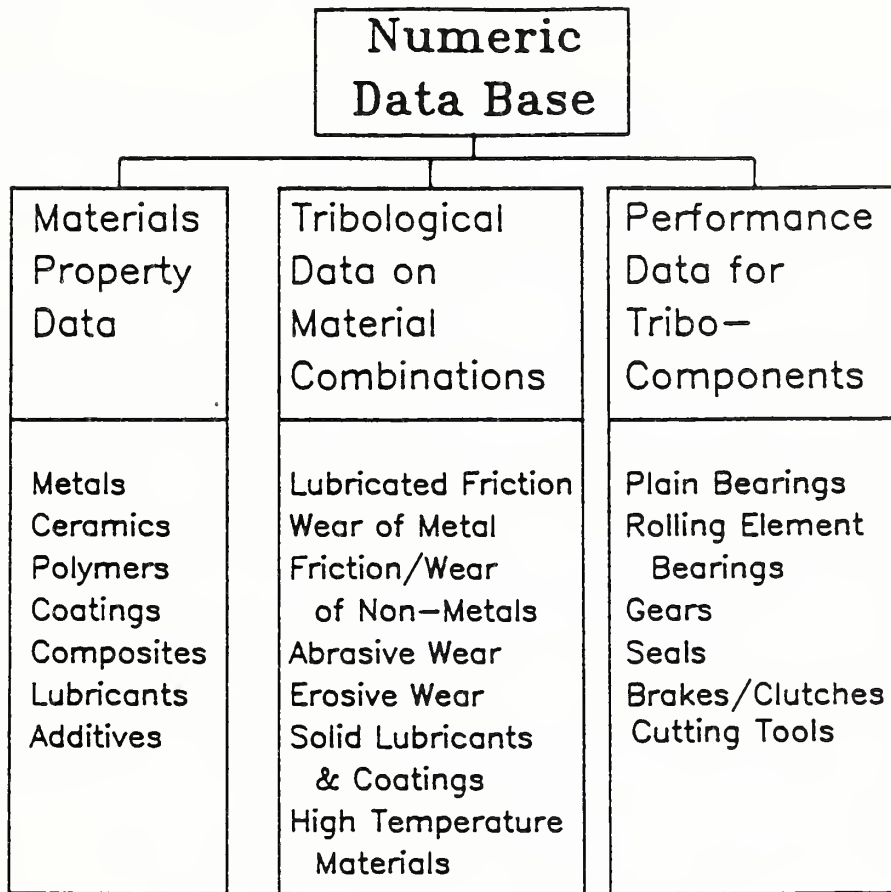| Materials Property Data	Tribological Data on Material Combinations	Performance Data for Tribo- Components

Metals
Ceramics
Polymers
Coatings
Composites
Lubricants
Additives
	Lubricated Friction
	Wear of Metal
	Friction/Wear
	  of Non-Metals
	Abrasive Wear
	Erosive Wear
	Solid Lubricants
	  & Coatings
	High Temperature
	  Materials
		Plain Bearings
		Rolling Element
		  Bearings
		Gears
		Seals
		Brakes/Clutches
		Cutting Tools

Figure 29: Three categories of data identified for inclusion
in the ACTIS numeric database. Initial emphasis has been
on material property data and tribological data.

Structural Ceramics Database

R. G. Munro, E. F. Begley, C. G. Messina[1] and T. L. Baker

[1]Consultant

Successful industrial applications of advanced materials depend critically on the availability of reliable materials property data often difficult to obtain. Further, if data are found, the design engineer usually does not have an opportunity to assess the quality of the data. The Structural Ceramics Database (SCD) is being developed to provide evaluated critical materials property data in a highly effective, easy to use format.

The prototype SCD, completed in mid-1989, contains thermal and mechanical property data for silicon carbides and silicon nitrides. Emphasis is placed on user-friendliness and the evaluation of the data in terms of accuracy, quality, reasonableness, and limitations. All data entries are documented as to source of data, material specification, measurement methods and procedures, and any limitations or cautions that might be important to the user.

The SCD is expected to have a significant impact on U.S. industries in several respects. Computerization of the data will directly enable more rapid access to new research results at considerable savings in terms of expenditures of time and money. Use of evaluated data can be expected to result in improved quality control and product reliability. Establishment of a reporting standard in a distributed database may also lead to more consistent treatment of data presented in the technical literature. More fundamentally, the collection of critical data under controlled conditions may provide an enhanced opportunity to understand the relations among materials properties, processing conditions, and performance characteristics.

The development of the SCD is being guided by focusing attention on specific applications. The notion of a focused database results in a system whose contents are determined specifically by the requirements of the application. Under funding from the Gas Research Institute, the initial focus is on ceramic heat exchangers and recuperators. In practice, the resulting database may be readily utilized in other application areas such as for valve train components in heat engines.

Development has progressed along two parallel paths, system design and data acquisition.

Three primary considerations were essential to the design of an innovative database for scientific and engineering applications. First, the needs of the user, both technical and cybernetic, had to be given highest priority. To achieve the highest degree of effectiveness, the system's design had to place very little demand on the user in terms of technical knowledge of computers or computer programming. Indeed, the emphasis had to be on user-friendliness. Second, the nature of the materials property data had to be recognized in selecting the supplementary information that would be

required to specify a material adequately and to describe thoroughly the
measurement techniques used to determine the property data. Third, the
state-of-the-art in database management system (dbms) languages had to be
considered as a constraint on the design since most dbms languages are
optimized for business rather than technical applications. To accommodate
the requirements of the SCD, a commercial dbms language that could be
tailored to the design specifications was selected.

User-friendliness was achieved through the development of a hybrid
interface that combined the characteristics of menu systems, fill-in-the-
blanks forms, and query-by-example search methods. Overall, more than 7000
lines of code have been generated to achieve user-friendliness.

The SCD interface allows the user to search for properties of a given
material or to determine materials satisfying given property values, with
equal ease. Figure 30a shows the general materials specification menu of
the SCD. Following the query-by-example method, the user only specifies
what is known about the material of interest. The user, however, does not
actually type anything into the blanks shown in the figure. Rather, the
user presses the function key, F2, whereupon the SCD presents a list, such
as Figure 30b, of the possible entries that are already known to be
acceptable to the system. The user merely selects the desired entry. In
this manner consistency is enforced by the system, typing errors are
minimized, and the user does not have to know a priori what values are
allowed or useful. Specification of numeric properties are made in an
analogous manner, with the exception that numeric values or ranges of
values must be entered by the user.

Data acquisition for the SCD has been pursued through searches for data in
the open technical literature. A computerized literature search provided
the basic key to the data. The search produced approximately 1000 titles
pertaining to silicon carbide or silicon nitride. A review of the titles
and abstracts was sufficient to reduce this number to 400 possible
references. Copies of the 400 papers were obtained and subjected to
further review. In general, papers were retained if: the material was
considered a monolithic ceramic; adequate materials specification
information was provided; thermal or mechanical properties were reported;
and sufficient details of the measurement methods and procedures were
described. This more stringent review reduced the number of acceptable
papers to approximately 75. Overall, data acquisition and assessment
involved approximately 750 staff-hours of effort.

A survey of the properties reported in these papers, showed that many of
the important properties had sparse data. The most frequently reported
property was flexural strength. These results show quite graphically the
lack of a broad database of materials property data for advanced ceramics.

Further review of the bibliographic data for the retained papers emphasized
another important reason for developing the present computerized database.
The papers that were retained were issued by 29 distinct publication
sources. The distribution of papers by sources showed that 38 percent of
the data was contained in papers from four sources; i.e., 62 percent of the
data was dispersed across numerous journals. Clearly, researching this
broad spectrum of journals each time a property value is sought could be a

very costly proposition in terms of monetary expenditures, personnel time, and project delays.

Currently, the prototype SCD is undergoing field tests at selected industrial and research centers. Evaluation of the data in the SCD is expected to be completed in the latter part of 1989. The goal is to have the SCD with materials property data on silicon carbides and silicon nitrides ready for distribution by mid-1990.

```
┌──────── ... Material Specification ... ─────────┐
│                                                  │
│    Material Class   :   Monolithic Ceramic       │
│                                                  │
│    Chemical Class   :   Carbide                  │
│                                                  │
│    Chemical Name    :   Silicon Carbide          │
│                                                  │
│                        ┌──────────────────┐      │
│    Common Name      :  │                  │      │
│                        └──────────────────┘      │
│ .  Processing Method:                            │
│                                                  │
└──────────────────────────────────────────────────┘
```

```
[F1] Help          [F3] Zoom        [Esc] Exit
[F2] Choices       [F9] OK          Arrows move cursor
```

Figure 30a: **The general material specification menu of the SCD.**

```
┌──────── ... Material Specification ... ────────────┐
│                                    ┌───────────────────┐
│  Material Class   :  Monolithic Ceramic │ Silicon Carbide │
│                                    ├───────────────────┤
│                                    │>Carborundum Hexoloy SA
│  Chemical Class   :  Carbide       │ EKA-50
│                                    │ GE Sintride (SSIC)
│                                    │ Norton NC-203
│  Chemical Name    :  Silicon Carbide│ ?
│                                    │ Erase current entry
│                      ┌──────────────┐└───────────────────┘
│  Common Name      :  │              │
│                      └──────────────┘
│  Processing Method:
│
└──────────────────────────────────────────────────┘
```

```
[F1] Help          [F3] Zoom        [Esc] Exit
[F2] Choices       [F9] OK          Arrows move cursor
```

Figure 30b: **The materials specification menu after the user has
            pressed the F2 function key for Common Name.**

FUNCTIONAL CERAMICS

FUNCTIONAL CERAMICS

Overview

Functional ceramics are those in which the primary interest is in other than structural properties, such as electrical/electronic, magnetic, optical, corrosion resistance, refractoriness, light weight, decorativeness, low cost, or ability to be cleaned and sanitized; about 95% of the roughly $35 B sales in 1988 by the U.S. ceramics industry were for such non-structural purposes. The U.S. ceramics industry is awakening (or in some cases already awake) to technology forced on it by aggressive foreign competitors and the current pace of technological advances. The Division's program in functional ceramics is structured to assist U.S. industry assimilate new technology into the manufacture of existing products and to prepare for the development of new ones.

The pressures on the U.S. ceramics industry are generally associated with cost and quality of existing products and emergence of opportunities for new products. The Division's program in functional ceramics attempts to produce technology base addressing as many such pressures as possible given the resources and capabilities available to the Division.

In superconducting ceramics the primary need is understanding how the materials work and how they can be fabricated into useful components. Divisional efforts emphasize aspects of the processing-structures-properties relationships not apt to be addressed by industry or other government programs. The emphasis on dielectrics, electronics packaging, and semiconductors reflects the importance of such materials to the electronics industry. Work on diamond thin film technology was occasioned by the recent discovery of ways of producing such films and the realization of the enormous potential of such films in electronic, optical and wear applications. The area of photonic materials (optoelectronic and electrooptic) has been recognized as a potential major growth area in the future and thus the Division has initiated work on ferroelectric oxide films. Optical detectors are important to current and future civilian and military photonic systems and thus two projects are underway in this area. Phase diagrams are the guides for most ceramic processes and are especially important for electronic and optical ceramics which tend to be considerably more complex than structural ceramics. Nondestructive evaluation techniques primarily affect cost and reliability and are becoming more important as the competitive pressures on the U.S. ceramics industry increase.

Program Structure

The Ceramics Division's current functional ceramics efforts focus on high temperature superconductors for bulk (non-thin-film) applications, electronic and optical materials, ceramic phase equilibria reference data and nondestructive evaluation. The main thrusts in superconductors are determinations of phase equilibria, explorations of chemical routes for producing powders, methods of processing the powders into bulk superconductors with optimal properties, and measurements of certain critical properties. Current efforts in electronics are aimed mainly at dielectrics, electronics packaging and semiconductors, both elemental and

alloy compound. The major effort in optical ceramics is on synthesis and characterization of diamond thin films which have potential electronic as well as optical applications. Other optical efforts address the synthesis and measurement of properties and structures of materials for transmitting and detecting infrared radiation and for optoelectronic switching and modulating visible radiation. The sole effort in reference data is a long-standing cooperative project with the American Ceramic Society (ACerS) aimed at providing the world ceramics community with the best phase diagrams available. Finally, there is a single effort aimed at investigating the use of thermal wave approaches for nondestructively characterizing near-surface regions of ceramics; it is expected that such work will increase in the future as the Division looks forward to the possibility of work in the general area termed "intelligent processing" of ceramics.

Project Listing

Projects comprising the functional ceramics program are as follows:

High Temperature Superconductors:

Thermomechanical Detwinning of Superconducting $YBa_2Cu_3O_{6+x}$ Single Crystals*

Crystal Chemistry and Phase Equilibria Studies*

Processing High T_c Superconductors*

Strength of Superconducting Ceramics*

Electrical Properties of High T_c Superconducting Ceramics*

Electronic Materials:

Electrostrictive Effects on Crack Growth*

Molecular Orbital Calculations of Strained Si-O Bonds

Synchrotron Diffraction Imaging Analysis of Advanced Single Crystals*

Advanced Synchrotron Radiation Analysis of Polycrystalline Ceramics*

X-ray Imaging for Studies of Interfaces

Thermal Wave Monitoring of Grinding Damage in Si_3N_4

*These projects are selected for expanded descriptions to illustrate the program.

Optical Materials:

Diamond Films Processing*

Characterization of CVD-Grown Diamond Films*

High Pressure Zinc Sulfide Studies

Processing of Lead Niobate-Lead Titanate

Reference Data:

Ceramic Phase Equilibria Program*

Significant Accomplishments

Significant technical accomplishments in the functional ceramics program include the following.

o   The phase equilibria in significant portions of the Bi-Sr-Ca-Cu-O superconducting system have been determined. These ternary diagrams illustrate the complexity in the processing steps needed to create the 80K and 110K superconducting compounds.

o   An optimum approach was developed to homogeneously precipitate Y-Ba-Cu-O (YBCO) precursors as Y, Ba and Cu hydroxycarbonates. Importance of proper precursor calcining and environmental control during phase development has been delineated.

o   Electrical fields have been shown to play a role in the extension of cracks in electrostrictive ceramics.

o   Volume 7 of Phase Diagrams for Ceramists (salt systems) and Volume 8 (systems at elevated pressure in the presence of water) were submitted to the American Ceramic Society for publication.

o   A region of solid solution around the 1-2-3 compound in the superconducting R-Ba-Cu-O system (where R is a lanthanide) was shown to grow larger as the size of the lanthanide atom increased.

o   A facility for the processing of thallium-based superconducting ceramics has been constructed and preliminary materials produced. This facility will be used to make materials for phase equilibria analyses in Tl-Ba-Ca-Cu-O system.

o   Superconducting ceramics in the Bi-Pb-Sr-Ca-Cu-O system were produced from glasses through suitable crystallization heat treatments. The development of such glass-ceramic processing techniques could lead to better methods of forming complex shapes of these materials.

o   Flexural strength data obtained on Y-Ba-Cu-O ceramics showed that the tetragonal-to-orthorhombic phase transformation in this system plays an important role in causing internal stresses which can lead to cracking.

o   The microstructure of Y-Ba-Cu-O ceramics was shown to be highly
    dependent on the temperature, time, and environment of sintering.
    Increases in sintering temperature and time and more oxidizing
    environments lead to larger, more highly elongated grains.

o   Design diagrams for polycrystalline silicon and zinc sulfide were
    created based on environmentally enhanced fracture data. These
    diagrams will be used by industry to design improved infrared
    transmitting windows.

o   The effect of gas composition on the morphology and growth of
    chemically vapor deposited (CVD) diamond films has been studied.
    Growth rates as a function of gas methane fraction were found to have
    a nearly linear dependence. The absorption edge at the electronic
    band gap of CVD diamond has been observed both in diffuse transmission
    spectroscopy and in excitation spectroscopy of photoluminescence.

o   A metallorganic CVD reactor for depositing ferroelectric thin films
    has been designed and construction of the reactor began.

o   A thermomechanical method was discovered for producing untwinned
    single crystals of Y-Ba-Cu-O. The crystals show a sharp
    superconducting transition near a transition temperature of 90 K.

o   An image detecting system which comprised X-ray image magnifiers and a
    two dimension charge coupled device (CCD) camera was completed and
    displayed 0.5 μm resolution in microradiography as well as diffraction
    imaging.

o   A high pressure furnace capable of reaching 900°C was constructed in
    collaboration with scientists in industry and was successfully applied
    in in-situ heating experiments with Si and HgCdTe crystals.

o   For polycrystalline characterization, a new diffraction technique was
    developed and applied to several materials for the determination of
    the shape, size and distribution of particle grains without ad-hoc
    mathematical models for particles.

o   For strains and lattice parameter variations, a new measurement
    technique which utilizes an additional X-ray analyzer crystal to
    obtain strain sensitivity less than 10^{-4} is being tested with ceramic
    superconductors to show not only its feasibility but great potential.

o   For characterization of defects in advanced ceramics, genesis of
    defects and effects of crystal growth conditions of GaAs, CdTe, InP
    and other alloy semiconductors were studied by synchrotron radiation
    analysis in collaboration with universities and other government
    agencies.

The Electronic Materials Group performs research in a number of different areas. A major effort is directed toward an understanding of the relationships between processing and properties of the high T_c superconducting ceramics. In this task, we are working closely with personnel throughout NIST as well as in industry and academia. One of the primary research objectives in the superconducting ceramics program is the development of phase equilibria data, leading to phase diagrams for the systems of primary interest. Phase transformations in superconducting and other materials are being investigated in various systems using X-ray diffraction techniques. In addition, techniques are being developed to determine critical currents in superconducting ceramics. In related work, there is an ongoing study on the reliability of piezoelectric components under cyclic loading including possible effects of electric fields on fracture. Preliminary work on the processing of lead niobate-lead titanate ceramics for infrared sensors has been conducted.

The Ceramics Phase Diagram Program which is conducted jointly with the American Ceramic Society is now part of the Electronic Materials Group. The primary objective of this program is the publishing of edited phase diagrams for use by ceramic scientists worldwide. We are exploring new directions for the program as well as other means for disseminating phase equilibria data.

Scientists in the Electronic Materials Group have been exploring high pressure techniques for preparing infrared transmitting materials. These techniques have been demonstrated to lead to harder, more fracture resistant materials which can be processed at lower temperatures than those made by conventional means.

Finally, there is an ongoing effort within this Group in the development of non-destructive evaluation techniques for ceramics. During this past year, this research has involved the use of thermal wave analysis for the determination of surface damage, the detection of delamination of thin films, and the observation of spatial inhomogeneities in the thermal diffusivity of electronic components.

Crystal Chemistry and Phase Equilibria Studies

W. Wong-Ng, R. S. Roth, C. J. Rawn, B. P. Burton[2], N. M. Hwang[1], E. R. Fuller, Jr., L. P. Cook, J. D. Whitler and B. Paretzkin[1]

[1] Guest Scientist
[2] Metallurgy Division

Despite recent worldwide efforts on superconductivity research, there is still a need for fundamental understanding of the crystal chemistry and phase equilibria in superconducting ceramic systems. The discovery that substitution for yttrium in $BaO-Y_2O_3-CuO$ by a large variety of lanthanides, R, also produces superconductors with $T_c \approx 90K$, provides numerous alternative materials for investigation. Since knowledge of phase equilibria and crystal chemistry is essential for controlling processing parameters and material properties, systematic studies of the $BaO-R_2O_3-CuO$

systems are crucial. In addition, comprehensive phase equilibria and crystal chemistry studies were undertaken on binary and ternary systems contained in the quaternary $SrO-CaO-Bi_2O_3-CuO$ system.

Two important factors, the progressively decreasing size of the lanthanides, known as the lanthanide contraction, as well as the stability of different oxidation states of these elements play important roles in governing compound formation in the $BaO-R_2O_3-CuO$ systems. We have initiated a systematic study to investigate the effect of the above two factors, in particular the size factor, on the _trend_ of phase formation and solid solution formation of selected binary and ternary compounds in the $BaO-R_2O_3-CuO$ systems, the _trend_ of phase diagrams, as well as the _trend_ of the structural phase transformation between the orthorhombic and tetragonal phases of the superconductor materials, $Ba_2RCu_3O_{6+x}$, as a function of the ionic size of the element R.

Solid Solution Formation in $Ba_{2-z}R_{1+z}Cu_3O_{6+x}$

Solid solution formation is usually technologically advantageous because it allows for greater control of processing parameters without the possibly deleterious occurrence of second phases. The superconductors $Ba_2RCu_3O_{6+x}$ were found to exist as solid solution series with formulas $Ba_{2-z}R_{1+z}Cu_3O_{6+x}$ for the larger size of R, namely, for La, Pr, Nd, Sm and Gd. Beyond Gd, only point compositions (z=0) were obtained. The size compatibility between the Ba^{2+} and R^{3+} is a predominant factor governing the formation of this solid solution. The amount of substitution of lanthanides for barium decreases with the decreasing size of R^{3+}; the larger the mismatch of the sizes of R^{3+} and Ba^{2+}, the narrower the solid solution extent. This extent, z, for R=La, Nd, Sm, Eu and Gd has been found to be $z \leq 0.7$, 0.7, 0.7, 0.5, 0.2, respectively.

Phase Diagrams

In air at 950°C the phase relationships in the CuO-rich region of the ternary diagrams $BaO-R_2O_3-CuO$ progressively change from the La system through the Nd, Sm, Eu, Gd, Y, and Ho systems to the Er system. Several features have been observed. First, the La system has the greatest number of ternary compounds. Second, the superconductor material, $Ba_2RCu_3O_{6+x}$, exhibits a solid solution of $Ba_{2-z}R_{1+z}Cu_3O_{6+x}$ for the first half of the lanthanide elements with a range of formation which varies with the ionic size of R. Third, a trend is observed regarding the tie-line connections between BaR_2CuO_5, CuO, the phases $Ba_{2-z}R_{1+z}Cu_3O_{6+x}$, and the binary phase along the R_2O_3-CuO edge. For the first half of the lanthanides, except for La, a compatibility join is found to connect R_2CuO_4 and the tetragonal end member of the $Ba_{2-z}R_{1+z}Cu_3O_{6+x}$ phase. In systems where R has a smaller ionic size, i.e., R = Eu and Gd, the tie-line connection switches to join the $BaEu_2CuO_5/BaGd_2CuO_5$ phase and the CuO phase, respectively.

New data were obtained for the binary systems, SrO-CaO, $SrO-Bi_2O_3$, and SrO-CuO. A new phase, identified as $Sr_6Bi_2O_9$, was discovered.

Studies in the ternary $SrO-\frac{1}{2}Bi_2O_3-CuO$, $CaO-\frac{1}{2}Bi_2O_3-CuO$, and $SrO-CaO-\frac{1}{2}Bi_2O_3$ systems are nearly complete. In the $SrO-CaO-\frac{1}{2}Bi_2O_3$ system, three new ternary solid solution phases were discovered and partially characterized.

This work has demonstrated that equilibria involving ternary phases is only obtained after repeated cycles of annealing and grinding, and that metastable Raveau solid solutions are typically the first ternary phases to form.

Phase Transformations

In order to understand the crystal chemistry and to gain insight into the effect of oxygen stoichiometry on superconductivity, we have investigated the phase transformations between the orthorhombic and tetragonal structures of several high T_c superconductors, $Ba_2RCu_3O_{6+x}$, where R = Sm, Gd, Y, Ho and Er, and x=0 to 1. Various techniques including X-ray diffraction, thermogravimetric analysis, neutron scattering, transmission electron microscopy, and determination of Meissner effect, have been used to study the nature of the phase transition.

AC magnetic susceptibility measurements suggest that the transformation from the oxygen-rich orthorhombic phase to the oxygen-deficient tetragonal phase involves two orthorhombic phases, designated here as O(A) and O(B). At present there is no clear evidence of where the phase boundary between O(A) and O(B) is. Electron diffraction patterns from an yttrium material quenched from 670°C show both a splitting of the strong diffraction spots as a result of twinning and also extra, weak, diffuse reflections indicating that the a-axis cell dimension is doubled. Neutron diffraction results show the absence of long-range ordering of oxygen; the electron diffraction results correspond to short-range oxygen ordering.

The structural phase transition temperatures, oxygen stoichiometry and characteristics of the Tc plateaus appear to follow a trend anticipated from the dependence of the ionic radius on the number of f electrons as R progresses across the lanthanide series. Lanthanide elements with a smaller ionic radius stabilize the orthorhombic phase to higher temperatures and lower oxygen content. Also, the superconducting properties, viz., the T_c values, are less sensitive to the oxygen content for materials with smaller ionic radius.

It is hoped that the relationships among compositions, structures and the size of R^{3+} which we have discovered will enhance the understanding of the physical properties of high T_c superconductors and improve the strategy both for processing these materials with improved properties and for the search for new materials. Further work will continue in the phase equilibria studies of these lanthanide systems including the investigation of melting relationships, primary phase field determination of selective $Ba_2RCu_3O_{6+x}$ phases and of mixed lanthanide phases.

Processing High Tc Superconductors

J. E. Blendell, M. D. Hill, E. R. Fuller, Jr., J. S. Wallace and C.K. Chiang

While it is known that the properties of high T_c ceramic superconductors are strongly influenced by processing, the mechanisms which control these effects are not known. We have undertaken this study in order to understand the effect of processing variables on the microstructure of $Ba_2YCu_3O_{6+x}$. Correlation of the observed microstructures with measured properties will allow definition of an optimum microstructure to achieve a desired property. Initial experimental variables include sintering temperature, the time at temperature, and the composition of the gas atmosphere during sintering.

In order to keep the number of experimental variables low, which would facilitate analysis of the interactions between variables, several conditions were held constant. A single batch of a commercial powder was used for all sintering experiments so that there would be no variations in powder chemistry or characteristics. All samples were heated at the same rate and in the same atmosphere as used for sintering. The cooling was always done in argon, and the oxidation kinetics were subsequently studied. The samples were sintered under two different oxygen partial pressures, 100 kPa (pure oxygen) and 2 kPa (balance was argon) with the total pressure at 100 kPa (1 atm). Three sintering temperatures (920°C, 935°C and 950°C) were used and the samples were held for different times (4, 7 or 10 hours) to measure the grain growth.

Major differences in the microstructure were observed under the different conditions. Representative microstructures are shown in Figure 31 for samples sintered in high and low oxygen partial pressures. For the samples sintered in 100 kPa oxygen, the grains were elongated and much larger than the equiaxed grains in the samples sintered in 2 kPa oxygen. The mean intercept length was more than 2 times larger in high PO_2 than low PO_2. This underestimates the difference in the microstructure, due to the change in aspect ratio. The high PO_2 samples had a very large aspect ratio (7.0) compared to the low PO_2 samples (1.5). It was also found that increased temperature and longer times increased both the mean intercept length and the aspect ratio. Statistical analysis indicates that there is a very complex relationship among all three variables.

The samples were oxidized after sintering by heating in oxygen to 600°C and then cooling to 420°C and holding at that temperature until there was no further weight gain. It was found that the kinetics of weight gain were the same for both types of microstructure. After oxidation, the samples were fully superconducting above 80K as determined by AC susceptibility measurements. Critical current density measurements showed highly variable results. There was a peak in J_c at intermediate grain sizes and aspect ratios, and a drop-off for large values of both parameters.

These results were contrary to what was expected. The elongated grain seen are usually associated with the presence of small amounts of liquid phase. However, liquid is formed at higher temperatures in high PO_2 than in low

88

PO$_2$, so the high aspect ratio is probably not due to the presence of a liquid phase at the sintering temperature. Another possibility is the formation of a low temperature liquid phase during heating, which coarsens the structure below the sintering temperature. Experiments performed with the atmosphere during heating different from the sintering atmosphere showed no difference in microstructure. Thus, a low temperature liquid phase, if present, is not important.
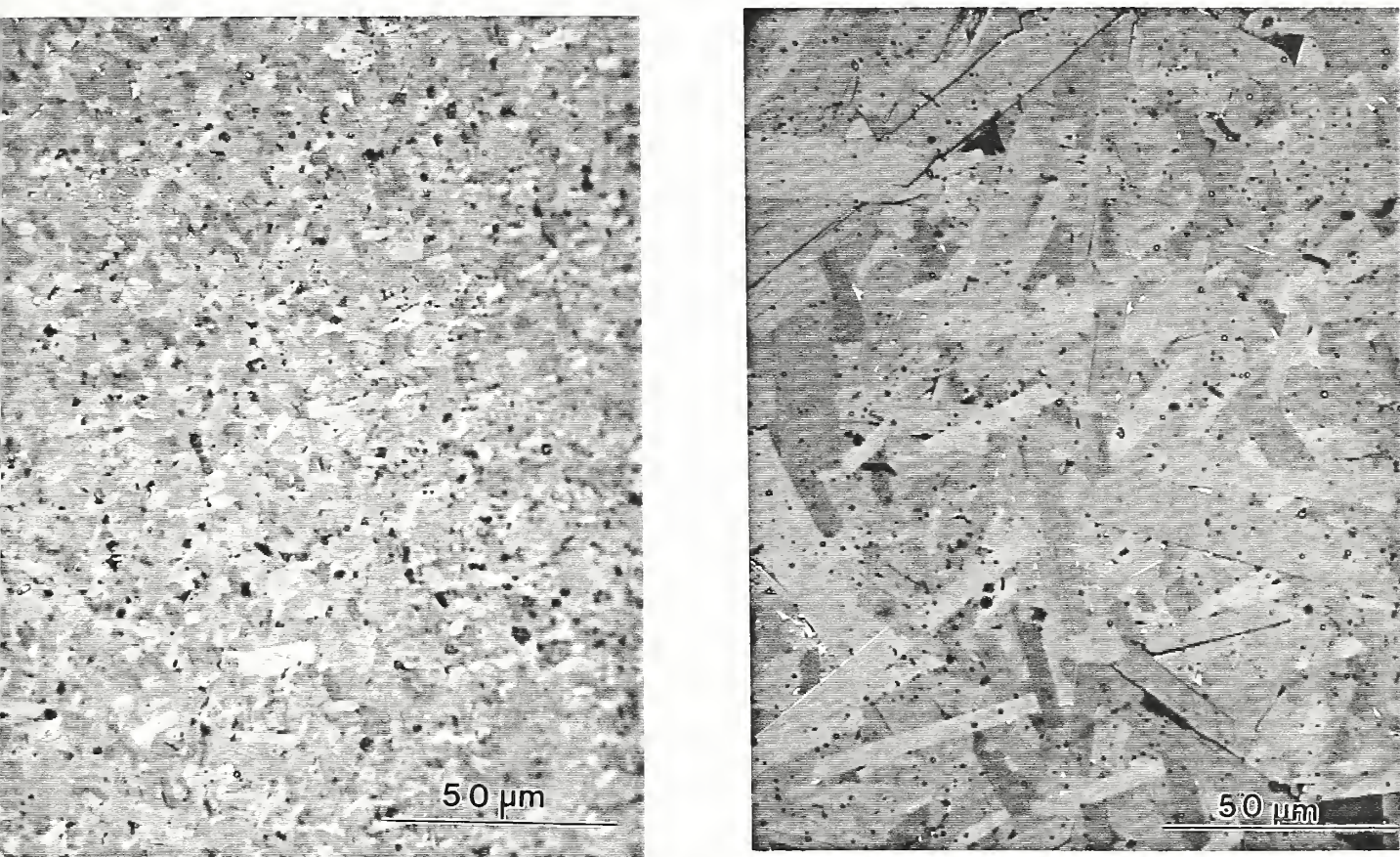

Figure 31. Microstructure of Ba$_2$YCu$_3$O$_{6+x}$ samples sintered under different PO$_2$ conditions; a)PO$_2$=2 kPa; b)PO$_2$=100 kPa. The larger grains in the high PO$_2$ samples are easily seen compared to the finer, equiaxed grain in the low PO$_2$ sample.

Strength of Superconducting Ceramics

J. S. Wallace, E. R. Fuller, Jr., A. S. Raynes, S. W. Freiman,
J. E. Blendell, M. L. Balmer and M. D. Hill

Mechanical reliability is an important aspect of the technological
application of high temperature ceramic superconductors. An acceptable
strength is on the order of 150 MPa, although larger values are clearly
desirable. Work has addressed the strength and fracture behavior of Ba-Y-
Cu-O superconducting ceramics, and more importantly, the influence that the
microstructures of these materials impart to the mechanical properties.
The sintering conditions for the ceramics have been seen to have a profound
effect on microstructure development. In addition, large internal strains
can develop on cooling from the sintering temperature. These strains
result either from the phase transformation that occurs during oxygenation
or from anisotropy in the thermal expansion. Since strain relief by
plastic deformation or diffusion is generally not active below the
sintering temperature, these strains are most easily accommodated by
microcracking.

In this study we have seen that the critical fracture toughness of these
materials varies from approximately 0.85 MPa$\cdot$m$^{\frac{1}{2}}$ to 1.1 MPa$\cdot$m$^{\frac{1}{2}}$ depending on
the processing conditions. Results of strength measurements for four
sintering-cooling conditions are presented in Table 1. The densities of
all of these materials were greater than 95% of theoretical. Those
materials sintered in 98% Ar - 2% O_2 were relatively fine-grained (grain
size 3.5 micrometers), while those sintered in O_2 had a bimodal grain size
distribution (60-150 micrometer plate-like grains and regions of 8-10
micron grains). As expected, the fine-grained materials had higher
strengths than the coarse-grained materials. The large facets in the
coarse-grained materials can become critical defects. The particularly low
strength of the specimens which were both sintered and annealed in O_2 is
apparently due to the fact that they were heavily microcracked. The
relatively low strength of the specimens which were sintered in 98% Ar - 2%
O_2 and then annealed in O_2 indicates that either these materials were
microcracked as as result of the anneal or that large internal stresses
resulting from the thermal expansion anisotropy or phase transformations
were superimposed on the externally applied stress. Since the fracture
toughness of all of these materials was relatively similar, the different
strengths most likely result from the different microstructures, i.e.,
different flaw sizes and internal strains.

TABLE 1: Strengths of Superconducting Ceramics

Flexural Strength (MPa)

Cooling/Annealing	Sintering Conditions	
	4.7 h., 930°C 98% Ar - 2% O_2	6.0 h., 950°C O_2
Ar; no hold	133 ± 19	96 ± 19
O_2; 20 h. at 420°C	70 ± 37	58 ± 6

Electrical Properties of High T_c Superconducting Ceramics

C. K. Chiang

In the case of the new, high T_c superconducting ceramics, electrical resistivity measurements provide one of the basic characteristics of the material, i.e., critical temperature. The shape of the resistivity-temperature curve as well as the absolute value of the superconducting resistivity provides feedback as to the quality of the processing procedure. Transport critical current measurements provide one of the most important parameters for practical applications of superconducting ceramics.

At present, we have measured both resistivity and transport critical current on ceramics in both the Ba-Y-Cu-O and Bi-Sr-Ca-Cu-O systems. Samples have been obtained from other investigators at NIST as well as from other laboratories.

One of the key problems associated with making critical current measurements is obtaining a sufficiently low-resistance contact between the lead wires and the specimen. The need for contacts having lower and lower resistance increases as the level of critical current in the materials is improved. The contact method used should be a nondestructive one, which means that the material itself should not be altered due to the temperatures and environments to which the specimen is subjected in order to make the contacts. For example, we do not heat a $Ba_2YCu_3O_{7-\delta}$ sample to a temperature above 350°C where oxygen atoms became mobile and the sample oxidation state might change. To date, three nondestructive contact methods have been used: a) silver paste which requires no heating; b) indium-silver alloy soldering, in which the sample is heated to 180°C at the contacts; and c) gold evaporation/sputtering. The contact resistance produced by all of these methods were in the range from 1×10^{-6} ohm/cm^2 to 1×10^{-3} ohm/cm^2. For a sample with the 0.8mm x 0.8mm cross-section, one could expect to measure the critical current up to 1000 A/cm^2. For higher critical current materials, we must use samples having smaller cross-sections.

A facility for making critical current measurements was designed and constructed. This system is capable of supplying current up to 100 A. The measurements can be performed in magnetic fields from zero to 10,000 gauss (1T). We have utilized the system to study high T_c ceramics materials prepared in our laboratory and also to examine materials from other agencies.

Electrostrictive Effects on Crack Growth

G. S. White, A. S. Raynes and S. W. Freiman

Mechanical reliability of electronic ceramics is becoming a matter of increasing concern. Electronic ceramics must not only survive mechanically applied stresses, they must also survive stresses resulting from electric fields. Yet, effects of electric fields on crack propagation have been investigated only slightly. The presence of electric fields can affect

electronic ceramics in a variety of ways, directly, through piezoelectric or electrostrictive effects, or indirectly through Joule heating.

We have been investigating crack propagation in an electrostrictive material, a lead magnesium niobate ceramic (provided by AVX Corporation), in the presence of an electric field. We were also interested in the applicability to crack growth of models predicting that electric fields would be enhanced at discontinuities such as voids. In materials with large electrostrictive coefficients, electric fields give rise to strains; if the electric fields are enhanced by the presence of discontinuities such as cracks, material in the vicinity of the cracks will experience greater strains than material in uncracked regions. The ramifications of such strains on crack extension, i.e., whether electric fields improve or degrade the fracture resistance of these ceramics, were experimentally investigated.

Vickers or Knoop indentations were placed in the ceramic between a set of parallel electrodes. The Vickers indentations were oriented such that the radial cracks from the corners of the indentation were either parallel or perpendicular to the applied electric field. Knoop indentations were oriented so that the cracks ran parallel to the electrodes, i.e., perpendicular to the electric field. Both sets of indentations were made either under 1) no voltage (E = 0 kV/cm) or 2) an applied voltage of 257 V (E = 17 kV/cm). The crack lengths were measured under the same voltage conditions for which they were introduced. Measurements were made on many indentations and the conclusions were drawn at the 95% confidence level.

Results showed that lengths of cracks oriented perpendicular to the applied electric field were reduced relative to those for which no field was present. These results were found to hold true for both Vickers and Knoop indentations and are in general agreement with expectations based upon a model which suggests that large tensile strains local to a crack situated perpendicular to an electric field would lead to compressive stresses in the near-crack-tip region because the material surrounding the highly strained region would lead to clamping.

High Pressure Zinc Sulfide Studies

S. Block, G. J. Piermarini, M. Vaudin and A. S. Raynes

Compaction and sintering studies in the Diamond Anvil Cell (DAC) were carried out on the optical materials ZnS, composites of ZnS and TlI (4-to-1 by volume, respectively), and CdY_2S_4. Also, relatively large compacts of ZnS were made by V. Bean of the NIST Temperature and Pressure Division, who used a large hydraulic press in a two-stage process to make cylindrical compacts approximately 0.635 cm (0.25 inch) in diameter and thickness. In these studies, powders are first compacted at very high pressures (up to 50 kbar) and then sintered at moderately high pressures (on the order of 5 kbar).

Based on these studies it was concluded that the quality of the final product is a function of the powder source and the processing parameters which include pressure, temperature, particle size, pore pressure (trapped

air) and sintering time. Pressure-induced sintering in pure ZnS has been shown to result in improved hardness and up to a 50% increase in fracture toughness over CVD or HIPed ZnS. The sintering temperature used to make the ZnS compacts (600°C) was found to be much lower than that used in conventional sintering processes (>900°C). Furthermore, no significant grain growth occurs at these lower temperatures. The hardness of the material increased with increasing compaction pressure. Fracture toughness was found to be a complex function of pressure, initially increasing, then decreasing at very high pressures because of spring-back processes arising from residual stress in the compact. The increased toughness is hypothesized to be due to the heavily deformed, very fine grains (< 1 micron) in the ZnS.

In addition, both NiS-ZnS and Tl-ZnS composites were investigated. The NiS-ZnS composites showed some promise in terms of increased fracture toughness over pure ZnS. However, the Tl-ZnS compacts made were inferior in comparison to CVD material, about 50% lower in fracture toughness and 40% lower in hardness.

Poor results were also obtained for CdY_2S_4 compacts. The volume compression and bulk modulus of CdY_2S_4 compacts were measured by X-ray diffraction. Assuming 0.3 for Poisson's ratio, a Young's modulus of 87 GPa was determined from compression data up to 2.5 GPa. This value is similar to that found for ZnS. The X-ray results also show a transition in CdY_2S_4 to an opaque phase in the pressure range 2.5<GPa<3.3. The high pressure phase has not yet been identified crystallographically.

Molecular Orbital Calculations of Strained Si-O Bonds

G. S. White, W. Wong-Ng and S. W. Freiman

Structural reliability is the key to the use of ceramics in a wide variety of applications. Consequently, there has been a considerable effort to understand the mechanisms of failure in brittle materials. A major component of this effort has been the investigation of environmentally enhanced fracture in ceramics, since, in the presence of a stress and an active environment such as water, subcritical flaws in these materials will grow, resulting in eventual mechanical failure. Therefore, studies involving a number of materials, e.g., SiO_2, Al_2O_3, GaAs, Si, and MgF_2, have been conducted and qualitative models describing environmentally enhanced fracture have resulted. However, it has been demonstrated that even qualitative models cannot safely be extrapolated to materials other than those for which they have been developed; details of environment/strained-crack-tip-bond interactions are too subtle to approximate with macroscopic material parameters. Rather, in order to understand environmentally enhanced fracture of ceramics, it is necessary to know how the atomic/electronic structure of the bonds at the crack tips change as they are subjected to strain and to the presence of reactive environments. Therefore, we have begun molecular orbital (MO) calculations of molecules simulating crack tips to try to determine how energy levels and electron distributions are affected by strain.

93

This year, we have incorporated a molecular orbital calculation program into the computer system at NIST. A number of preliminary computations have been made of the Si-O system in which different basis sets, molecule sizes and bond angle orientations have been investigated. In particular, we investigated whether d-orbitals should be included in the basis sets (their presence substantially increases the length of each computer run). Although there was little difference in the energy values calculated for strained Si-O bonds for basis sets which included the d-orbitals compared with those which did not, we have chosen to retain the d-orbitals because of their possible contributions during further calculations of environmental interactions. Energy dependence of the SiO bond on both Si-O angle and bond length were calculated and were found to behave in agreement with previous workers. We have begun 2-parameter calculations, which are made as both the bond angles and bond lengths are strained, a situation more realistic than treating the angle and bond length independently. Preliminary calculations have shown that the energy of the Si-O bond does depend on the neighboring Si-O bond angle (the Si-O bonds at the crack wall, not at the crack tip). These calculations suggest that the existence of highly strained sites, proposed on both experimental and theoretical grounds, are reasonable for amorphous silica, which contains randomly oriented SiO_2 tetrahedra.

Ceramic Phase Equilibria Program

H. M. Ondik, S. W. Freiman, M. A. Clevinger, S. K. Peart[1], K. M. Kessel[1] and C. G. Messina[1]

[1]American Ceramic Society Industrial Research Associates

The purpose of the Ceramic Phase Equilibria Program is to provide the ceramics user community with evaluated phase equilibria data covering all non-alloy, inorganic systems. This past year has been the fourth full year of operation of the Ceramics Phase Diagram Data Center under the expansion plan sponsored cooperatively by NIST and the American Ceramic Society (ACerS). About $2,500,000 has been raised by the ACerS from industrial and private sponsors for the support of the program.

The major accomplishments during the past year include:

Camera-ready copy for Volume 7 on salts and Volume 8 on high-pressure aqueous systems was delivered to the ACerS. Volume 7 contains 1057 diagrams discussed in 934 commentaries. Publication is expected in October 1989. Volume 8 contains 915 diagrams discussed in 295 commentaries, and should be published in the late fall of 1989.

Chemical Abstracts are being searched and papers retrieved by the Data Abstract Search Service (DASS) working under a contract to the ACerS. The current search began with Chemical Abstracts issues of January 1988. A retrospective search is also being conducted. New data files generated since September 1988 contain about 6600 entries, each representing a diagram. There are about 2800 entries for oxide and salt systems combined, about 600 for boride, carbide, and nitride systems, about 2500 for systems containing elements of Groups IVa, Va, and VIa of the Periodic Table, and

about 700 for aqueous systems. These entries represent about 4500 papers.
Some 200 new papers are currently in hand for Data Center review and
preparation for data entry.

Planning for the revised chemical system sort program was postponed
until a significant number of new references had been examined. After
about 2000 new references have been examined, and chemical systems
assigned, the logic for the revised chemical sort software has been
established and the computer programming is being done. Some modifications
have been made to the digitization software to accommodate the needs of the
non-oxide, non-salt systems.

Examination, evaluation, and digitization of diagrams for inclusion in the
next two volumes of Phase Diagrams for Ceramists has begun. These volumes
will contain systems of interest to the structural ceramics community
(boride, carbide, nitride systems, etc.) and the semiconductor community
(systems containing Groups IVa, Va, and VIa elements).

Thermal Wave Monitoring of Grinding Damage in Si_3N_4

G. S. White

Measurements of thermal diffusivity, α, of silicon nitride, Si_3N_4, have
been made both as a function of grinding grit size and as a function of
depth beneath the surface using the mirage effect thermal wave technique.
The purpose of the work was to determine if values of α measured near the
surface differed from bulk values, reflecting the existence of a layer of
grinding damage. Modern structural ceramics are almost always ground to
final dimensions, and the grinding procedures are known to generate a wide
variety of flaws: cracks normal and parallel to the surface, local melting,
residual stresses, etc. These flaws are often the strength limiting
features of the ceramic, yet they are so small and so numerous that
identification of a single critical flaw is not possible. Consequently,
this work attempts to determine the average damage resulting from
particular grinding processes rather than to detect specific flaws. To
determine the average damage, α was measured both within the specimen, to
obtain the undamaged value, and at successively more shallow depths, to
find measurements of α which have been affected by the grinding process.
Both the probe depth and the measured values of α were found to correlate
with grinding coarseness, suggesting that the measurement technique may
provide an evaluation of grinding damage when calibrated with strength
measurements. In addition, measurements made at separate regions of the
specimens provided data which were essentially identical, showing that the
technique gives a true measure of the average surface.

The objective of the Optical Materials Group is to provide data, measurement methods, standards and reference materials, concepts, evaluated data, and other technical information on the fundamental aspects of processing, structure, properties and performance of optical and optoelectronic materials for industry, government agencies, universities, and other scientific organizations. The program supports generic technologies in crystalline, glassy, and thin film inorganic optical materials in order to foster their safe, efficient and economical use. Research in the group addresses the science base underlying new advanced optical materials technologies together with associated measurement methodology.

The effort of the Optical Materials Group has been directed into three principal areas: diamond film processing and characterization, metallorganic chemical vapor deposition (CVD) of ferroelectric oxides, and single-crystal high-temperature superconducting ceramics. A significant accomplishment in high temperature superconductivity was the result of a unique combination of talent, prior experience and serendipitous circumstances.

Diamond Film Processing

E. N. Farabaugh and A. Feldman

Diamond films were grown by the hot-filament technique with three broad objectives: to examine the effect of deposition parameters on film growth rate and diamond quality; to provide specimens for properties measurement such as thermal conductivity, wear, and adhesion; and, to enhance our film growth capabilities.

The effect of $CH_4:H_2$ gas volume ratios on diamond growth rate and morphology was studied. $CH_4:H_2$ ratios in the range 0.1-1.0% were employed. The other deposition parameters were: filament material, tungsten; filament temperature, 1800 °C; gas pressure, 40 torr; gas flow rate, 52 sccm except for the 0.1% $CH_4:H_2$ ratio deposition in which the flow rate was 120 sccm. The films were characterized by scanning electron microscopy (SEM) and x-ray diffraction (XRD). Diamond films were produced on single crystal silicon (Si) and polycrystalline mullite ($3Al_2O_3 \cdot 2SiO_2$) substrates by hot filament chemical vapor deposition. These substrate materials provide a good thermal expansion match to diamond.

SEM micrographs were taken both of film surfaces and cross-sections. The cross-sectional micrographs served both to examine the internal growth features of the films and to provide a means of measuring film thickness. The surface micrographs revealed that the roughness of the films decreased with increasing CH_4 content during growth with the effect appearing to be more pronounced for the films grown on mullite. The best defined crystal faceting was present in the films grown with the lowest CH_4 concentrations. Mean growth rates, as determined from thickness measurements and deposition times, were seen to increase with increasing CH_4 concentrations. Growth rate, normalized by flow rate, versus gas fraction of methane is shown in

Figure 32. The highest growth rate was of the order of 0.2 μm/hr. The slightly higher observed growth rate on mullite may be explained by the diamond polishing preparation of the mullite surface. This preparation may have provided a higher density of nucleation sites for film growth. The cross-sectional SEM micrographs also show that the films possess columnar growth features. The columnar growth appears to be better defined in the lower CH_4 concentration growth.

XRD patterns, taken with a Read Camera, suggest that the crystallite size increases with decreasing CH_4 gas content. No preferred crystallographic orientation could be observed in any of the diffraction patterns.

Isolated particles were also grown on Si substrates under the same deposition conditions as film growth. SEM micrographs revealed that as the CH_4 gas fraction increased, the particles displayed increasing rates of secondary particle nucleation resulting in a less well faceted morphology. Under identical growth conditions, the dimensions of the largest isolated particles were greater than the film thicknesses. The largest particles, which were found in the 1.0% CH_4:H_2 ratio deposition, were 30-40 μm across, whereas the film grown under identical conditions was 13μm thick. This result is consistent with earlier reports showing that diamond particles have a higher growth rate than diamond films.

In addition to the above work, films have been grown for cathodoluminescence studies of defects, optical transmission measurements, thermal diffusivity measurements, wear, adhesion, and Raman spectroscopy of nondiamond phases of carbon present in the diamond.

The second generation hot-filament CVD reactor, described in a previous annual report, has been placed into operation and used to prepare the diamond film specimens used in these studies. A new microwave assisted CVD reactor is nearly ready to be put in operation. With the microwave assisted reactor and another hot-filament reactor under construction, we anticipate three hot-filament reactors and one microwave reactor to be on line in 1990. This will provide us with the capability to prepare specimens under a wider range of deposition conditions, and to dedicate individual reactors to particular other agency projects without interfering with other important research projects.

In collaboration with Chrysler Corporation, we have grown diamond films on WC cutting tools using the hot-filament CVD technique. These films grew easily and displayed the characteristic diamond film morphology. These tools were tested at Chrysler in a turning operation; however, the diamond film delaminated from the tool. Research in the area of diamond coated cutting tools needs further investigation and will be expected to have commercial impact very shortly.

Future work includes: establishing deposition parameters that provide the fastest growth rate; work on the proof on concept of smooth sided diamond films or plates; placing the microwave and another hot-filament reactor on line; collaboration in adhesion studies of diamond films; and collaboration on tribological studies; specimens thermal diffusivity measurements, Raman spectroscopy and luminescence studies of defect states.
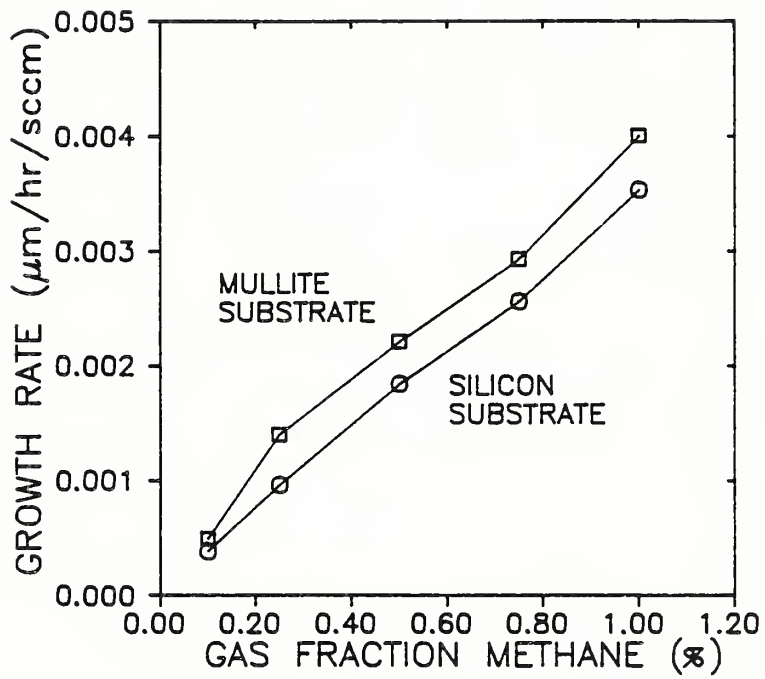
Figure 32.   Normalized growth rate vs. gas fraction of methane
              in hot-filament CVD of diamond films on mullite
              and on silicon.

Characterization of CVD-Grown Diamond Films by Cathodoluminescence Imaging
Spectroscopy and Other Optical Spectroscopies

L. H. Robins, L. P. Cook[1], E. N. Farabaugh, A. Feldman and E. Etz[2]

1Electronic Materials Group
[2]Gas and Particulate Science Division/Center for Analytical Chemistry

Thin diamond films that are synthesized by chemical vapor deposition have
the potential to be utilized in a number of applications in optics and
optoelectronics. An example of a potential optical application is an anti-
reflection coating for a high-index infrared window material such as
germanium. A potential optoelectronic application is a blue or violet
visible light-emitting diode.

The goals of this project are to determine which properties of the films
need to be modified for the films to perform well in various
optical/optoelectronic applications; to find relationships between the key
properties and film processing parameters; and to produce films with
improved properties for optical/optoelectronic applications. The influence
of structural defects and chemical impurities on the optical and
optoelectronic properties of the films is one of the key areas where
additional fundamental knowledge is needed, for the following reasons: (1)
the intrinsic optical properties of diamond, in the absence of defects and
impurities, are already well characterized; (2) performance of the films in
many of the intended applications is expected to be limited by defect-
related rather than intrinsic properties.

We have selected luminescence spectroscopy, in particular
cathodoluminescence (CL) imaging spectroscopy in the scanning electron
microscope (SEM), as a primary characterization technique. This technique
has the following advantages. Luminescence is a very sensitive probe of
the optical transitions of defects and impurities. Defects may often be
observed by luminescence when the optical transitions are too weak to
observe directly by optical absorption, especially in the case of thin
films. Further, unlike optical reflectance and transmittance measurements,
luminescence does not require films with optical-quality surfaces. This is
important because the diamond films grown at present are polycrystalline
and have rough, highly faceted surfaces. When CL is excited in the SEM,
the electron optics can be used to map the spatial distribution of
luminescence centers (those defects or impurities that give rise to
observable luminescence) with sub-μm resolution. Further, the CL image of
a given sample can easily be compared to the corresponding secondary-
electron image. The distribution of luminescence centers can thus be
correlated with film morphology and microstructure.

CL spectra have been examined for a number of films grown in our lab by the
hot-filament CVD method. The films were grown in two different hot-
filament deposition systems, and the following deposition parameters were
varied: (1) substrate temperature; (2) gas composition (methane/hydrogen
ratio); (3) deposition time. As reported last year, by searching the
literature we tentatively identified four distinct luminescent defect
structures in a set of films grown at different temperatures. These
structures are: (a) single-atom vacancy; (b) vacancy paired with nitrogen

impurity atom; (c) nitrogen impurity, either in interstitial site or paired with carbon interstitial; and (d) defect associated with dislocation, possibly donor-acceptor pair. More recently we have observed the same defects in films grown with different gas compositions and deposition times. We also observed CL from defect (d) in a large, gem-quality diamond. Our analysis shows that CL arises primarily from the {100} crystal surfaces in both the CVD-grown films and the gem; further, the CL intensity from the best CVD-grown films is similar to that from the gem.

Other spectroscopic characterization techniques, which provide related or complementary information to the CL experiment, are also being used to study the diamond films. Two such techniques are photoluminescence (PL) and Raman scattering excited by an argon-ion laser. Raman scattering is a probe of the lattice vibrational frequencies and thus of the short-range structural order. Laser Raman and PL spectra have been measured as a function of two deposition parameters, methane/hydrogen ratio and deposition time. The Raman spectra indicate that the structural order is very sensitive to methane/hydrogen ratio, with non-diamond carbonaceous phases playing an increasing role in the films grown with methane/hydrogen ratios greater than 0.5%. As a function of deposition time, the non-diamond phases seem to grow most rapidly at the same time that a continuous polycrystalline film is first formed, and are less noticeable at earlier or later times. (This interpretation of the data is still speculative, and will require further experimental confirmation.) A very broad and structureless PL spectrum, which underlies the Raman spectrum, appears to be directly correlated with the non-diamond carbon phases. This PL is probably different from any of the emissions observed in CL.

Another technique that we are using is PL excitation (PLE) spectroscopy. In this experiment, PL is excited by a wavelength-tunable ultraviolet light source; the total PL intensity is monitored as the excitation wavelength is varied. The fundamental optical absorption edge of diamond, at 5.5 eV, has been observed in several films by this technique. By comparing the results of the PL excitation and Raman measurements, we find that the PLE efficiency just above the fundamental absorption edge is inversely correlated with the presence of non-diamond phases (or directly correlated with the structural perfection of the diamond). In Fig. 33, we shown PLE spectra of a high-quality CVD film, grown with a methane/hydrogen ratio of 0.0025 at 750°C, and also the PLE spectrum of a diamond gem. The optical absorption spectrum of one film, grown on a fused-silica substrate, was measured more directly by the integrating-sphere diffuse transmittance method. For diamond films deposited under similar conditions, the line shape of the absorption spectrum in the region of the fundamental edge, as measured by diffuse transmittance, is found to correlate very well with the line shape of the PL excitation spectrum in the shape spectral region. In Figure 34, we show the diffuse transmittance spectrum of the film on the fused-silica substrate together with the PLE spectrum of a similar film.

We plan to continue and broaden our studies of the effect of process parameters on the luminescence and optical properties of diamond films. One area that we have begun to study and would like to understand better is the development of different bonding structures and defects as a function

of deposition time. We plan to begin to investigate some additional processes that are likely to introduce new types of optically active defects or impurities into the films. One such process is doping the films with optically active impurities such as nitrogen, boron, or lithium. We have made tentative arrangements to study lithium- or boron-doped films supplied by an outside source; boron and lithium are of interest as electrically as well as optically active impurities. Other potentially important post-deposition processing steps are radiation-induced damage (e.g., electron beam, ion beam, synchrotron), which can lead to the creation of additional defects in the films, and thermal annealing, which can lead to aggregation or other changes in the structure of pre-existing defects and impurities. Experiments on other types of diamonds suggest that complex defect structures can be formed by various combinations of chemical doping, radiation damage, and thermal annealing steps. One such complex defect in diamond, the H3 center (nitrogen-vacancy-nitrogen), has been observed to be laser-active.
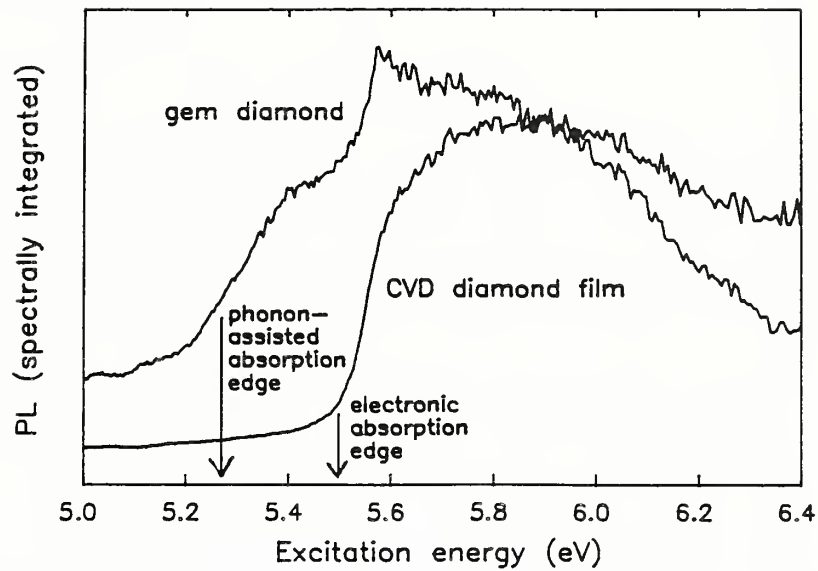
Figure 33.   PLE spectra of CVD-grown film, grown with
methane/hydrogen ratio of 0.0025 at substrate
temperature of 750° C for 72 hours, and of gem
diamond; same excitation conditions for both
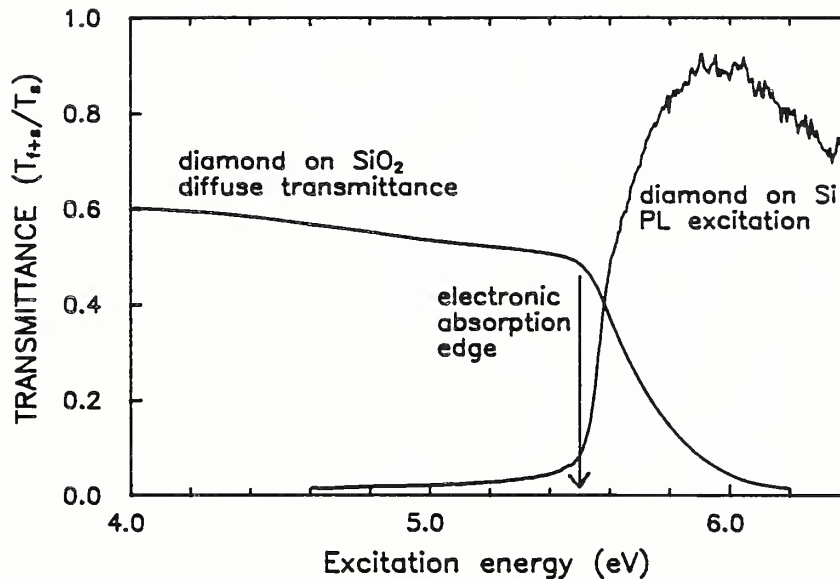spectra.

Figure 34.   Diffuse transmittance spectrum of CVD-grown film on
fused-silica substrate, and PLE spectrum of film on
silica substrate. Both films were grown with a
methane/hydrogen ratio of 0.0025 and a substrate
temperature of 750° C.

Thermomechanical Detwinning of Superconducting $YBa_2Cu_3O_{6+x}$ Single Crystals

D. L. Kaiser, F. W. Gayle[1], L. J. Swartzendruber[1], W. Wong-Ng[2], S. F. Watkins[3], F. R. Fronczek[3] and R.S. Roth[2]

[1]Metallurgy Division
[2]Electronic Materials Group
[3]Department of Chemistry, Louisiana State University, Baton Rouge, LA

The presence of twins in "single crystal" and polycrystalline ceramic specimens of the superconducting, orthorhombic $RBa_2Cu_3O_{6+x}$ phases (R = rare earth elements) has hindered our ability to resolve the effect of a-b anisotropy on the physical properties. Furthermore, the role of twins and twin boundaries in important physical phenomena such as magnetic flux pinning is not known. These issues can only be addressed through studies on untwinned crystals.

We have developed a novel process, which depends upon ferroelastic behavior of the material, to completely remove twins from $YBa_2Cu_3O_{6+x}$ single crystals. In the process, a uniaxial compressive stress is applied to a twinned crystal along an a/b axis at elevated temperature. Under such an applied stress, conditions are energetically favorable for the smaller a-dimension to be aligned along the direction of the stress. This occurs when oxygen atoms within the domains with the b-axis aligned along the stress direction jump into adjacent sites, converting these domains into the more favorable a-axis configuration. The end product is a fully untwinned crystal.

For these investigations, single crystals were grown from Y-Ba-Cu-O melts in gold crucibles. The crystals were annealed in oxygen gas to obtain sharp superconducting transitions at 90 K as measured by d.c. magnetic susceptibility. The crystals had smooth, flat facets which allow for the application of a uniform compressive stress on two opposing parallel faces. Typical crystal dimensions were 100-400 μm in the a/b directions and 50-100 μm in the c direction. In the detwinning experiments, a crystal was placed between two fused quartz slides held in a parallel geometry by a clamp (see Figure 35). The spacing between the slides was established by a thickness of gold filler sheets. A force due to the weight of stainless steel blocks was applied to the crystal. The mass of the weight (typically 50 to 400 g) was selected to yield an applied stress in the range of 45-260 MPa. The rig was then heated to temperatures in the range of 420 to 600°C for 1 to 40 hrs.

Reflected polarized light optical microscopy was used for the initial determination of twin removal. A crystal observed with reflected polarized light is shown before and after a detwinning treatment in Figure 36. The as-grown, orthorhombic crystal exhibits characteristic (110) type twin bands (Figure 36a). After twin removal, the crystal contains a single apparent orientation (Figure 36b, 36c). Since polarized light optical microscopy is not sensitive to microtwinning, the crystals were examined with a Buerger x-ray precession camera, which is sensitive to microtwinning. A typical precession photograph of a twinned crystal exhibits splitting of some of the spot reflections; the absence of spot

splitting in the detwinned crystals confirmed that the crystals were fully untwinned.

At 600°C, twins were completely removed after 1 hr. However, oxygen loss at this temperature reduced T_c to 54K. Subsequent annealing in oxygen gas at 420°C for extended times (> 200 hrs) raised T_c to 89K. Detwinning at lower temperatures (420-450°C) required several 40-hour treatments at successively higher applied pressures for complete twin removal. These crystals did not lose oxygen and thus had T_c values of 90K after detwinning.

Magnetic susceptibility measurements were performed on the crystals with a Superconducting Quantum Interference Device (SQUID) magnetometer. These measurements give T_c (which relates directly to the oxygen concentration) and critical current density (which relates to the degree of flux pinning). Magnetic studies were conducted throughout this investigation to determine the conditions of the detwinning and post-annealing processes needed to obtain untwinned crystals with sharp (2-3K wide) superconducting transitions at 90K. Measurements of magnetization vs. applied magnetic field loops have shown that flux pinning behavior and critical current densities are comparable in twinned and untwinned crystals, suggesting that twin boundaries are not the principal flux pinning sites in this material. However, the significant size and shape corrections which are required to compare different crystals make these results preliminary. To obtain unambiguous information on the effect of twin boundaries on flux pinning, it is necessary to measure the same crystal in the twinned and untwinned states.

In conjunction with this investigation, recent studies on a single crystal which contains predominantly one variant of twin boundary have provided the first direct evidence of an effect of twin boundaries on magnetic properties. Further studies are in progress to fully understand the role of twin boundaries in flux pinning and to determine anisotropy of the magnetic properties along the a and b crystallographic directions.

Crystal structure determination of $YBa_2Cu_3O_{6+x}$ has been complicated by the presence of twins. We have performed single crystal x-ray diffraction studies on twin-free crystals in collaboration with Louisiana State University to obtain unambiguous structural data. Measurements at 115K and room temperature have been completed on a crystal with T_c=54K. Determinations of oxygen positions and occupancies in the Cu-O basal plane have been refined, showing that the O(5) site is completely vacant, and the O(4) atoms are offset from the crystallographic mirror plane positions by 0.15 Å in a zig-zag fashion. These results represent the first observation of zig-zag Cu-O chains by an x-ray study. Gold, which is a common impurity in crystals grown by the present technique, was found to occupy Cu(1) sites only. Weak superlattice reflections were also observed, suggesting a possible three-dimensional ordering of O and/or Au. Measurements are in progress on an untwinned crystal with T_c=89K. Superlattice reflections were also observed in this crystal. Further experiments will be conducted to determine the nature of these superlattice reflections.
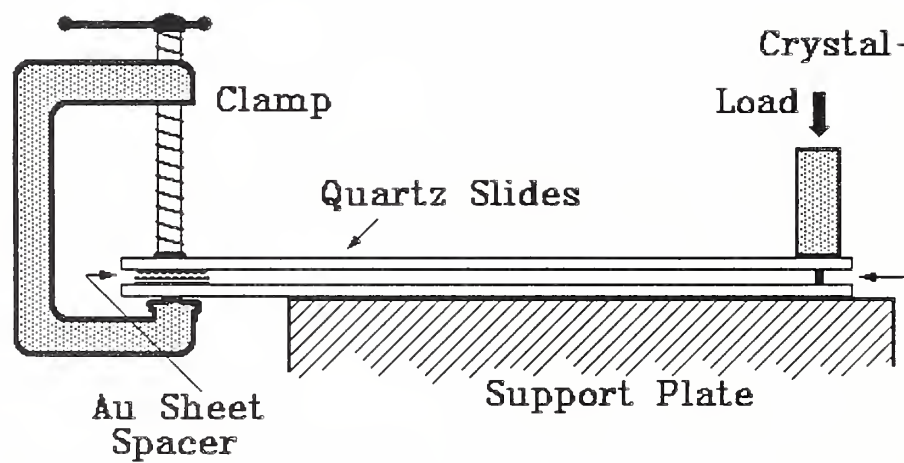
Figure 35.   Schematic diagram of the experimental apparatus
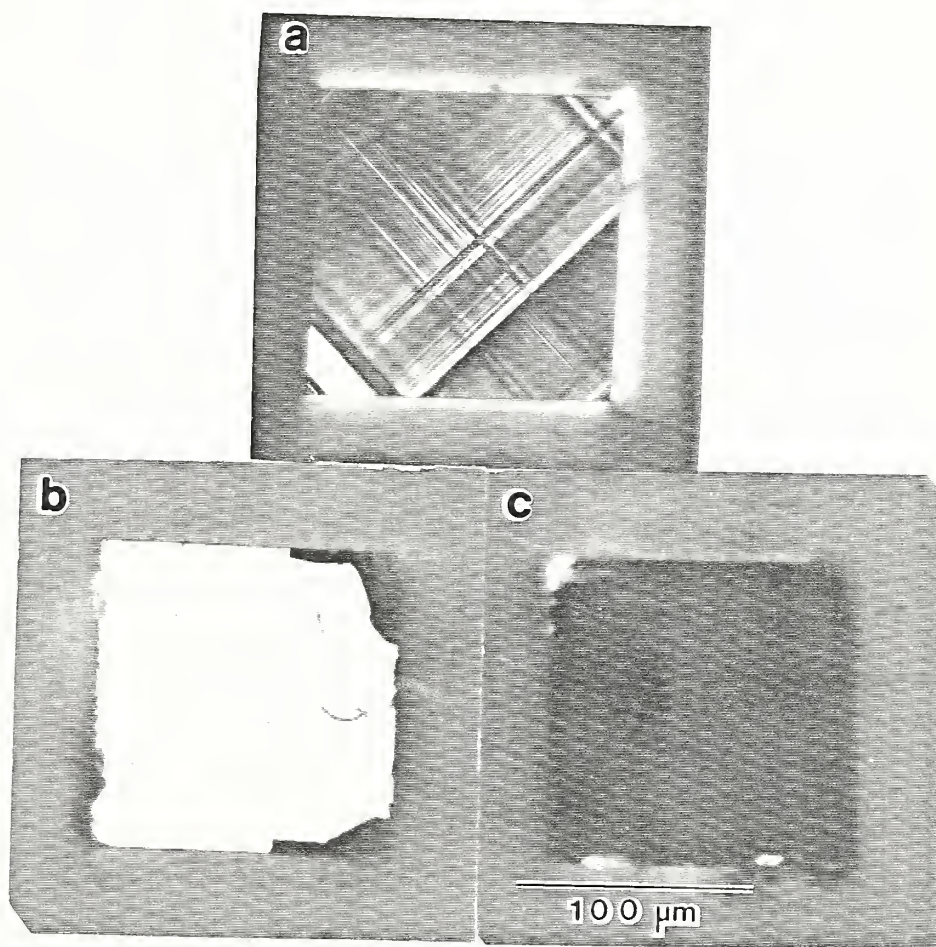used to detwin $YBa_2Cu_3O_{6+x}$ single crystals.

Figure 36.   Polarized light optical micrographs:(a) twinned
crystal; (b) the same crystal after the detwinning
treatment. The crystal has been rotated 90° from
(b) to (c) showing the a-b anisotropy in the
reflectivity associated with the orthorhombic
structure.

High resolution X-ray imaging with synchrotron radiation is being developed on NIST/IMSE beamline X23A3 at NSLS. The sample is illuminated by nearly parallel radiation from a double flat crystal monochromator using asymmetrically cut crystals. The sample image, which may be radiographic or topographic, is magnified in two dimensions by extremely asymmetric diffraction from two flat crystals. Magnification factors over 100 have been achieved. The magnified image is detected by an X-ray sensitive charge coupled device (CCD) area detector with 20 micron square pixels. Thus, submicron sample features may conceivably be resolved. So far, a resolution of 1 to 2 microns has been demonstrated for both radiography and topography.

A key goal is an understanding of the factors which limit the resolution, in hope that they can be circumvented. From the standpoint of geometrical optics, the resolution may be computed from the source characteristics and the transfer functions of the optical elements. The least known source characteristic, its size, has been carefully measured on beamline X23A3. It remains to compute the resolution, using theoretical values for the transfer functions. For asymmetrically diffracting optical elements, it is expected that wavelength dispersion may be an important factor affecting the resolution. From the standpoint of physical optics, Fresnel diffraction may be important. Intensity oscillations across a knife edge have been observed, similar to Fresnel diffraction. Diffraction calculations are contemplated, taking into account the non-plane wave, non-spherical wave nature of synchrotron radiation.

Development of Micron-Resolution, Two-Dimensional X-Ray Imaging for Studies of Interfaces.

R. C. Dobbyn, R. D. Spal and M. Kuriyama

Electron microscopy and scanning microscopy show the presence, an outline, of microscopic device features, but fail to reveal the microstructural or mesoscopic details of changes in these features created during processing, because of a lack of sensitivity to lattice irregularity. Highly parallel synchrotron X-radiation can reveal not only the outline of these structures (by microradiography) but also sensitive details of their microstructure before, during and after processing (by monochromatic diffraction imaging).

These challenges can be met using the high brilliance, highly collimated, tunable synchrotron radiation in combination with two dimensional X-ray image magnification and high-resolution digital video detection, as developed within IMSE. In collaboration with scientists from industry, one micron-size feature in electronic device materials have been successfully imaged in real time, using a two dimensional CCD imaging detector with $20\mu m$ square pixels in combination with 80x - X-ray image magnification. Preliminary results show that these new techniques are not only feasible but possess great potential.

For device materials, such as GaAs, InP, energy tunability of the synchrotron radiation is a powerful tool to increase the penetration of X-rays through the materials. However, the anomalous transmission effect in

dynamical diffraction permits X-rays to go through a one-half millimeter-thick sample, easily, almost regardless of X-ray energy. This mode of observation, diffraction imaging, does not give a direct radiographic image but does provide a microstructurally sensitive image in both the transmission and the Bragg diffracted directions.

Figure 37 shows an anomalous transmission image under the (220) diffraction condition, precisely tuned to the surface region of a solid state laser device, V-shaped groove features (A) in InP. The image magnification used in the observation of this region (A) was 16x with 12 keV radiation. These "grooves" were designed to have a 1.5μm width. However, the observed images are much wider, indicating that a diffusion layer must have increased the size of the designed crescent laser region and created a strain field around it.
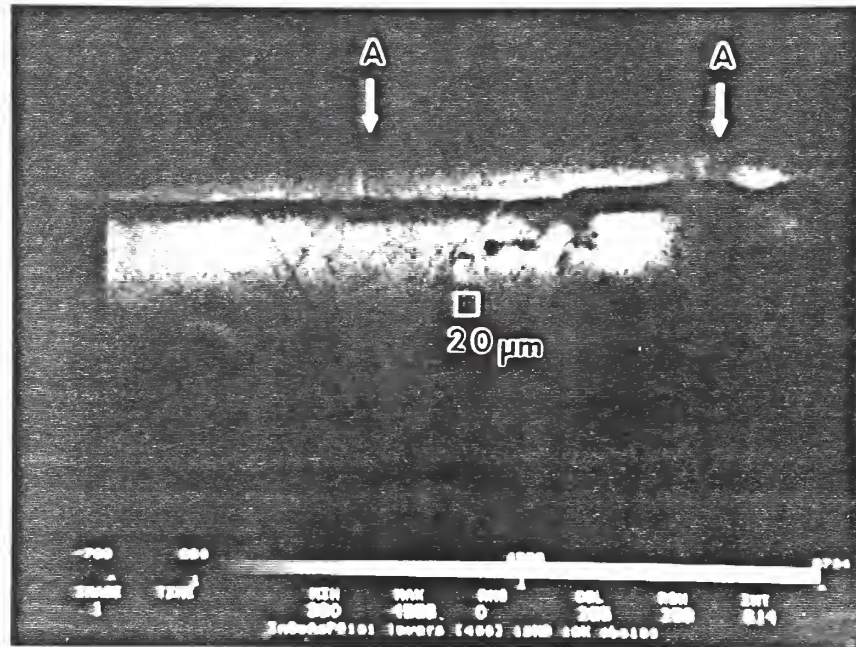
Figure 37.   Anomalous transmission image of a solid state laser device in InP. (In collaboration with scientists at Rockwell International.) This is a cross-sectional view, in which the surface region (A's) is tuned to the precise Bragg condition.

Advanced Synchrotron Radiation Analysis of Polycrystalline Ceramics.

D. R. Black, H. E. Burdette, R. D. Spal and M. Kuriyama

Consolidation of structural materials as industrial products often requires the preselection of the size and shape of individual component particles, such as powder, before they are formed in shape for processing. Normally, particle size, orientation, shape, strain and their distributions are considered to be determined by a traditional diffraction profile analysis using a commercial θ-2θ scanning diffractometer. However, this analysis method is not only cumbersome, but quite inaccurate, depending entirely on the investigators' chosen mathematical models of particle size and shape and the assumption of statistically uniform distributions. The advent of a highly parallel (a few arc second divergence) X-ray beam prepared from synchrotron radiation eliminates dependence on these models.

In conventional diffractometry a large sample volume is bathed by a divergent X-ray beam and a detector is placed on an X-ray focussing circle (Rowland circle). This X-ray optical arrangement relies on an underlying assumption that the property (such as shape, size and strain) to be measured is spatially invariant over the dimensions of the experimental probe (that is, the beam size) so that a spatial average of that property has meaning. If this assumption is true, diffraction profiles are smooth with a high signal-to-noise ratio. Each particle makes a contribution, but the actual contribution of any individual particle is not distinguishable. Because of this averaging, extraction of information, if successful, about the particles requires sophisticated mathematical analysis based on models. As new materials are developed by more sophisticated processes the validity of this ensemble average needs to be examined by techniques that treat the particles at a more fundamental level.

With a highly parallel beam, diffraction lines are actually composed of numerous small image spots, although they are grouped to form a "Debye-Scherrer" ring. The technique developed at the IMSE synchrotron beamline is to image individual particle spots with a real time video camera or film, located at the scattering angle for the desired Bragg diffraction, while the sample is rotated. A special coupled rotation stage was developed to guarantee the sample and detector rotational axes to be coincident. The incident beam divergence is normally 2 arc seconds in the vertical direction and 30 arc-seconds in the horizontal direction, with a 1mm x 0.2mm cross-section. These conditions can be adjusted as required. The following figures show some of the results obtained with 10 and 8 keV monochromatic beams from several samples.

Figure 38 shows enlarged diffraction images of individual particles of SiC. A variety of microstructures are revealed, although each particle is indeed a "single" crystal.

Figure 39 shows the distribution of particle sizes which were measured from the diffraction images. Comparison is made with optical microscope measurements of the original powder.
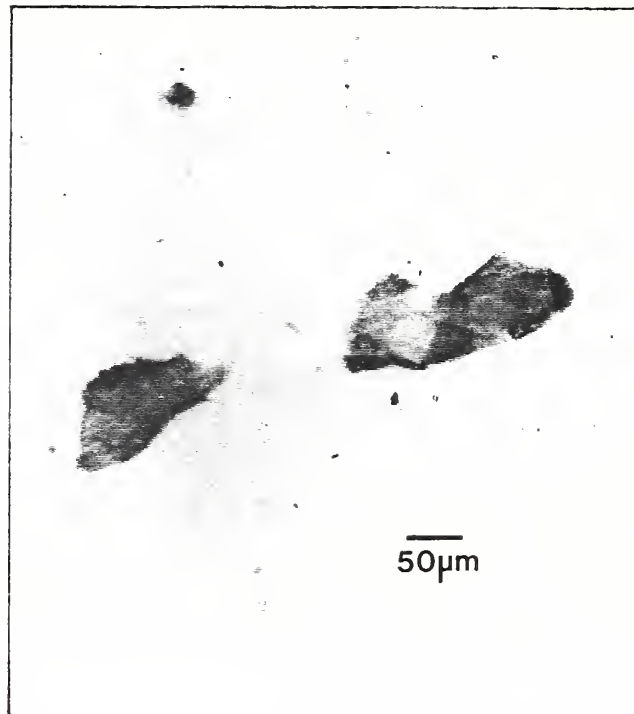
Figure 38.   Diffraction images, using 10 keV X-rays, from single particles of SiC.
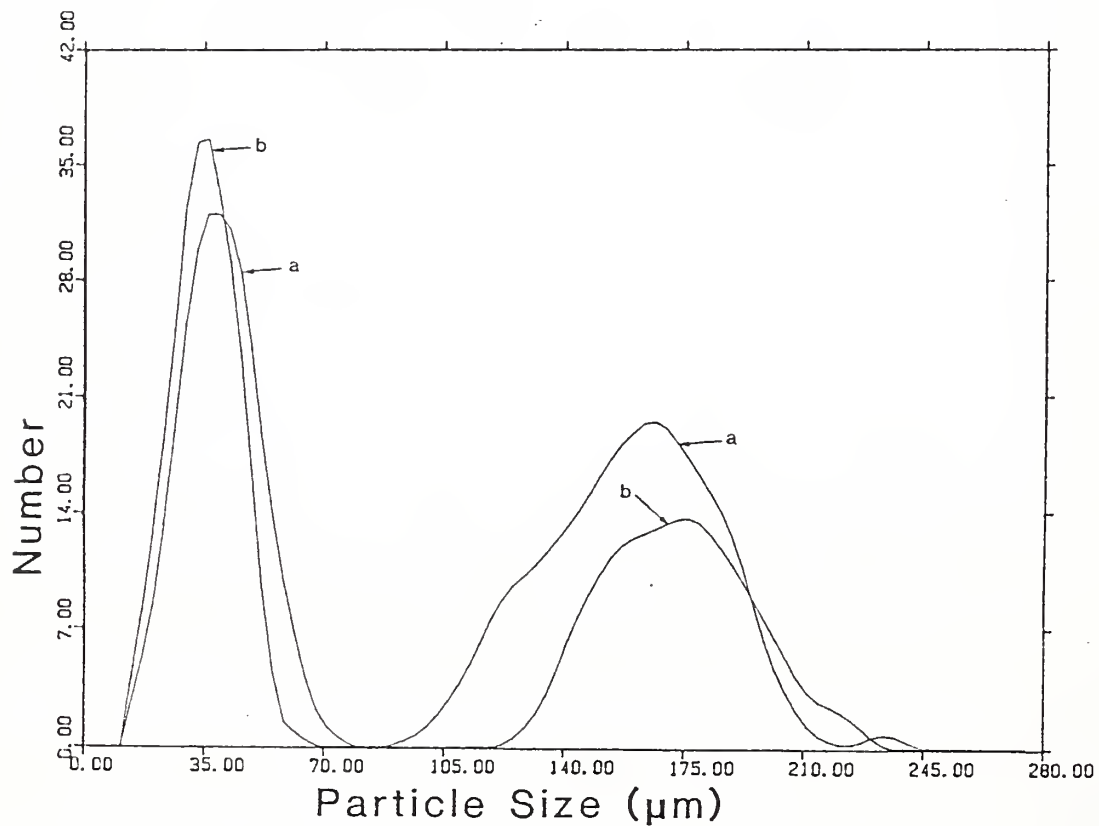

Figure 39.   Measured particle size distributions of a mixture of 80 (177 μm) and 280 (35μm) grit SiC powder from a) diffraction images and b) optical microscopy.

Figure 40 shows the degree of preferred orientation in 95% rolled copper
compared with the unpreferred annealed original material. The(220) plane
in each particle becomes parallel to the material surface after
rolling. Particularly the [112] was shown to be parallel to the direction
of rolling, judging from images taken with different azimuthal orientation.

The use of an additional X-ray analyzer crystal placed after the sample
enables us to distinguish the misorientation of each grain from lattice
parameter variations, or strain variation, with high precision. This
figure shows the diffracted intensity from the analyzer as it is scanned
through the scattering vectors corresponding to the (100) and (010) lattice
parameters of a high T_c superconducting single crystal.
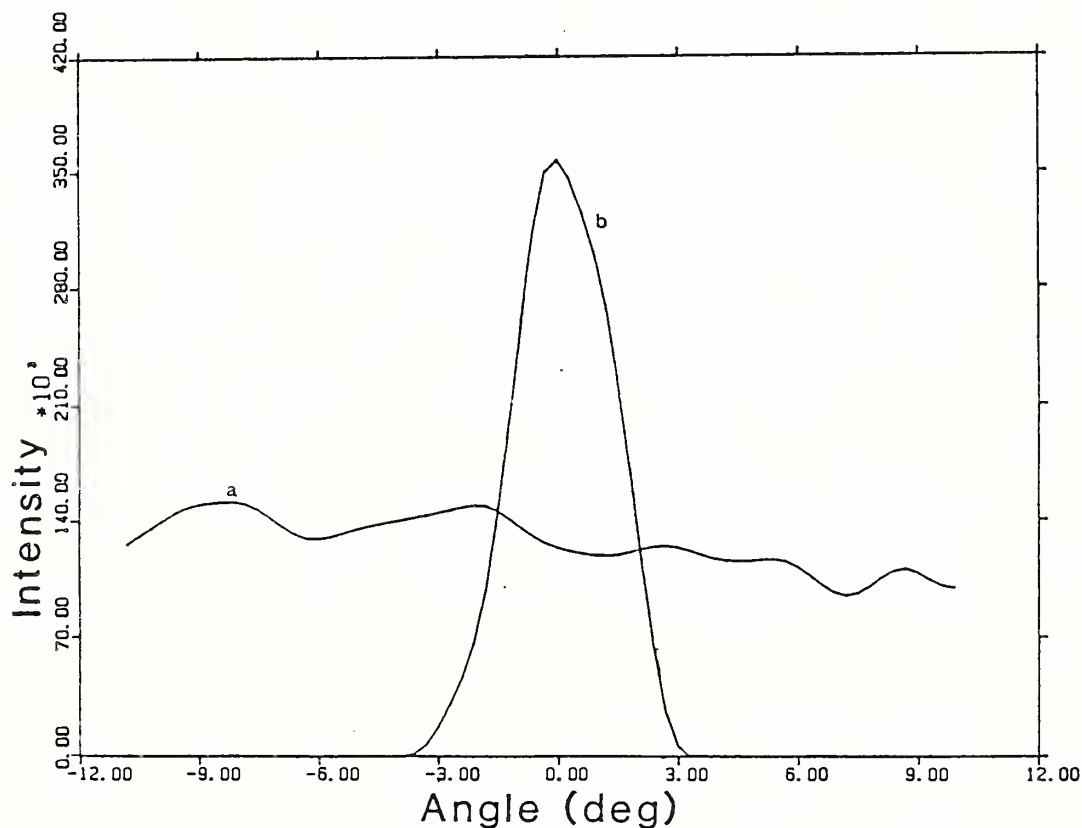
Figure 40.   The intensity of the (220) diffraction, at 8 keV, as a
              function of angle with respect to the sample normal, 0°, of
              a) annealed copper and b) 95% rolled copper. Negative angle
              is toward grazing incidence.

113

Synchrotron Diffraction Imaging Analysis of Advanced Single Crystals for Electronic and Photonic Applications.

B. W. Steiner, R. C. Dobbyn, H. E. Burdette and M. Kuriyama

The Institute's ultrahigh resolution diffraction imaging beam line (X23A3) at the National Synchrotron Light Source at Brookhaven National Laboratory has been devoted in part to determination of the mesoscopic structure of a variety of electronic and photonic materials. Initial effort in this area has been concentrated on a study of undoped semi-insulating gallium arsenide.

The principal defects observed in undoped gallium arsenide by many techniques are: 1) a cellular structure and 2) a set of orthogonal, very low angle subgrain boundaries in (110) planes. The former were widely assumed to result from polygonized dislocations, and this seemed to have been confirmed by thermal calculations involving a critical stress model; no detailed causal connection with the subgrain boundaries had been postulated. However, research both by conventional x-ray topography and electron microscopy had led the most careful workers to conclude that the cellular structure was unrelated to dislocations because it did not obey the traditional visibility laws of diffraction imaging.

High resolution work carried out on our beam line has shown for the first time that the observation of the cellular structure indeed obeys new visibility law (Kuriyama, et. al: Phys. Rev. B (1989) 38 12421). We have shown that this structure is due to interfaces formed in (110) planes that fulfill two additional criteria: 1) coherence is preserved across the interface, and 2) an atomic phase shift occurs at the interface. These characteristics have led us to postulate that these interfaces are in fact antiphase boundaries incorporating a lattice tilt of about 2 arc seconds (Steiner, et. al: J. Appl. Phys. (1989) 66 559). This postulate satisfactorily explains for the first time all of the observations of mesoscopic structure in undoped gallium arsenide: the cellular structure and its visibility as a function of diffraction conditions and angular resolution; the very low angle subgrain boundaries; and futhermore, the anomalously increased angular broadening observed under the {444} asymmetric diffraction conditions. The tilt may be ascribed to the differing nature of the (homopolar) chemical bonds across the antiphase interface.

To understand the structural nature of these interfaces, diffraction imaging work has been extended to undoped samples prepared under different growth conditions and under different heat treatments after growth, in collaboration with scientists in universities and industry. For this purpose, a systematic analysis of images as a function of process parameters is required, and is being carried out.

Research is being continued to determine what types of mesoscopic structure becomes typical in different electronic and photonic materials, such as doped GaAs, and CdTe, particularly under specific growth conditions and heat treatments. Real time, in-situ observation of structural changes at elevated temperatures has been initiated with various materials.

EXPLORATORY PROJECTS

Microwave Processing of Ceramic Materials

J. S. Wallace

Recent work has indicated exciting and potentially enormous possibilities for utilizing microwave energy in processing of materials. Some of the most exciting possibilities exist for ceramic materials where the microwave energy can be directly dissipated within the material. This offers wide range of uses, including direct heating of ceramic powders to temperatures where densification, or sintering, occurs. In addition, microwaves might also be used as a probe for identifying internal changes within a material, such as reactions and melting. Since microwave energy is absorbed according to not only the chemistry, microstructure and temperature of the material, but also the frequency of the microwaves, the possibility of tailoring the energy input also exists. For example, it may be possible to selectively deposit energy into a precursor material in order to decompose it without significantly heating the surrounding material.

Since the conditions of energy absorbtion are selective, a wide range of materials must be investigated to understand and appropriately apply microwave processing to ceramics. In order to determine the effects of microstructure, chemistry and crystallinity on material interactions with microwave energy, amorphous, single crystal and polycrystalline materials, both pure and doped, are scheduled to be investigated. These materials are to include alumina, silica and zirconia because of their commercial importance, and dopants such as iron oxide and magnesia because of their common occurrence in oxide ceramics. Reports of grain boundary melting during sintering of oxide ceramics also make it necessary to investigate the effect of microstructure on energy absorbtion. This effect will be characterized by comparing single crystal with polycrystalline materials. Measurement of amorphous and crystalline silica will give further insight into the effect of microstructure.

Because the deposition of energy is dependent upon physical relaxation phenomena which are rate and mobility dependent, measurements must be made over a wide range of frequencies and temperatures. Understanding of these energy absorptive mechanisms in well characterized ceramics is necessary to understand how microwaves interact with the more complex commercially available materials. Indeed, this and similar data may allow tailoring of new materials to make optimum use of microwave absorbtion. With this set of data on well-characterized ceramic materials, the full potential of microwave energy in processing of ceramic materials can be accurately evaluated.

Preliminary dielectric constant measurements have been made on pure fused silica at room temperature. The measured data correlate well with those in the literature over the frequency range measured, 9 to 11 GHz. Significant difficulties have been identified, however, in making similar measurements over a wide range of elevated temperatures at microwave frequencies. Under these conditions, coefficient of thermal expansion differences can result in large measurement errors for the wave guide technique utilized here.

Metallorganic Chemical Vapor Deposition of Ferroelectric Oxides

D.L. Kaiser

Ferroelectric oxides, such as $LiNbO_3$, have large electro-optic coefficients, which are important for optoelectronic applications. Single crystals or epitaxial films of these materials are useful for switches and modulators in optical signal processing and optical communications systems. Expense in growing high-quality single crystals and difficulties in growing epitaxial films by standard processes have limited the commercial implementation of optoelectronic devices based on ferroelectric oxides.

This project was undertaken to explore the feasibility of metallorganic chemical vapor deposition (MOCVD) processes for thin film growth of ferroelectric oxides for optoelectronic applications. An MOCVD system was designed for the experiments. The system is considerably more complex than the commercially available semiconductor deposition systems due to the higher temperatures required for vaporization of the metallorganic compounds for oxides. In additional, the system was designed for maximum flexibility of the processing parameters (gas flow rates, total gas pressure, precursor and substrate temperatures) to allow for film growth of a wide variety of oxide materials. Construction of the system is nearing completion. Initial experiments will focus on deposition of $BaTiO_3$.

RESEARCH STAFF

Powder Synthesis and Characterization

Bartenfelder, David C.   o Ceramic powders and suspensions characterization
    o Surface chemistry of powders

Cline, James P.   o High-temperature X-ray diffraction
    o Microstructural effects in X-ray diffraction
    o Standard reference materials

Hegemann, Bruce E.   o Time-resolved micro-Raman spectroscopy
    o Micro-FTIR spectroscopy
    o Laser-induced fluroescence spectroscopy

Kelly, James F.   o Quantitative scanning electron microscopy
    o Image analysis
    o Microstructure analysis
    o In-situ crack propagation studies

Long, Gabrielle G.   o Small angle neutron scattering
    o Small angle X-ray scattering
    o Surface EXAFS

Lum, Lin-Sien H.   o Powder characterization
    o Instrumental analysis

Malghan, Subhas G.   o Powder and dense slurry characterization
    o Colloidal processing and forming
    o Interfacial and surface chemical studies

Minor, Dennis B.   o Analytical SEM of ceramics and particulates
    o Powder test sample preparation
    o Powder characterization
    o High temperature ceramic synthesis

Pei, Patrick   o Chemical instrumental analysis
    o Separation of complex organic mixtures
    o Characterization of lubricants and lubricant products
    o Trace organic compound identification

Ritter, Joseph J.   o Ceramic powders from organometallic precursors
    o Ceramic powders from solution precipitation reactions

Wallace, Jay S.   o Processing-microstructure-property relationships
    o Forming, compaction and sintering
    o Processing of high T_c ceramic superconductors
    o Processing of structural ceramics

Wang, Pu Sen   o Solid state NMR
    o Nuclear magnetic imaging of materials
    o Surface characterization by X-ray photoelectron and Auger spectroscopy

Mechanical Properties

Blackburn, Douglas H.
- o Glass properties
- o Melting of glasses

Chuang, Tze-jer
- o Ceramics
- o Diffusional crack growth
- o Finite element analysis
- o Creep theory

Coyle, Thomas W.
- o Processing/microstructure/fracture relations
- o Toughening mechanisms in ceramics
- o Processing and properties of ceramic composites
- o Stress induced transformations

Cranmer, David C.
- o Ceramics and glasses
- o Ceramic matrix composites
- o Viscosity

Hockey, Bernard J.
- o Ceramics
- o Scanning and transmission electron microscopy
- o Interfaces
- o Microstructure

Horn, Roger G.
- o Surface forces
- o Tribology
- o Colloidal science

Kauffman, Dale A.
- o Glass melting

Krause, Ralph F. Jr.
- o Fracture mechanics of ceramics
- o Creep and creep rupture behavior
- o Hot pressing and composite fabrication
- o Vaporization equilibria

Lawn, Brian R.
- o Microstructure/strength relations
- o Fracture mechanics
- o Contact phenomena
- o Surface forces in fracture

Ostertag, Claudia P.
- o Influence of heterogeneities on sintering
- o Processing and sintering of reinforced ceramics
- o Processing & reinforcing ceramic superconductors
- o Grain alignment of high T_C ceramic superconductors

Roberts, D. Ellis
- o Mechanical Properties

Smith, Douglas, T.
- o Surface forces

Wiederhorn, Sheldon M.
- o Ceramics
- o Fracture
- o Reliability
- o Creep rupture

Tribology

Duvall, William W.   o Wear test analysis

Ives, Lewis K.   o Wear of materials
                           o Transmission electron microscopy
                           o Mechanical properties

Jahanmir, Said   o Wear mechanisms
                           o Boundary lubrication
                           o Mechanical behavior of materials

Ku, Chia-Soon   o Lubrication of ceramics
                           o Lubricant oxidation, thermal stability and
                             volatility
                           o Lubricant degradation mechanisms

Perez, Joseph M.   o Additive chemistry and deposits
                           o Thermal and oxidation stability of fluids
                           o Fuels, lubricants and diesel engines

Peterson, Marshall B.   o Wear of materials
                           o Solid film lubricants
                           o Mechanical behavior

Ruff, Arthur W.   o Wear of materials
                           o Microstructure effects
                           o Mechanical behavior

Strakna, Timothy J.   o Self lubricating components

Whitenton, Eric P.   o Electronics
                           o Computer science
                           o Surface measurement

Electronic Materials

Blendell, John E.   o Ceramic processing and clean-room
                             processing
                           o Sintering and diffusion controlled
                             processes
                           o Processing high T_c ceramic
                             superconductors
                           o Activation chemical analysis

Block, Stanley   o Ceramic processing and high pressure
                             sintering
                           o Pressure-induced transformation
                             toughening
                           o High pressure physical properties and
                             structures
                           o High pressure X-ray diffraction and
                             spectroscopy

123

Chiang, C. K.	o Electronic ceramics
	o Superconductivity
Clevinger, Mary, A.	o Phase diagrams for ceramists
	o Computerized data
Cook, Lawrence P.	o Thermodynamics
	o Electron microscopy
	o Phase diagram evaluation
Freiman, Stephen W.	o Electronic ceramics
	o Mechanical properties
	o Composites
Hill, Michael D.	o Piezoelectric materials
	o Ceramic processing
Ondik, Helen M.	o Phase diagrams for ceramists
	o Database management systems
Piermarini, Gasper J.	o Ceramic processing and high pressure sintering
	o Pressure-induced transformation toughening
	o High pressure physical properties and structures
	o High pressure X-ray diffraction and spectroscopy
Rawn, Claudia J.	o Phase diagrams
	o X-ray diffraction
Raynes, Alan S.	o Fracture
	o Microstructure
Roth, Robert S.	o Crystal chemistry
	o Phase diagrams
	o Phase equilibria
Vaudin, Mark	o Electron microscopy of ceramic superconductors and of ceramic-ceramic and ceramic-metal composites
	o Microscopy and diffraction studies of interfaces
	o Computer modelling of grain boundary phenomena
	o Microstructural properties of advanced ceramics
White, Grady S.	o Ceramics and glass
	o Nondestructive evaluation
	o Subcritical crack growth

Wong-Ng, Winnie	o X-ray analysis
	o X-ray standards

Optical Materials

Farabaugh, Edward N.	o Thin film deposition and analysis
	o Scanning electron microscopy of diamond films
	o Surface analysis
	o Diamond films processing
Feldman, Albert	o Thermal properties of diamond films
	o Thin film optical properties
	o Diamond films processing
Frederikse, Hans P. R.	o Thin film thermal wave analysis
Kaiser, Debra L.	o MOCVD of oxide optical films
	o Single cyrstal high temperature superconductors
Robins, Lawrence H.	o Photoluminescence, cathodoluminescence of diamonds
	o Optical properties of diamond films

Synchrotron Radiation Analysis

Black, David R.	o Inelastic X-ray scattering
	o Energy dispersive diffraction
	o Fluorescence and absorption
	o Polycrystalline diffraction imaging
Burdette, Harold E.	o X-ray optics engineering
	o Crystal growth
	o Instrumentation
Dobbyn, Ronald C.	o X-ray imaging
	o X-ray optics
	o Microradiography
	o Diffraction imaging
Kuriyama, Masao	o Scattering physics
	o Condensed matter physics
	o Crystallography
Spal, Richard D.	o X-ray optics
	o X-ray image detectors
	o Condensed matter physics
	o Diffraction physics
Steiner, Bruce W.	o X-ray diffraction imaging
	o Optoelectronic materials
	o Crystal growth

Data Base Activities

Begley, E. F.
- o Database management for scientific and engineering data
- o User-friendly interfaces
- o Materials property databases

Messina, C. G.
- o Bibliographic data modules
- o Data entry consistency specifications
- o System validation routines

Munro, R. G.
- o Material properties of advanced structural ceramics
- o Wear of ceramics under harsh tribological conditions
- o Analysis of complex and multivariate data relations

Division Office

Carpenter, J. A., Jr.,
- o Functional ceramics applications
- o Technical assessments
- o Industrial liaisons

Dapkunas, S. J.
- o Structural ceramics applications
- o Technical assessments

Hsu, S. M.
- o Tribology of ceramics materials
- o Advanced high temperature lubrication concepts
- o Wear maps concepts and methodology

Fuller, Edwin R.. Jr.
- o Influence of microstructure on fracture and other physical properties of materials
- o Toughening mechanisms in ceramics and ceramic composites, and their relations to processing
- o Interfacial fracture and toughening mechanisms in reinforced ceramic composites
- o Processing/property relations and phase equilibria of high T_c ceramic superconductors

GUEST SCIENTISTS AND GRADUATE STUDENTS

Amman, Mary	University of Maryland
Baker, Theresa L., Dr.	Ohio St. University
Balasubramanian, Raghuraman	Clarkson University
Barta, J., Dr.	ISCAR Ceramics, Inc.
Bennison, S. J., Dr.	Lehigh University
Brandon, D., Dr.	Technion, Israel
Bulter, Elizabeth	Lehigh University
Cho, Seong-Jai	Korea Standards Research Institute
Curtis, Martin	Naval Surface Warfare Center
Dally, James	University of Maryland
Deckman, Douglas E.	Pennsylvania State University
Divakar, Ramesh	Carborundum Company
Dong, Jie-Yi	E. China University, PRC
Dong, Xiaoyan	University of Tsinghua, PRC
Duvall, William W.	University of Maryland
Finkelstein, Y.	Rafael Laboratory, Israel
Gangopadhyay, A.	University of Maryland
Gartstein, Efim, Dr.	Georgia Institute of Technology
Gates, Richard S.	Pennsylvania State University
Gerhardt, R. A., Dr.	Rutgers University
Huang, N. M.	Korea Institute of Standards
Inglehart, L., Dr.	Johns Hopkins University
Kruger, Jerome	Johns Hopkins University
Laor, Uri, Dr.	Nuclear Research Center, Israel
Larsen-Dasse, J.	National Science Foundation

Lathabai, S., Dr.	Lehigh University
Lee, Soo W.	University of Illinois
Lim, Dae-Soon	University of Illinois
Liu, W.	University of Tsinghua, PRC
Miller, P. J., Mr.	Naval Surface Warfare Center
Mizuhara, Kazuyuki	Ministry of International Trade, Japan
Moudgil, Brij	University of Florida - Gainesville
Nakamura, T.	Meiji University, Japan
Paulik, Steven	Northwestern University
Ritter, Andrew, Dr.	Martin Marietta
Stewart, J., Dr.	University of Maryland
Strakna, Timothy J.	University of Maryland
Tanaka, D. K.	Johns Hopkins University
Trivedi, S. B.	Primrose Corporation of America, Inc.
Vandiver, P. B., Dr.	Smithsonian Labs
Wan, K-T.	Lehigh University
Wang, Yusha	University of Tsinghua, PRC
Whitler, John D.	University of Maryland
Wilson, Annie, M.	Oberlin University
Yellets, Jeffrey P.	Pennsylvania State University
Ying, Tsi-Ning	University of Tsinghua, PRC
Ying, X. T.	Fudan University, PRC
Zhang, Y.	University of Maryland
Zhang, Z.	Johns Hopkins University
Zheng, Pei-Yi	Research Institute of Petroleum Processing, Beijing, PRC

OUTPUTS AND INTERACTIONS

SELECTED TECHNICAL PUBLICATIONS

Powder Synthesis and Processing

Cline, J. P.; Kreider, K. G.; Shapiro, A.; Pens, A. R.; Rojas, A.; Azamar, J. A.; Maldonado, L. and Del Castillo, L. "Sputtered Thin Film YBa_2Cu_3O," AIP/AVS Proceedings of Topical Conference on High T_c Superconductors, ed. by George Margaratando, 1989.

Cline, J. P; Kreider, K. G.; Shapiro, A. and Moreland, J. "High T_c Superconducting Films on Silicon Wafers," submitted to Solid Thin Films.

Cline, J. P. and Shull, R. D. "High Temperature X-ray Diffractometry of Ti-Al Alloys," Proceedings of the 6th International Conference on High Temperatures, Chemistry of Inorganic Materials, ed. by J. W. Hastie, Humana Press, in press.

Hegemann, B. E.; Perez, J. M.; Ku, C. S.; Pei, P. and Hsu, S. M. "Characterization of Tricresylphosphate Lubricating Film by Micro-Fourier Transform Infrared Spectroscopy," STLE Trans., in press.

Hegemann, B. E.; Gangopadhyay, A. and Jahanmir, S. "Reduction of Friction Coefficient in Sliding Ceramic Surfaces by In-Situ Formation of Solid Lubricant Coatings," submitted to Leeds-Lyon Tribology Conference Proceedings.

Long, G. G.; Krueger, S. T. and Gerhardt, R. A. "SANS Characterization of Microporous Silica." To be published in Characterization Techniques for Ceramics.

Long, G. G.; Black, D. R. and Tanaka, D. K. "Refl-EXAFS at the Carbon K-Edge." Synchrotron Radiation in Materials Research, M.R.S. Vol. 143, pp. 157-162, 1988.

Long, G. G. and Krueger, S. T. "MSANS Characterization of the Densification of Alumina." Accepted for publication in J. Appl. Cryst.

Malghan, S. G. and Ostertag, C. Stress Relaxation in Sintering of Fiber Reinforced Composites Through Fiber Coating. 13th Annual Conference on Composites and Advanced Ceramic Materials, 1989.

Ritter, J. J. and Kelly, J. F. "A Study of the Hydroxycarbonate Precursor Route to the $YBa_2Cu_3O_{7-x}$ High T_c Superconductor", Proceedings of the 118th Meeting of the Metallurgical Society, Las Vegas, NV, February 27-March 2, 1989, WERB Approved, accepted for Proceedings.

Ritter, J. J.; Roth, R. S.; Rawn, C. J. and Burton, B. "Phase Equilibria in Portion of the System - SrO-CaO-Bi$_2$O$_3$-CuO, Part 1 - The System SrO-CaO-CuO", Journal American Ceramic Society - Communications, accepted for publication in August 89.

Ritter, J. J.; Lundy, D.; Swartzendruber, L. J.; Shull, R. D. and Bennett, L. H. "Studies of Magnetic Flux Penetration in a Chemically Synthesized Bi(Pb)SrCaCuO Superconductor", Journal of Superconductivity, Journal accepted 12/1/88.

Ritter, J. J.; Shull, R. D.; Shapiro, A. J.; Swartzendruber, L. and Bennett, L. H. "Magnetic Properties of Iron/Silica Gel Nanocomposites", Multicomponent Ultrafine Microstructures (edited by L. E. McCandlish, B. H. Kear, D. E. Polk, and R. W. Siegel) MRS Symposium Proc., Vol. 132 (1989), p. 179.

Wallace, J. S.; Fuller, E. R.; Raynes, A. S.; Freiman, S. W.; Blendell, J. E.; Balmer, M. L. and Hill, M. "Strength and Fracture Behavior of Ba-Y-Cu-O Ceramics." Accepted for publication in TMS proceedings, Las Vegas, NV (1989).

Wallace, J. S.; Mueller, D. R.; Ederer, D. E.; Rubensson, J-E.; Shuker, R.; Zhang, C. H.; Jai, J.; Callcott, T. A.; Dhong, D.; Toth, L. E.; Raynes, R. and Osofsky, M. "A Soft X-Ray Emission Spectroscopy Investigation of Bi$_2$Sr$_2$CaCu$_2$O$_8$," submitted for publication.

Wallace, J. S.; Bender, B. A. and Schrodt, D. J. "Effect of Thermochemical Treatment on the Strength and Microstructure of SiC Fibers," submitted to J. Mat. Sci.

Wang, P. S.; Hsu, S. M. and Wittberg, T. N. "Oxidation Kinetics of Silicon Carbide Whiskers Studied by X-Ray Photoelectron Spectroscopy," submitted to J. of Materials Science (London).

Mechanical Properties

Horn, R. G.; Hirz, S. J.; Hadziioannou, G.; Frank, C. W. and Catala, J. M. J. Chem. Phys., 90 (1989) 6767-6774, "A Re-evaluation of Forces Measured Across Thin Polymer Films: Non-Equilibrium and Pinning Effects".

Horn, R. G.; Smith, D. T. and Haller, W. Chem. Phys. Letters (in press, 1989), "Surface Forces and Viscosity of Water Measured Between Silica Sheets".

Aimard, N.; Wan, K. T.; Lathabai, S.; Horn, R. G. and Lawn, B. R. Submitted to J. Mater. Res. "Interfacial Energy States of Moisture-Exposed Cracks in Mica".

Helm, C. A.; Israelachvili, J. N.; McGuiggan, P. M. and Horn, R. G. Submitted to J. Colloid Interface Sci. "Molecular Mechanisms and Forces Involved in the Adhesion and Fusion of Bilayers".

Horn, R. G. and Smith, D. T. Submitted to J. Non-Cryst. Solids, "Measuring Surface Forces to Explore Surface Chemistry".

Cranmer, D. C. (INVITED), Bulletin ACerS, 68 [2] 415-419 (1989), "Fiber Coating and Characterization".

Ostertag, C. Accepted for publication in Advances in Ceramics, Proceedings of the Coble Symposium on Sintering of Ceramics. "Reduction in Sintering Damage of Fiber Reinforced Composites".

Ostertag, C. and Malghan, S. To be published in Cer. Eng. Sci. Proc., 1989. "Stress Relaxation in Sintering of Fiber Reinforced Composites Through Fiber Coating".

Bennison, S. and Lawn, B. Accepted for publication in Acta Metall. "Role of Interfacial Grain-Bridging Sliding Friction in the Crack-Resistance and Strength Properties of Nontransforming Ceramics".

Cho, S.-J.; Hockey, B.; Lawn, B.; and Bennison, S. Accepted for publication in J. Amer. Ceram. Soc., "Grain-Size Dependence of Brittle Wear of Ceramics with R-curve Behavior".

Lathabai, S. and Lawn, B. Accepted for publication in J. Mater. Sci. "Fatigue Limits in Noncyclic Loading of Ceramics with Crack Resistance Curves".

Lathabai, S.; Mai, Y. and Lawn, B. Accepted for publication in J. Amer. Ceram. Soc. "Cyclic Fatigue Behavior of an Alumina Ceramic with Crack Resistance Characteristics".

Hockey, B. J. and Wiederhorn, S. M. "Effect of Microstructure on the Creep of Reaction Bonded Silicon Carbide" Submitted to J. Amer. Ceram. Soc.

Wiederhorn, S. M.; Hockey, B. and Carroll, D. "Creep of Two Phase Ceramics". Accepted for publication in Advances in Ceramics, Proceedings of the Coble Symposium on Sintering of Ceramics.

Carroll, D. F. and Wiederhorn, S. M. J. Amer. Ceram. Soc., 72 [9] (1989). "A Technique for Tensile Creep Testing of Ceramics".

Cranmer, D. C. To be published in Proceedings of the International Symposium on Advances in Processing and Application of Ceramic and Metal Matrix Composites. "Determination of Fiber/Matrix Interfacial Properties of Ceramic and Glass Matrix Composites".

Cranmer, D. C.; Deshmukh, U. V. and Coyle, T. W. To be published in ASTM STP, Thermal and Mechanical Behavior of Ceramic and Metal Matrix Composites, 1989. "Comparison of Methods for Determining Fiber/Matrix Interface Frictional Stresses in Ceramic Matrix Composites".

Cranmer, D. C.; Freiman, S.; Fuller, E.; Haller, W.; Koczak, M.; Barsoum, M. and Deshmukh, U., NISTIR 89-4073, January, 1989. "Mechanical Property Enhancement in Ceramic Matrix Composites.

Tribology

Weeks, S.; Lawson, R.; Pei, P. and Hsu, S. M.   "The Design and
Construction of a Chemiluminescence Apparatus for the Study of Complex
Hydrocarbon Oxidation," Lub. Eng., 45, 1, 9-15, 1989.

Lockwood, F. E.; Bridger, K. and Hsu, S. M.   "Heats of Immersion, Friction,
and Wear of Base Oil Fractions," J. of Tribology, in press.

Munro, R. G. and Hsu, S. M.   "Advanced Ceramics: A Critical Assessment of
Wear and Lubrication," GRI-88/0290, Gas Research Institute, Chicago, IL,
January 1989.

Hsu, S. M.; Klaus, E. E. and Cheng, H. S.   "A Mechano-Chemical Descriptive
Model for Wear under Mixed Lubrication Conditions," Wear, 128, 307-323,
1988.

Hsu, S. M.; Pei, P.; Ku, C. S.; Lin, R. S. and Hsu, S. T.   "Mechanisms of
Additive Effectiveness," Lub. Sci., 1, 2, 165-184, 1989.

Gates, R. S.; Jewett K. L. and Hsu, S. M.   "A Study on the Nature of
Boundary Lubricating Film: Analytical Method Development," STLE Preprint
No. 88-Tc-5A-3, October 1988, accepted in Tribology Trans.

Hsu, S. M.; Wang, Y. S. and Munro, R. G.   "Quantitative Wear Maps as a
Visualization of Wear Mechanism Transition in Ceramic Materials," Wear of
Materials, Vol 2, p. 723, ASME, 1989.

Hsu, S. M.; Lim, D. S.; Wang, Y. S. and Munro, R. G.   "Ceramic Wear Maps:
Concepts and Method Development," accepted for publication ASME/STLE
Tribology Conference, October 1989.

Wang, Y. S.; Hsu, S. M. and Munro, R. G.   "Ceramic Wear Maps: Alumina,
"Accepted for publication, ASME/STLE Tribology Conference, October 1989.

Gates, R. S. and Hsu, S. M.   "Tribochemical Mechanism of Alumina with
Water," Tribology Trans., 32, 3, 357-363, 1989.

Perez, J. M.; Ku, C. S.; Pei, P.; Hegemann, B. E. and Hsu, S. M.
"Characterization of Tricresyl Phosphate Lubricating Films by Micro-Fourier
Transform Infrared Spectroscopy," Tribology Trans., in press.

Jahanmir, S., Deckman, D. E., Ives, L. K., Feldman, A. and Farabaugh, E.
"Tribological Characteristics of Synthesized Diamond Films on Silicon
Carbide," Wear, in press.

Ruff, A. W. and Wang, Z. X.   "Sliding Wear Studies of Nickel-Copper
Composition-Modulated Coatings on Steel," Wear, in press.

Gangopadhyay, A.; Jahanmir, S. and Hegemann, B. E.   "Reduction in Friction
Coefficient in Metal-Ceramic Contact by Solid Lubrication," to be published
in Tribology Transactions.

Whitenton, E. P. and Deckman, D. E. "Measuring Matching Wear Scars on Balls and Flats," to be published in Surface Topography.

Jahanmir, S. and Peterson, M. B. "The Development and Use of a Tribology Research-in-Progress Database," to be published in Lubrication Engineering.

Ruff, A. W. "Comparison of Standard Test Methods for Non-Lubricated Sliding Wear," to be published in Wear, 1989.

Dally, J. W.; Chen, Y-M. and Jahanmir, S. Analysis of Subsurface Crack Propagation and Implications on Wear of Elastically Deforming Materials," submitted to Wear.

Database Activities

Munro, R. G., Hwang, F. Y. and Hubbard, C. R. "The Structural Ceramics Database: Technical Foundations," J. Res. Natl. Inst. Stand. Technol. 94, 37 (1989).

Munro, R. G. and Hubbard C. R. "Development of the Property Database for Gas-Fired Applications of Ceramics," CAM Newsletter 3 (1), 1 (1989).

Munro, R. G. and Begley, E. F. "Materials Property Database Requirements for Gas-Fueled Ceramic Heat Exchangers," ASTM Second International Symposium on Computerization of Materials Property Databases, Nov. 29-Dec. 1, (1989).

Electronic Materials

White, G. S.; Freiman, S. W. and Wilson, A. "Environmentally Enhanced Fracture of GaAs", to be published in J. Am. Cer. Soc.

Block, S.; Piermarini, G.; Balmer, M. and Bean, V. "Pressure Induced Sintering of ZnS" to be published in proceedings of SPIE Symposium on IR Applied Science and Engineering, Vol. 1112 (1989)

Wong-Ng, W.; Cook, L. P.; Chiang, C. K.; Swartzendruber, L. J. and Bennett, L. H. (1988). "Structural Phase Transition Study of $Ba_2RCu_3O_{6+x}$." Ceramic Superconductors II, edited by M. F. Yan, Am. Ceram. Soc., 27 (1988).

Wong-Ng, W.; Paretzkin, B.; and Fuller, E.R., Jr. (1989). "Crystal Chemistry and Phase Equilibria Studies of the $BaO-R_2O_3-CuO$ Systems." Advances in X-ray Analysis, accepted for publication.

Wong-Ng, W.; Gayle, F. W.; Kaiser, D. L.; Watkins, S. F. and Fronczek, F. R. (1989). "X-ray Diffraciton Study of a Thermomechanically Detwinned Single Crystal of $YBa_2Cu_3O_{6+x}$." Phys. Rev. B, accepted for publication.

Cook, L.; Schenk, P.; Zhao, J.; Farabaugh, E.; Chiang, C. K., and Vaudin, M. "Ceramic Thin Films by Laser Deposition", submitted to American Cer. Soc.

Roth, R. S.; Rawn, C. and Bendersky, A. "Crystal Chemistry of the Compound $Sr_2Bi_2CuO_6$", accepted for publication by J. Mater. Res.

Blendell, J.; Wong-Ng, W.; Chiang, C. K.; Shull, R. and Fuller, E. R. "Phase Composition and Superconducting Propoerties of the High T_c Ceramic Materials," Proc. of TMS Meeting on High Temperature Superconductivity.

Freiman, S. W. and Pohanka, R. C. "A Review of Mechanical Failures of Ceramic Capacitors and Capacitor Materials", accepted for publication by J. Am. Cer. Soc.

Optical Materials

Feldman, A. "Diamond and Diamond-Like Materials: An Emerging Technology - - Status and Applications, Chapter on "Applications", prepared for National Materials Advisory Board/National Academy Report

Robins, L. H.; Cook, L. P.; Farabaugh, E. N. and Feldman, A. "Cathodoluminescence of defects in diamond films and particles grown by hot-filament chemical vapor deposition". Phys. Rev. B, 39, 13367-77 (1989-II)

Feldman, A.; Ying, X. and Farabaugh, E. N. "Optical Properties of Mixed Yttria-Silica Films," submitted to Applied Optics.

Ying, X.; Feldman, A. and Farabaugh, E. N. "Fitting of Transmission Data for Determining the Optical Constants and Thicknesses of Optical Films." Submitted to Journal of Applied Physics.

Kaiser, D. L.; Gayle, F. W.; Roth, R. S. and Swartzendruber, L. J. "Thermomechanical Detwinning of Superconducting $YBa_2Cu_3O_{7-x}$ Single Crystals," J. Mat. Res., 4, 745 (1989).

Wong-Ng, W.; Cook, L. P.; Chiang, C. K.; Vaudin, M. D.; Kaiser, D. L., Beech, F. W.; Swartzendruber, L. J.; Bennett, L. H. and Fuller, E. R., Jr. "Structural Phase Transformation Studies of the High T_c Superconducting Materials, $Ba_2RCu_3O_{6+x}$, in Air," submitted to Trans. of AIME.

Wong-Ng, W.; Gayle, F. W.; Kaiser, D. L.; Watkins, S. F. and Fronczek, F. R. "X-ray Diffraction Study of a Thermomechanically Detwinned Single Crystal of $YBa_2Cu_3O_{6+x}$," submitted to Phys. Rev. B.

Etz, E. S.; Farabaugh, E. N.; Feldman, A. and Robins, L. H. "Raman spectroscopy of synthesized diamond grown by hot filament chemical vapor deposition" Proceedings, SPIE, Vol. 969, Diamond Optics, Albert Feldman, Sandor Holly, Chairs/Editors (SPIE, Bellingham, Washington, 1989).

Frederikse, H. P. R.; Ying, X. T. and Feldman, A. "Thermal Properties of Non-Metallic Films By Means of Thermal Wave Techniques" Proceeding of the Materials Research Society, in press.

Feldman, A.; Robins, L. H.; Frederikse, H. P. R.; Farabaugh, E. N. and Etz, E. "Physical and Chemical Properties of Chemical Vapor Deposited (CVD) Diamond", Proceedings of the Electro-Chemical Society, Diamond and Diamondlike Films, 1989.

Frederikse, H. P. R.; Ying, X. T. and Feldman, A. "Thermal Diffusivity of Thin Diamond Films,", Proceedings of the 6th International Topical Meeting on Photoacoustic and Photothermal Phenomena, in press.

Cook, L. P.; Schenck, P. K.; Zhao, J.; Farabaugh, E. N. and Chiang, C. K. "Ceramic Thin Films By Laser Deposition," to be published in the Proceedings of Thick and Thin Films Symposium, American Ceramic Society, 1989)

Feldman, A. and Holly, S., Chairs/Editors, Diamond Optics, Proceedings SPIE, Vol. 969, SPIE, Bellingham, Washington, 1989.

Synchrotron Radiation Analysis

Kuriyama, M.; Steiner, B. and Dobbyn, R.   "Streaking Images that Appear Only in the Plane of Diffraction in Undoped GaAs Single Crystals: Diffraction Imaging (Topography) by Monochromatic Synchrotron Radiation," Phys. Rev. B, 38, 12421-12427 (1988).

Kuriyama, M.; Steiner, B.; Dobbyn, R. "Structural Anomalies in Undoped Gallium Arsenide Indicated in High Resolution Diffraction Imaging with Monochromatic Synchrotron Radiation", J. Appl. Phys., 66, 559-568 (1989).

Kuriyama, M.; Steiner, B. and Dobbyn R. "Dynamical Diffraction Imaging (Topography) with X-Ray Synchrotron Radiation", Ann. Rev. of Mats. Sci., 19, 183-207 (1989).

CONFERENCES SPONSORED

SDIO/IST-ONR Diamond Technology Initiative Symposium, July 11-13, 1989 (Albert Feldman)

Sumposium on Diamond Optics II, at 33rd Annual International Technical Symposium on Optical and Optoelectronic Applied Science and Engineering, August 7-8, 1989 (Albert Feldman)

TTCP Ceramic Matrix Composites Workshop, June 22-23, 1989 (D. Cranmer)

Engineering Foundation Conference on Structural Ceramics - Science and Technology, March 12-17, March 1989 (S. Wiederhorn)

4TH U.S.-Japan Workshop on Dielectric and Piezoelectric Materials, October 30-November 2, 1988 (S. W. Freiman)

NIST/ONR Workshop on Fracture Computations, September 7-8, 1989 (G. S. White)

Superconductor and Related Materials Session, 1989 Annual Meeting of Crystallographic Association, July 24-29, 1989 (W. Wong-Ng)

American Chemical Society - Special Symposium on "Chemistry and Chemical Engineering in Tribology, April 12-12, 1989 (S. M. Hsu)

Alternatives in Glass Research Symposium, March 23, 1988 (M. Cellarosi)

SELECTED TECHNICAL/PROFESSIONAL COMMITTEE LEADERSHIP

American Ceramics Society
    Glass Division
        Committee on Glass Standards Classification and
        Nomenclature
            M. J. Cellarosi, Chairman
        Editorial Committee
            S. M. Wiederhorn, Subchairman
    Basic Science Division
        Editorial Committee
            B. R. Lawn, Chairman
        Program Committee
            E. R. Fuller, Jr., Chairman
    Communication of the American Ceramic Society
            E. R. Fuller, Jr., Contributing Editor
    Baltimore-Washington Section
            J. S. Wallace, Vice Chairman

American National Standards Institute (ANSI)
    Committee 43.1--Safety Standards for X-ray Diffraction and
               Fluorescence Analysis Equipment
        S. Block, Chairman

ASM International
    Energy Division
            S. J. Dapkunas, Chairman
    Journal of Engineering Materials
            S. J. Dapkunas, Associate Editor

American Society for Testing and Materials
    C14: Glass and Glass Product
            M. J. Cellarosi, Chairman
    C14.01: Nomenclature of Glass and Glass Products
            M. J. Cellarosi, Chairman
    C28.05: Task Group on Powder Characterization
            S. G. Malghan, Working Group Chairman
    D2: Petroleum Products and Lubricants
    D2.09G: Response of Base Oils to Oxidation Inhibitors
            J. M. Perez, Chairman
            C. S. Ku, Secretary
    E29.01: Advanced Ceramics, Organizational Meeting
            M. J. Cellarosi
    F1: Electronics
    F1:02: Lasers
            A. Feldman, Subcommittee Editor
    G2: Erosion and Wear
    G2.2.02: Solid Particle Erosion
            A. W. Ruff, Task Group Leader
    G2.4.04: Pin-on-Disk
            A. W. Ruff, Chairman

American Society of Mechanical Engineers
      Tribology Division Executive Committee
              S. Jahanmir, Member
      Research Committee on Tribology
              S. Jahanmir, Chairman
              S. M. Hsu, Member
      Wear of Materials Conference Steering Committee
              A. W. Ruff, Member

American Society for Testing and Materials
      Wear of Materials Conference Steering Committee
              A. W. Ruff

COMAT Subcommittee on Structural Ceramics
              S. M. Hsu, Member
COMAT Subcommittee on Superconductivity
              S. J. Dapkunas, Member

International Commission for Optics
      U. S. National Committee
              B. Steiner, Chairman

International Energy Agency
      Task II - International Standards
              S. M. Hsu, Overall Task Leader on Powder Characterization
          Subtask 6 Powder Characterization Subgroup
              S. G. Malghan, U. S. Task Leader
          Assignment II-0-3 Ceramic Characterization
              E. R. Fuller, Jr., Member

International Union of Crystallography (IUCr)
      Commission on Crystallographic Studies at Controlled
      Pressures and Temperatures
              G. J. Piermarini, Chairman

National Materials Advisory Board, National Academy of Sciences
      Committee on Ceramic Tribology
              S. M. Hsu, Member
              S. Jahanmir, Member
      Committee on superhard Materials
              A. Feldman, Member

Oak Ridge National Laboratory
      High Temperature Materials Laboratory Advisory Committee
              S. M. Wiederhorn, Chairman

Powder and Bulk Engineering Journal
              S. G. Malghan, Member Editorial Advisory Board

Society of Automotive Engineers
      Task Group on Recommended Practices for the Measurement of Unregulated
      Diesel Emissions
              J. M. Perez, Chairman

Society of Mining and Metallurgical Engineers
    Mining Processing Division
        Concentration Committee
            S. G. Malghan, Chairman
    Mining and Metallurgical Processing Journal
        Editorial Board
            S. G. Malghan, Member

Society of Tribologists and Lubrication Engineers
    Annual Meeting Program Committee
        S. Jahanmir, Member
    Board of Directors
        S. M. Hsu, Director
    Ceramics and Composite Committee
        S. Jahanmir, Chairman

Superconductor Applications Association
        E. R. Fuller, Jr., Member of Advisory Board

Versailles Project on Advanced Materials and Standards (VAMAS)
    International Round-Robin in Ceramic Working Area
        S. W. Freiman, Co-chairman
        E. R. Fuller, Jr., Co-chairman
    Subcommittee on Wear
        S. Jahanmir, U. S. Representative

INDUSTRIAL AND ACADEMIC INTERACTIONS

The Ceramics Division actively participates with industry, academia and other government laboratories in research programs of mutual interest. The following examples are illustrations.

INDUSTRIAL

1. 3M, Incorporated (M. S. Leitheriser)

   This is a collaborative project to examine the surface chemistry of ceramic powders.

2. Accumetrix Corporation (Dr. D. Greenspan)

   This is a program to study the thermal and adhesive properties of plasma sprayed ceramic films. The films are prepared at Accumetrix and their properties were measured at NIST by means of photothermal radiometry.

3. Advanced Composite Materials Corporation (Dr. James F. Rhodes)

   The project is to characterize the microstructures of silicon carbide whisker-reinforced alumina composites. Mechanical properties (fracture toughness and creep behavior) are correlated with microstructural properties and processing conditions.

4. Applied Physics Laboratory (Dr. Moorjani)

   This is to study the laser-ablated thin films of both the BiSrCaCuO and BiPbSrCaCuO high T_c superconductor systems. Initial results indicate an improvement in superconductivity in the thin films when compared to this property in the target from which they are derived.

   Applied Physics Laboratory (Dr. K. Moorjani)

   This is an investigation of the processing conditions and superconducting properties of Bi-Sr-Ca-Cu-O materials. Emphasis has been on fabricating thin films using a laser ablation technique and measuring the properties of the resulting films.

5. AT&T Bell Labs (Dr. P. Gallagher)

   This is a joint research on the phase relations in superconducting ceramics.

6. AVX Corporation (Dr. Bharat Rawal)

   The joint effort is to understand the mechanical properties of multilayer ceramic capacitors. AVX is preparing specimens of differing composition and properties. These are subsequently tested at NIST.

7. Battelle Columbus Laboratories (Dr. W. Glaeser)

    A joint activity is underway to prepare a wear atlas from selected
    literature and research findings at Battelle Columbus Laboratories
    and NIST. Battelle and NIST are evaluating 250 publications in wear
    and friction to select authoritative findings that relate wear and
    friction with materials properties and surface morphology. The
    findings will be published as an atlas under a cooperative effort
    that also includes the West German Bundesanstalt fur Materialprufung.

8. Boeing Company

    An activity has begun with Boeing Company, Seattle, WA, to examine
    the wear characteristics of SiC-coated carbon composites at high
    temperatures. Specimens have been prepared, and have been examined
    so far in the high temperature microindenter system. A significant
    temperature dependence of microhardness was found which should assist
    in interpreting the wear data to be obtained.

9. Carborundum Company (Dr. R. Divakar)

    Dr. Divakar is a Research Associate in the Tribology Group,
    participating in a joint program on the wear mechanisms of advanced
    ceramics and composites at elevated temperatures.

10. Catalyst Research Corporation (D. Schrodt)

    This is a project to develop laboratory procedures for designing
    tests for Li-batteries.

11. Chrysler Corporation

    A collaborative program is in place to evaluate the durability of CVD
    diamond coated WC cutting tools.

12. Clarkson University

    This is a consortia program to study electrooptic material crystal
    growth.

13. Cummins Engine Co. (Dr. D. Steuhower)

    A simple bench test method to evaluate diesel engine oil performance
    was developed in cooperation with Cummins Engine Co. Validation of
    the method was performed using samples from Detroit Diesel Allison
    Division, GMC and Caterpillar, Inc.

14. E.I. Dupont de Nemours and Company (Drs. David Roach, P. Morris,
    F. Tabbe, and R. French)

    Research is being conducted for the Dupont Co. to evaluate the static
    fatigue behavior of polycrystalline aluminum oxide fibers intended for
    reinforcement of other ceramic materials. In this project, the
    strength, toughness and resistance of these fibers to environmentally

induced fracture will be evaluated at room temperature. The NIST clean room is being used in joint research projects addressing production of barium titanate and sintering of ultra high purity alumina.

E. I. Dupont de Nemours (C. Torardi, J. B. Parise)

Structural characterization of Ca-Bi-O compounds. Solved the crystal structure of a $Ca_4Bi_6O_{13}$ single crystal that was grown in our laboratory; they also demonstrated the acentricity of this structure on a powder sample that we synthesized. We are currently collaborating on structural studies of the compound "$Ca_7Bi_6O_{16}$" (possibly $Ca_2Bi_2O_5$).

15. Electric Power Research Institute (Mr. W. Bakker)

    EPRI is funding a program in the Electronic Materials Group to develop more economical superconducting ceramics for conductor applications.

16. Ford Motor Company (Drs. K. R. Carduner and M. J. Rokosz)

    Applications of NMR spectroscopy and imaging to characterize ceramic materials for automotive applications. The first stage involves using Si-27 CP/MAS NMR for phase composition determination of silicon nitrides and carbides. The current collaborative relation is analysis of NIST samples by Ford's spectrometer. In the future, we will provide imaging capability for Ford's applications.

17. Garrett Ceramic Components (Dr. B. Busovne)

    This project is related to pressure slip casting of colloidal suspensions by using a special hardware designed by Garrett Ceramic Components.

18. Gas Research Institute and Pennsylvania State University
    (Prof R. Tressler, Prof. D. Green)

    The Division is leading an effort with GRI and PSU to develop a materials property computerized database targeted for gas-fueled heat exchangers and recouperators as well as conducting research addressing the tribological properties of materials for gas-fired applications.

19. ISCAR Ceramics, Inc. (Dr. Joseph Barta)

    Statistically designed experiments were performed to establish interrelations amongst processing parameters, microstructure, mechanical properties, and machining performance of silicon carbide whisker-reinforced alumina composites. Processing parameters were correlated by regression analysis with microstructure (density, alumina grain size, and homogeneity), mechanical properties (flexural strength, hardness, and fracture toughness), and machining performance (flank and nose wear). An industrial Research Associate,

Dr. Joseph Barta, from ISCAR Ceramics worked with Division personnel on this project.

20. John Deere and Company (Dr. P. Swanson)

This program is concerned with investigating problems connected with the measurement of galling damage and the development of tests to evaluate alloys used in agricultural and industrial equipment where severe wear is a serious problem.

21. Martin Marietta (G. T. Davis and W. C. Moshier)

Measure refl-EXAFS of thin films on $A\ell$ and $A\ell$-Mo alloys to study the role of Mo and molybdates.

22. Max Planck Institute, Stuttgart, Federal Republic of Germany

Collaborative research with the processing group of Max Planck Institute on the clean room processing of advanced ceramic material is in progress. The influence of clean room processing on chemical and phase composition of ceramic superconductors in the barium-yttrium-copper-oxide system and in similar systems with lanthanide (rare earth) substitutions for yttrium has been examined.

23. Naval Research Laboratory (D. Schrodt, B. Bender, R. Soulen, S. Wolf)

The project is on the thermochemical treatment of polymer-derived SiC fibers and the degradation mechanisms of these fibers during high-temperature heat treatments (Schrodt, Bender). A project is also underway to characterize YBaCuO single crystals by magnetic susceptability and cyclotron resonance measurements (Soulen, Wolf).

24. Naval Surface Weapons Center (Dr. P. Miller)

This research characterizes the influence of pressure on the decomposition kinetics of energetic materials by a combination of FTIR and x-ray diffraction techniques.

25. Norton Company (Dr. P. Tewari, Dr. K. E. Amin)

An FTIR study of aqueous slurries and surface treatments of Si_3N_4 and SiC is in progress (Tewari). A collaborative program is in place to study the effects of processing wear phenomena.

26. Oak Ridge National Laboratory (Dr. T. M. Besmann)

The project is on the microstructural and structural characterization of ceramic matrix composites produced by chemical vapor infiltration (CVI). Mechanical properties are correlated with microstructure and processing.

27. Raytheon Corporation

A joint activity has been initiated to examine the toughness of CVD and HIPed zinc sufide materials by a microindentation techniques.

28. Southwest Research Institute (Dr. R. Page)

The project is to conduct SANS beam broadening experiments to follow pore evolution during early and intermediate stages of alumina sintering.

29. VAMAS Standardization

An international round-robin to develop test procedures for determining the stress corrosion susceptibility of advanced ceramic materials is conducted. Approximately 20 laboratories in 6 countries are participating in the interlaboratory testing program. A second cooperative program is underway to evalute the tribology of structural ceramics.

30. W. R. Grace (Dr. L. Dolhert)

This research addresses sintering properties of barium-yttrium-copper-oxide superconductor materials which have been prepared by chemical routes and milled to different size fractions.

UNIVERSITIES

1. University of Dayton Research Institute (T. N. Wittberg)

Using UDRI's X-ray photoelectron spectrometer (XPS) and Auger electron spectrometer (AES), the surface structures and reactivities have been investigated and results published for ceramic materials.

2. Drexel University (Dr. M. Koczak)

This is a joint program with Dr. M. J. Koczak of Drexel University on the fracture behavior of ceramic matrix composites.

3. University of Florida (Prof. B. M. Mougdil)

In this collaborative project the characterization and structure of flocs in dense slurries will be examined using interfacial, rheological, and neutron and X-ray scattering techniques.

4. University of Illinois (Dr. S. W. Lee, Prof. S. Danyluk)

The project centers on an investigation of the fundamental mechanisms of friction, wear, and surface damage in tribological applications of advanced ceramics.

5. The Johns Hopkins University (Drs. Bohandy, B. F. Kina, F. J. Adrian, K. Moorjani)

   This project addresses characterization of YBaCuO single crystals by magnetically modulated microwave absorption.

   The Johns Hopkins University (J. Kruger)

   Measure refl-EXAFS of ultra-thin oxide films on Fe and FeCr alloys near the initiation of breakdown.

6. Lehigh University (Prof. M. Harmer)

   Joint research on the effect of microstructure on the fracture resistance of ceramic materials. The materials under study will be manufactured at Lehigh University and will be characterized and tested at the NIST.

7. Louisiana State University (Dr. S. F. Watkins, Dr. F. B. Fronczek)

   This project involves single crystal X-ray diffraction studies to determine the structure of YBaCuO using untwinned single crystals.

8. University of Maryland (Profs. J. Dally, and J. Stewart)

   Two projects are underway; one a joint research project on wear models of ceramics; and, the other on the determination of residual stresses in ceramics by X-ray techniques.

   University of Maryland (Prof. Luke Chang and Dr. Y. Zhang)

   The projects include the investigation of ceramic surface reactivities with surface lubricants at high temperature by TGA/DSC as well as surface film formations. The lubricant oxidations through free radical formation and recombinations are also studied by the electron spin resonance (ESR) method.

9. University of Michigan (Dr. T. Y. Tien)

   This is joint research on the creep and creep rupture behavior of SiAℓON composites at high temperature. These materials were manufactured at the University of Michigan and characterized both microstructurally and mechanically at NIST.

10. University of Minnesota (Dr. D. Pui)

    This is a collaborative project on the aerodynamic sizing of fine ceramic powders and on computer fitting of standard particle size distribution functions to particle size distribution data.

11. Northwestern University (Prof. H. Cheng)

    Joint research involves lubrication modeling. The research focuses on the microelastohydrodynamic theories under wearing conditions. This

is the first attempt at combining surface chemistry with surface mechanics to create a predictive wear model.

Northwestern University (Prof. K. Faber and S. W. Paulik)

Collaborative research is performed (i) to elucidate the fundamentals of microcrack generation in noncubic polycrystalline ceramics due to thermal expansion anisotropy and/or phase transformation strains; (ii) to develop fabrication strategies, based on control of grain size, grain texture and thermal treatments, which suppress the formation of microcracks; and (iii) to elucidate the influence of processing strategies of the fracture properties of these materials. The ceramic superconductor, $Ba_2YCu_3O_x$, was chosen as one model system due to its extreme anisotropy in thermal expansion coefficients and the potential for control of crystallographic texture.

Northwestern University (J. Weertman and P. Jemian)

Anomalous small angle X-ray scattering to separate contributions from various scattering species in a complex material. With this technique it is possible to follow the microstructure evolution due to simple aging or creep or cyclic stresses for example.

12. University of Pennsylvania (Prof. P. Davies)

This is a collaborative project on the properties and structure of microwave dielectrics and high T_c superconductors.

13. Pennsylvania State University (Dr. E. Klaus)

The research joint projects include fundamental studies on the vapor phase lubrication of ceramic materials at high temperature; microstructural effects in ceramic wear processes; high temperature friction and wear tribometer design; and ceramic wear modeling which seeks to establish a theoretical understanding of ceramic wear processes.

14. Rutgers University (Dr. R. Gerhardt)

This is a collaboration on the characterization by SANS of microporous silica as a function of thermal processing.

Rutgers University (Dr. J. Wachtman, A. Zutshi)

This cooperative study involves the fabrication of low iron impurity, hot-pressed silicon nitride and the wear testing of same to investigate effects of Fe impurities on the lubrication chemistry of silicon nitride. Will also include wear testing of silicon nitride made from the same powder but with different processing technique to look at processing-microstructure-performance relationships.

15. Southwest Research Institute (R. A. Page) and S. T. Krueger (Reactor Division, NIST)

   MSANS studies of pore evolution in pure alumina.

16. University of Maryland (Prof. Luke Chang and Dr. Y. Zhang)

   The projects include the investigation of ceramic surface reactivities with surface lubricants at high temperature by TGA/DSC as well as surface film formations. The lubricant oxidations through free radical formation and recombinations are also studied by the electron spin resonance (ESR) method.

17. Tsinghua University (J. Dong, X. Dong, Y. Wang, T. Ying)

   This joint research activity is concerend with the mechanisms of wear and lubrication of ceramics.

18. Technion, Israel Institute of Technology

   Quantitative techniques are developed and characterized for the measurement of interfacial frictional stresses and interfacial fracture toughness in reinforced ceramic composites. A novel technique was developed which involves the compression of an aligned composite disc normal to the reinforcement between a rigid ceramic platen and a ductile metallic plate. Differential elastic properties of the fibers and the matrix result in a protrusion of the fibers, which can be measured at load from the metallic replica and after elastic/frictional recovery from the residual protrusion of the fibers. The technique has a major advantage that measurements are made on actual processed composites.

STANDARD REFERENCE MATERIALS

The Division provides science, industries, and government a central source of wellcharacterized materials certified for chemical composition of physical or chemical properties. These materials are issued with a certificate and are used to calibrate instruments, to evaluate analytical methods, or to produce scientific data which can be referred to a common base.

DESCRIPTION	SRM NUMBER
Alumina Elasticity	718
Alumina Glass Anneal Point	714
Alumina Glass Anneal Point	715
Alumina Melting Point	742
Aluminum Magnetic Susceptibility	763-1
Aluminum Magnetic Susceptibility	763-2
Aluminum Magnetic Susceptibility	763-3
Barium Glass Anneal Point	713
Borosilicate Glass Composition	93(A)
Borosilicate Glass Thermal Expansion	731L1
Borosilicate Glass Thermal Expansion	731L2
Borosilicate Glass Thermal Expansion	731L3
Cadmium Vapor Pressure	746
Chlorine in Base Oil	1818
Container Glass Composition	621
Container Glass Leaching	622
Container Glass Leaching	623
Copper Thermal Expansion	736L1
Fused Silica Thermal Expansion	739L1
Fused Silica Thermal Expansion	739L2
Fused Silica Thermal Expansion	739L3
Glass Analytical Standard	1835
Glass Dielectric Constant	774
Glass Electrical Resistance	624
Glass Fluorescence Source	477
Glass Liquidus Temperature	773
Glass Refractive Index	1820
Glass Sand (High Iron)	81A
Glass Sand (Low Iron)	165A
Glass Stress Optical Coefficient	708
Glass Stress Optical Coefficient	709
Glass Viscosity Standard Renewal	717
Gold Vapor Pressure	745
High Boron Glass Viscosity	717
Intensity XRD Set	674
Lead Barium Glass Composition	89
Lead Glass Anneal Point	712
Lead Glass Viscosity	711
Line Profile	660

FACILITIES

FACILITIES

High Temperature X-ray Diffraction - J. P. Cline

The X-ray diffraction facility at NIST consists of a high temperature
machine of theta-two theta geometry equipped with an incident beam
monochromator and a position sensitive proportional counter. The position
sensitive detector allows for data collection at a rate two orders of
magnitude faster than conventional detectors. The furnace is an enclosed
high vacuum chamber capable of reaching 3000K; it is also equipped with a
mass flow controller for atmospheric control. This equipment is used for
the study of high temperature phase equilibria, high temperature reaction
kinetics, sintering of monolithic ceramics, and strain development during
sintering of ceramic composites.

Small Angle Neutron Scattering (SANS) - Ceramics Furnace - G. G. Long

The SANS-ceramic furnace is associated with the NIST 20 MW research
reactor. This system will allow in-situ densification and microstructural
studies of ceramic powders during sintering.

Electrokinetic Sonic Amplitude (ESA) Measurement - D. C. Bartenfelder, L.
Lum, and S. G. Malghan

The Matec ESA unit has the unique capability of measuring colloidal
properties in dense slurries. This is a major breakthrough, since previous
techniques were restricted to dilute slurries. The analytical capabilities
of the unit include performance in the following modes: potentiometric
titration, conductometric titration, time-series titration, and
concentration series titration. In the selected mode, the equipment can
monitor: electrokinetic sonic amplitude, zeta-potential, electrophoretic
mobility, electrical conductivity, isoelectric point, surface charge
density, and phase angle of the material with the specified experimental
conditions.

Slurry Rheology - D. C. Bartenfelder, S. G. Malghan

The RTI unit allows for viscosity (stress/rate) as well as rheology
characterization of ceramic slurries. Rheological measurements are more
informative and flexible with respect to the various slurry properties:
ideal (Newtonian), pseudoplastic, plastic, dilatant, and thixotropic. The
modeling of these rheological properties as a function of sample treatment,
colloidal and surface chemical properties is paramount in developing and
improving processing technology.

Nuclear Magnetic Resonance (NMR) - P. S. Wang

The facility includes a Bruker MSL-400 NMR system capable of performing almost all NMR active nuclei in the periodic table in both solid and liquid states as well as performing NMR imaging in proton and carbon-13 frequencies. Currently, the operation parameters for both states at proton, deuterium, carbon-13, and aluminum-27 have been defined and proved by documented NMR spectra of organic and inorganic molecules. The equipment will be tuned to Si-29, Cu-63, and Y-89 in the near future.

Scanning Electron Microscopy/Image Analysis (SEM) - J. F. Kelly

A new scanning electron microscope facility is being used to characterize ceramic powders in terms of fundamental size and shape data. The capacity for characterizing thousands of individual features has been developed through the installation of a computer controlled Amray 1830 scanning electron microscope with a Kevex Quantum V energy dispersive (EDS) X-ray and image analysis system.

An in-situ fracture stage has been developed for the SEM to enable real time observation of crack propagation in ceramic wafers. This capability provides greater detail of the role of grain morphology in the mechanism of bridging behind the advancing crack tip.

Quantitative EDS X-ray techniques are being used to measure the blending homogeneity of SiC whiskers within an alumina matrix and the chemical homogeneity of Y-Ba-Cu-O high T_c superconductors.

The SEM is now modified to obtain single-grain electron backscatter diffraction patterns from bulk specimens. This permits the measurement of crystallographic orientation in ceramic specimens.

ISI Super III-A SEM with EDX - D. B. Minor

This is a general-use SEM that is inherently user-friendly both for microphotography and qualitative EDX. The beam source is a tungsten hairpin filament and features a 200 micron final aperture. The unit is equipped with a +700 VDC phototube and a +100 VDC backscattered detector.

Time-Resolved Micro-Raman - P. S. Wang

This versatile facility consists of a pulsed Nd-YAG laser, a CW Ar-ion laser, a triple monochromator, and a gated intensified diode array detector. This facility, therefore, provides a wide variety of Raman analysis techniques in both time-resolved and continuous operation modes, using either visible or ultra-violet excitation sources for either operation mode. Either bulk macro-Raman or 5 μm resolution micro-Raman analysis is available.

Chemical Laboratory - P. Pei

A new chemical characterization facility is being established. This facility will contain equipment to characterize ceramic surfaces as well as bulk composition. Some examples of the equipment are: infrared and Fourier transform infrared (FTIR) pectrometers for measuring absorption and specular and diffuse refractance; micro-FTIR spectrometer for absorption at small areas; gel permeation chromatograpy/graphite furnace atomic absorption (GPC/GFAA) for molecular size distribution and metal ion determination; and various chromatographic techniques for isolation of minor components for chemical characterization.

Thermal Analysis Facility - J. Wallace and J. Blendell

A thermal analysis facility has been set up for measurement of behavior of ceramic materials in a wide range of atmospheric conditions and temperatures. The equipment is comprised of a computer-controlled differential pushrod dilatometer capable of measurement of thermal expansion or sintering shrinkage in vacuum or inert, oxidizing or reducing atmospheres with temperatures from room temperature to 1600°C. The atmosphere can be monitored using either a zirconia oxygen cell, which is connected to the dilatometer data acquisition system, or an external mass spectrometer with its own associated computerized data acquisition system.

The second major piece of equipment is a simultaneous thermal analysis (STA) system capable of performing simultaneous thermogravimetric and differential thermal analysis from room temperature to 1700°C. Atmospheres can be varied from vacuum to single and mixtures of gases using a four-channel mass flow controller. The STA is also connected to the mass spectrometer system and its associated data acquisition system. The quadrapole mass spectrometer system has a capability of analyzing to 512 AMU.

High Temperature Creep Apparatus - D. Cranmer, S. Wiederhorn

A series of four high temperature tensile creep rigs (T_{max} = 1500°C) equipped with laser displacement sensors is available to determine the behavior of materials at elevated temperatures. Additionally, a rig capable of 1800°C in air equipped with the same laser displacement sensor is available.

Surface Forces Laboratory - D. Cranmer, R. Horn

The surface forces laboratory consists of a semi-clean room preparation facility and a crossed cylinders surface forces apparatus. The crossed cylinders apparatus permits measurements of the forces associated with surfaces brought to within ~2 nm of one another through contact. It can be operated with a variety of liquid or gaseous environments, thus allowing investigations of the effects of chemical changes on forces between two surfaces.

Instrumented Indenter - D. C. Cranmer

This apparatus is designed to enhance the ability to measure the properties of the fiber/matrix interface in ceramic matrix composites. The instrumented indenter permits measuring the force on and displacement of a fiber directly during loading and unloading. Previous methods for examination of these properties could only measure the maximum applied load and inelastic displacement.

Glass Melting - D. Blackburn, D. Cranmer

Extensive glass melting and annealing facilities for production of melts up to 1600°C are available. Batch sizes up to about 2.5 -3 kg can be produced using this equipment. Special facilities for melts containing heavy metals such as thallium and lead are also available.

Viscometers - D. Blackburn, D. Cranmer

Rotating bob, fiber elongation, and bending beam apparatus for determining the complete range of viscosity from about 10^{14} to 10^1 poise over the temperature range from room temperature to 1600°C are available.

Diamond Film Deposition - A. Feldman, E. Farabaugh

Facilities consist of three hot-filament CVD reactors and a microwave-enhanced CVD reactor.

Optical Characterization - L. Robins, A. Feldman

Facilities include a Cary spectrophotometer for measuring optical transmittance in the spectral range 0.2 μm to 2.5 μm, optical spectrometers for measuring photoluminescence and Raman spectra, and an argon ion laser.

Surface Analysis - E. Farabaugh

Surface analysis with capabilities for Auger spectroscopy, electronic energy loss spectroscopy, X-ray photoelectron spectroscopy, and secondary ion mass spectroscopy. Facility includes a HP-1000 computer for data acquisition.

Ceramics Processing Laboratory - J. Blendell, J. Wallace, S. Malghan

A processing laboratory for the synthesis and production of well controlled ceramics has been assembled. Equipment includes: cold isostatic process, hot presses, furnaces, milling equipment, a sinter forge and tape caster.

Level 10 Clean Room - J. Blendell

A Level 10 Clean Room has been constructed for the processing of ceramics in a controlled environment where the presence of air low contaminants can seriously affect the final products properties. The room is provided with separated work stations to allow simultaneous conduct of experiments.

Tribology Research Facilities - S. Jahanmir

Several types of equipment for friction and wear evaluation are available, including: a 1000°C single pass, unidirectional sliding, pin-on-flat geometry, tester; a modified four ball tester adaptable to ball on three flats with controlled environment; standard test machines such as block on ring, crossed cylinder, dry and wet sand rubber wheelabraders; high load, single pass galling wear tester, single and multiple particle erosive test systems. Computer controlled surface profilometer and scratch hardness testers are also available for surface analysis.


Thermal Wave Analysis Facility - A. Feldman, G.S. White

This facility is used for characterizations based on variations of thermal diffusivities. Equipped with both an Ar-ion and CO_2 laser, the facility permits analyses by infrared and Mirage methods. It is especially useful as a nondestructive method of detecting flaws in ceramics especially in near-surface regions.

APPENDIX

U.S. DEPARTMENT OF COMMERCE
National Institute of Standards and Technology
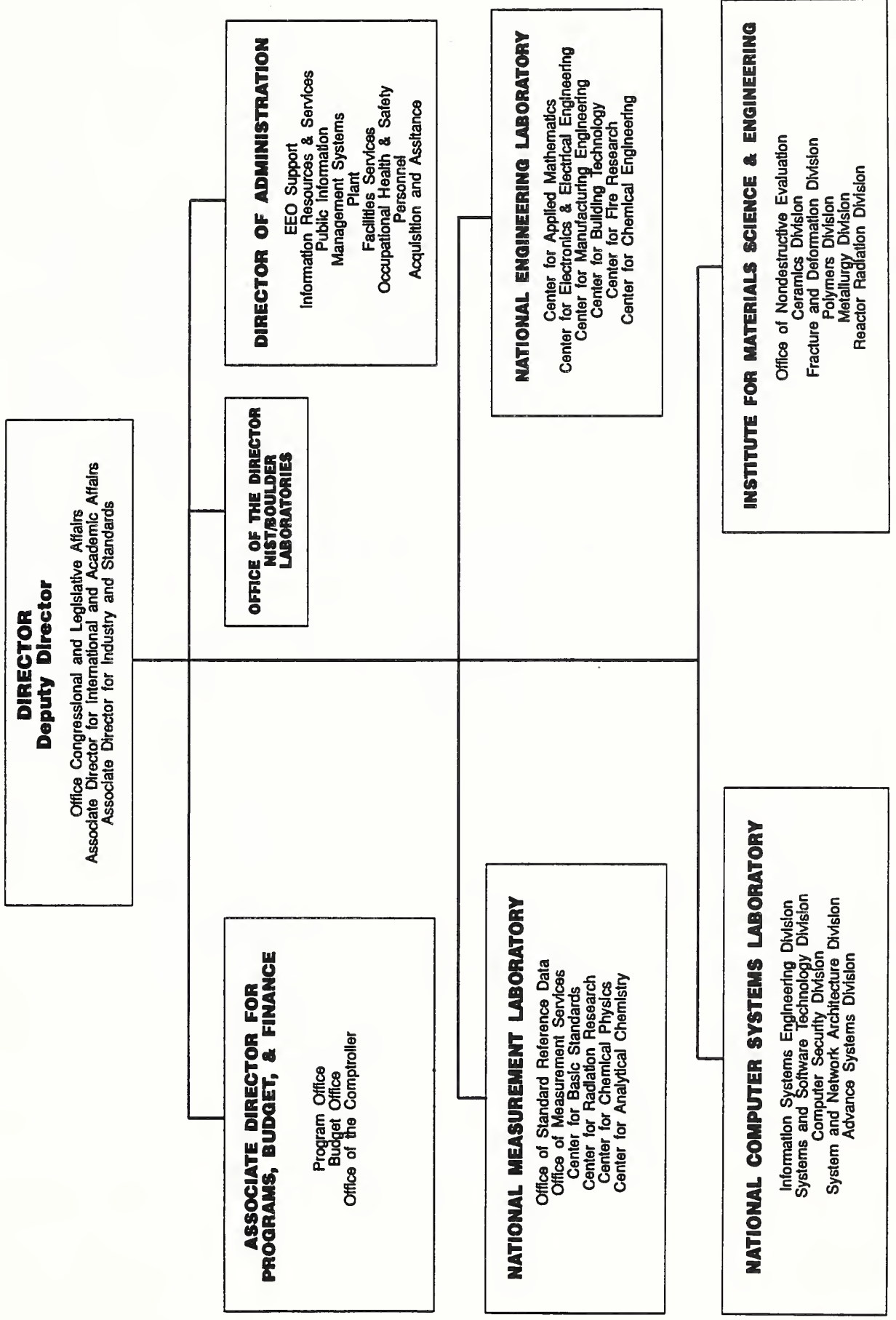
DIRECTOR
Deputy Director

Office Congressional and Legislative Affairs
Associate Director for International and Academic Affairs
Associate Director for Industry and Standards

OFFICE OF THE DIRECTOR
NIST/BOULDER
LABORATORIES

DIRECTOR OF ADMINISTRATION

EEO Support
Information Resources & Services
Public Information
Management Systems
Plant
Facilities Services
Occupational Health & Safety
Personnel
Acquisition and Assitance

NATIONAL ENGINEERING LABORATORY

Center for Applied Mathematics
Center for Electronics & Electrical Engineering
Center for Manufacturing Engineering
Center for Building Technology
Center for Fire Research
Center for Chemical Engineering

INSTITUTE FOR MATERIALS SCIENCE & ENGINEERING

Office of Nondestructive Evaluation
Ceramics Division
Fracture and Deformation Division
Polymers Division
Metallurgy Division
Reactor Radiation Division

ASSOCIATE DIRECTOR FOR
PROGRAMS, BUDGET, & FINANCE

Program Office
Budget Office
Office of the Comptroller

NATIONAL MEASUREMENT LABORATORY

Office of Standard Reference Data
Office of Measurement Services
Center for Basic Standards
Center for Radiation Research
Center for Chemical Physics
Center for Analytical Chemistry

NATIONAL COMPUTER SYSTEMS LABORATORY

Information Systems Engineering Division
Systems and Software Technology Division
Computer Security Division
System and Network Architecture Division
Advance Systems Division

Institute for Materials Science and Engineering

L. H. Schwartz, Director
H. L. Rook, Deputy Director

Institute Scientists

J. W. Cahn
R. M. Thomson
S. M. Wiederhorn

Nondestructive Evaluation

H. T. Yolken, Chief
L. Mordfin, Deputy

Ceramics

S. M. Hsu, Chief
S. J. Dapkunas, Deputy

Polymers

L. E. Smith, Chief
B. M. Fanconi, Deputy

Metallurgy

E. N. Pugh, Chief
J. H. Smith, Deputy

Reactor Radiation

J. M. Rowe, Chief
T. M. Raby, Deputy

Fracture and Deformation

H. I. McHenry, Chief
C. M. Fortunko, Deputy

NIST-114A (REV. 3-89)	U.S. DEPARTMENT OF COMMERCE NATIONAL INSTITUTE OF STANDARDS AND TECHNOLOGY	1. PUBLICATION OR REPORT NUMBER NISTIR 89-4148
		2. PERFORMING ORGANIZATION REPORT NUMBER
	BIBLIOGRAPHIC DATA SHEET	3. PUBLICATION DATE December 1989

4. TITLE AND SUBTITLE

Ceramics Division - Technical Activities 1989

5. AUTHOR(S)

S. M. Hsu

6. PERFORMING ORGANIZATION (IF JOINT OR OTHER THAN NIST, SEE INSTRUCTIONS) U.S. DEPARTMENT OF COMMERCE NATIONAL INSTITUTE OF STANDARDS AND TECHNOLOGY GAITHERSBURG, MD 20899	7. CONTRACT/GRANT NUMBER
	8. TYPE OF REPORT AND PERIOD COVERED

9. SPONSORING ORGANIZATION NAME AND COMPLETE ADDRESS (STREET, CITY, STATE, ZIP)

NIST - Ceramics Division 420
Building 223/A256
Gaithersburg, MD 20899

10. SUPPLEMENTARY NOTES

☐ DOCUMENT DESCRIBES A COMPUTER PROGRAM; SF-185, FIPS SOFTWARE SUMMARY, IS ATTACHED.

11. ABSTRACT (A 200-WORD OR LESS FACTUAL SUMMARY OF MOST SIGNIFICANT INFORMATION. IF DOCUMENT INCLUDES A SIGNIFICANT BIBLIOGRAPHY OR LITERATURE SURVEY, MENTION IT HERE.)

Current programs of the Ceramics Division are reviewed.

12. KEY WORDS (6 TO 12 ENTRIES; ALPHABETICAL ORDER; CAPITALIZE ONLY PROPER NAMES; AND SEPARATE KEY WORDS BY SEMICOLONS)

Advanced Ceramics; Data Bases; Electronic Ceramics; Mechanical Properties, Optical Materials; Powder Characterization and Processing; Tribology, Superconductors; Synchrotron Radiation

13. AVAILABILITY	14. NUMBER OF PRINTED PAGES
[X] UNLIMITED	
☐ FOR OFFICIAL DISTRIBUTION. DO NOT RELEASE TO NATIONAL TECHNICAL INFORMATION SERVICE (NTIS).	155
☐ ORDER FROM SUPERINTENDENT OF DOCUMENTS, U.S. GOVERNMENT PRINTING OFFICE, WASHINGTON, DC 20402.	15. PRICE
[X] ORDER FROM NATIONAL TECHNICAL INFORMATION SERVICE (NTIS), SPRINGFIELD, VA 22161.	A08

ELECTRONIC FORM